NVO-140

VOLUME II

ENEWETAK RADIOLOGICAL SURVEY

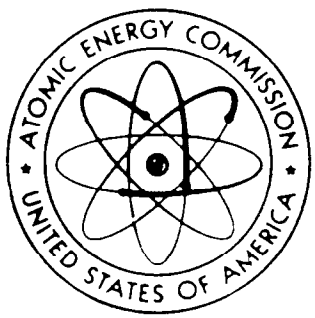

OCTOBER 1973

UNITED STATES ATOMIC ENERGY COMMISSION

NEVADA OPERATIONS OFFICE

LAS VEGAS, NEVADA

Appendix II - Survey Results by Island

INTRODUCTION

This appendix is a compilation of radiological survey results for each of the islands in Enewetak Atoll. The information for each island includes a color aerial photograph, a series of photographs overprinted with survey data, and a set of analytical data. It should be noted that several islands (i.e., IRENE, YVONNE, ELMER, FRED, and IRWIN) have been subdivided into sections (e.g., IRENE A and IRENE B) because of their relatively large size. In addition, it should be pointed out that the sets of overprints are not necessarily the same for all islands. Thermoluminescent detectors (TLD's), for example, were not used on all islands. For ease of comparison and clarity, the same data parameter for each island is overprinted on the same color of photograph.

For a discussion of the techniques used in collecting the data presented on the photographic overprints, the reader is referred to the appropriate section in Vol. I of this document.

A typical set of survey results is outlined below for ALICE, together with the page and figure designation scheme used.

ALICE

At the end of Volume III, after the section on LEROY, is a section containing microfiche transparencies reproducing all of the analytical data obtained in this survey. Instructions on the use of microfiche film are also included in that section.

Table B.1. Cross-reference list of island names.

Site	Native names from U.S. Hydrographic Office charts 1946	Native names from U.S. Hydrographic Office charts 1968	Native names from Dr. Jack A. Tobin
ALICE	Bogallua	Bogallua	BOKOLUO
BELLE	Bogombogo	Bogombogo	BOKOMBAKO
CLARA	Ruchi	Eybbiyae	—[a]
DAISY	—[a]	Lidilbut	LOUJ
EDNA	—[a]	—[a]	—[a]
HELEN	Bogairikk	Bogeirik	BOKAIDRIK
IRENE	Bogon	Bogon	BOKEN
JANET	Engebi	Engebi	ENJEBI
KATE	Muzinbaarikku	Mujinkarikku	MIJIKADREK
LUCY	Kirinian	Billee	KIDRINEN
PERCY	—[a]	—[a]	—[a]
MARY	Bokonaarappu	Bokonarppu	BOKENELAB
NANCY	Yeiri	Yeiri	ELLE
OLIVE	Aitsu	Aitsu	AEJ
PEARL	Rujoru	Rujiyoru	LUJOR
RUBY	Eberiru	Eberiru	ELELERON
SALLY	Aomon	Aomon	AOMON
TILDA	Biijiri	Biijiri	BIKILE
URSULA	Rojoa	Rojoa	LOJWA
VERA	Aaraanbiru	Arambiru	ALEMBEL
WILMA	Piiraai	Piirai	BILLAE
YVONNE	Runit	Runit	RUNIT
SAM	—[a]	—[a]	—[a]
TOM	—[a]	—[a]	ANEROWIJ
URIAH	—[a]	—[a]	—[a]
VAN	—[a]	—[a]	—[a]
ALVIN	Chinieero	—[a]	JINEDROL
BRUCE	Aniyaanii	Japtan	ANANIJ
CLYDE	Chinimi	Chinimi	JINIMI
DAVID	Japtan	Muti	JAPTAN
ELMER	Parry	Parry	MEDREN
WALT	—[a]	—[a]	—[a]
FRED	Eniwetok	Eniwetok	ENEWETAK

Table B.2 (Continued)

Island	Altitude flown, ft	Scale
TOM	2000	1 cm = 8 m
URIAH	2000	17
VAN	4000	20
ALVIN	2000	15
BRUCE	5000	42
CLYDE	2000	12
DAVID	5000	44
REX	2000	18
ELMER A, B, C, D	5000	47
WALT	2000	15
FRED A, B, C, D, E, F	5000	48
GLENN	9000	77
HENRY	6000	55
IRWIN A, B	3000	29
JAMES	3000	16
KEITH	3000	26
LEROY	3000	20
YVONNE E, F	10000	95

Table B.3. Contour map key for use with the EG&G aerial radiological survey figures in Appendix II.[a]

Symbol	^{241}Am concentration[b] (assumed 10-cm relaxation depth)		^{137}Cs[c]		^{60}Co[d]		Gross count exposure rate,[e] μR/hr
	Total μCi/m^2	averaged over top 10 cm, pCi/g	Concentration ±50% for 1 cm (relaxation depth < 10 cm), μCi/m^2	Exposure rate, μR/hr	Concentration ±50% for 1 cm (relaxation depth < 10 cm), μCi/m^2	Exposure rate, μR/hr	
A$^-$			0-0.1	0-0.34			
A$^-$			0.1-0.2	0.34-0.68	0-0.04	0-0.59	
A	0-21	0-9	0.2-0.4	0.68-1.36	0.04-0.08	0.59-1.14	0-1.0
B	21-30	9-13	0.4-0.6	1.36-2.0	0.08-0.12	1.14-1.7	1.0-1.5
C	30-45	13-19	0.6-0.8	2.0-2.7	0.12-0.16	1.70-2.3	1.5-2.0
D	45-66	19-28	0.8-1.6	2.7-5.4	0.16-0.32	2.3-4.6	2.0-4
E	66-100	28-42	1.6-3.1	5.4-11	0.32-0.64	4.6-0.9	4-8
F	100-145	42-61	3.1-6.2	11-22	0.64-1.3	9.2-18	8-16
G	145-210	61-89	6.2-12	22-44	1.3-2.5	18-36	16-33
H	210-300	89-130	12-25	44-88	2.5-5.0	36-72	33-66
I	300-450	130-190	25-50	88-170	5-10	72-140	66-130
J			50-100	170-340	10-20	140-290	130-260
K			100-200	340-700	20-40	290-580	260-520
L			200-400	700-1400	40-80	580-1200	520-1050

[a]See chapter on the EG&G aerial radiological survey in Vol. 1.

[b]Shown in "c" figures in this Appendix.

[c]Shown in "k" figures in this Appendix.

[d]Shown in "m" figures in this Appendix.

[e]Shown in "b" figures in this Appendix.

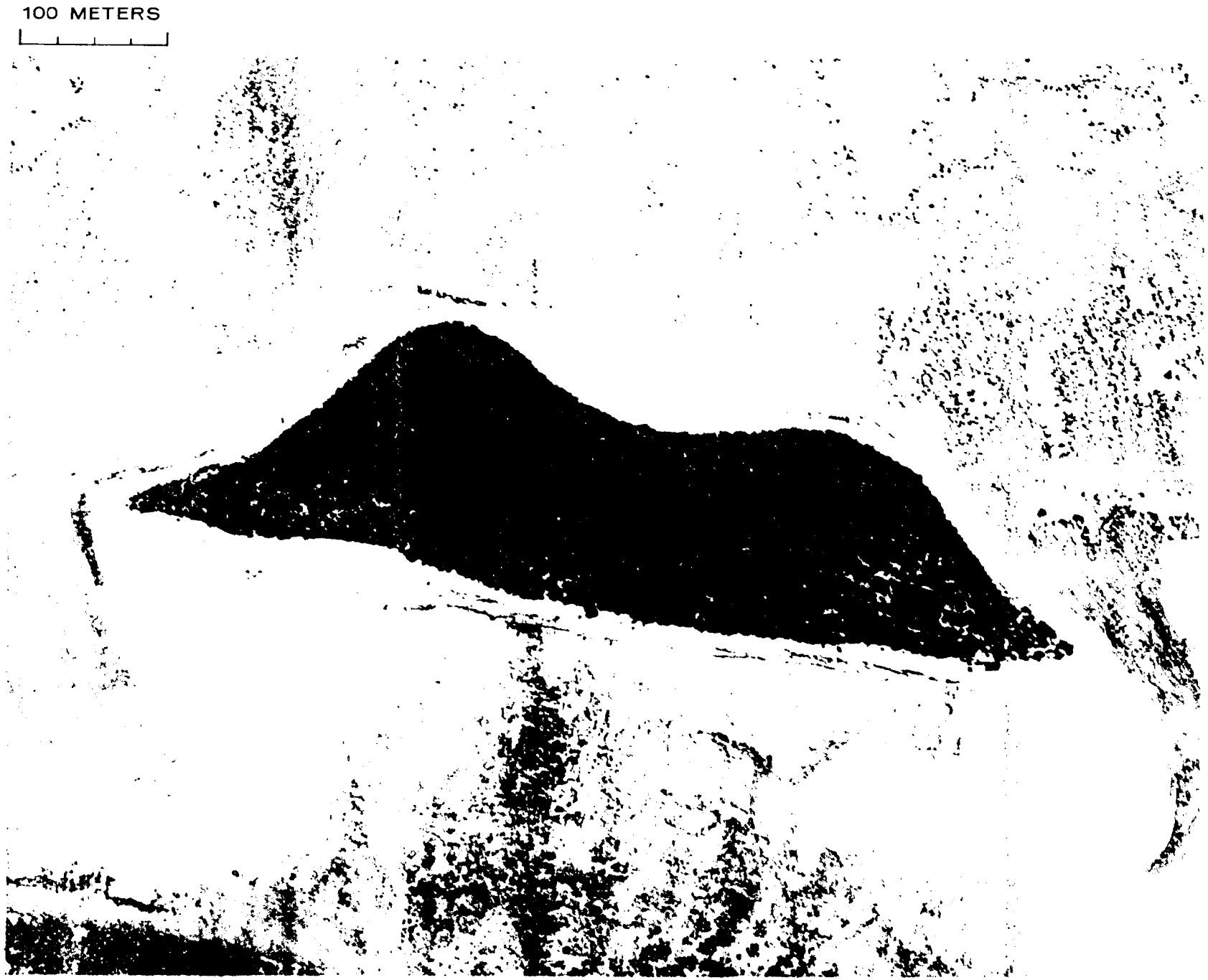

Fig. B.1.1.a.

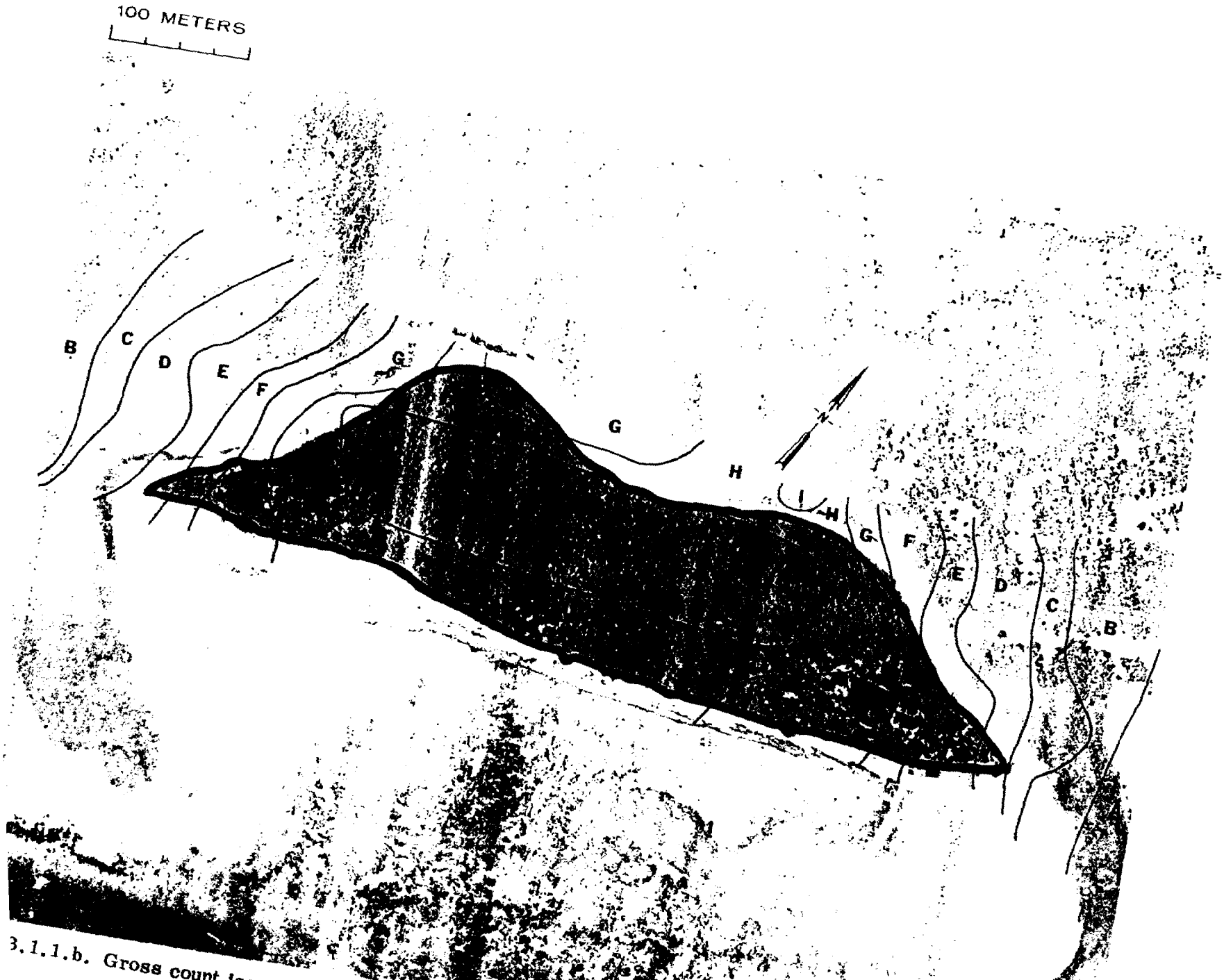

3.1.1.b. Gross count

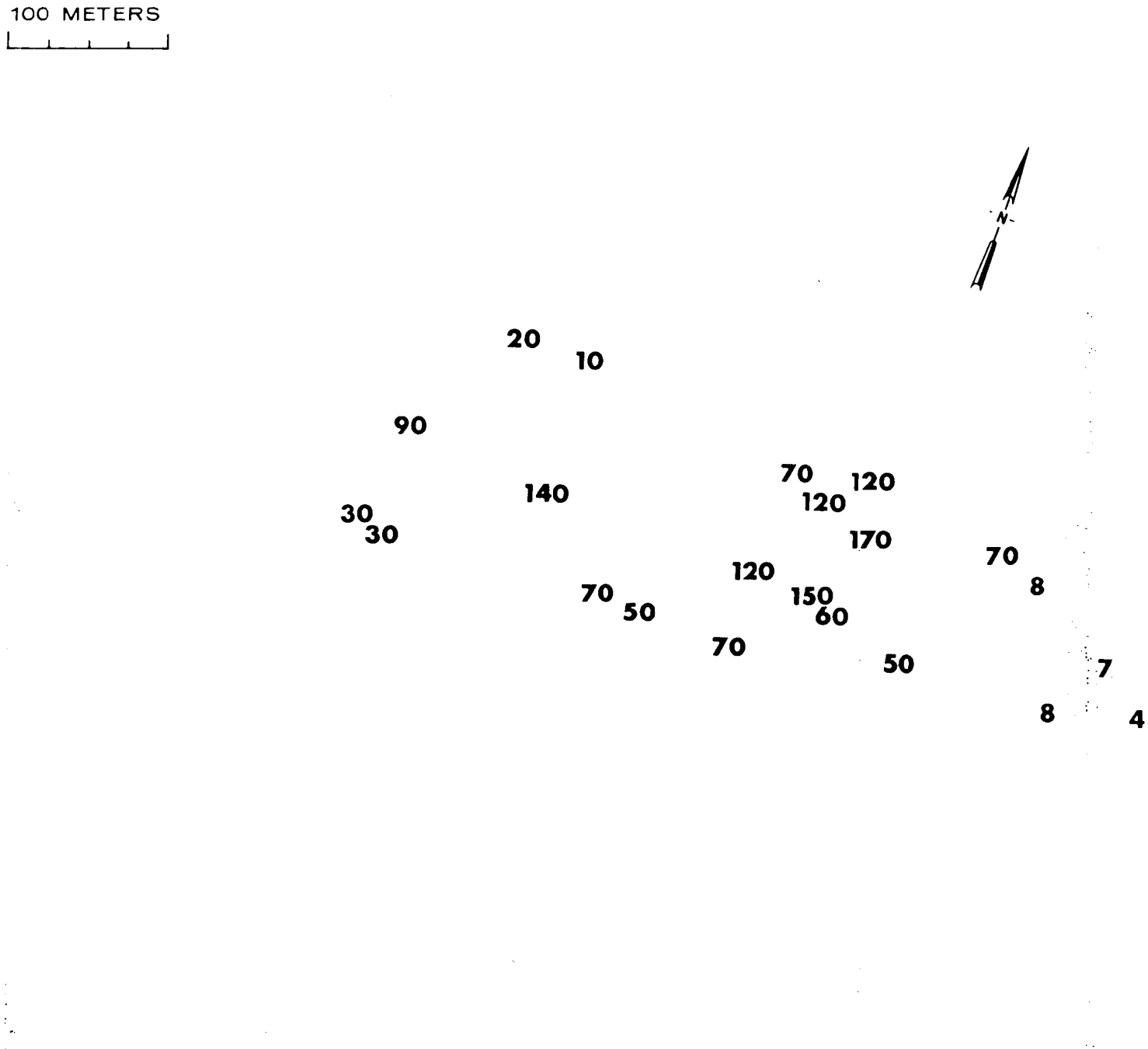

Fig. B.1.1.d. The gamma background exposure rate (μR/hr) at 1 m above the ground, measured with a portable NaI scintillation counter.

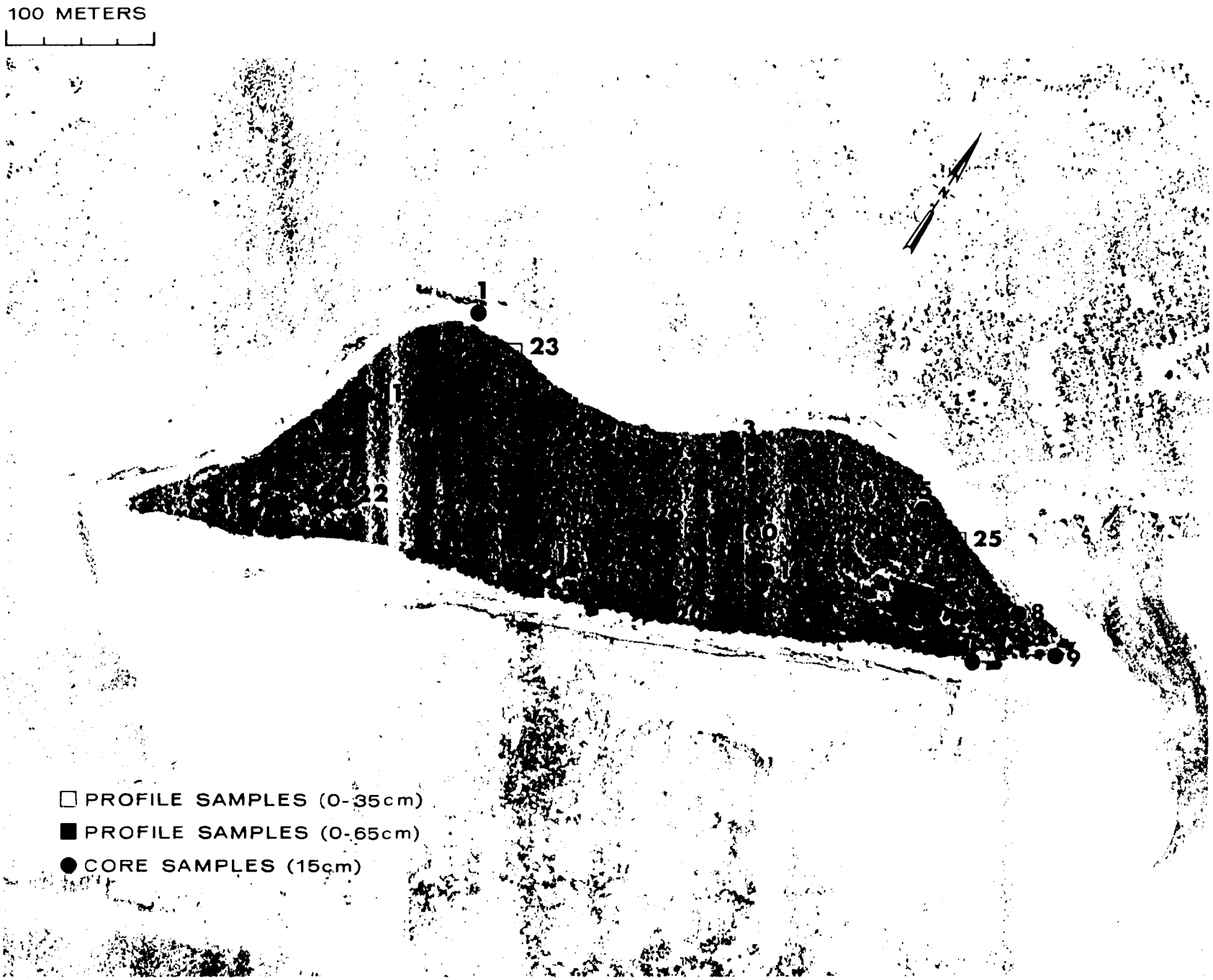

Fig. B.1.1.f. Soil-sample locations.

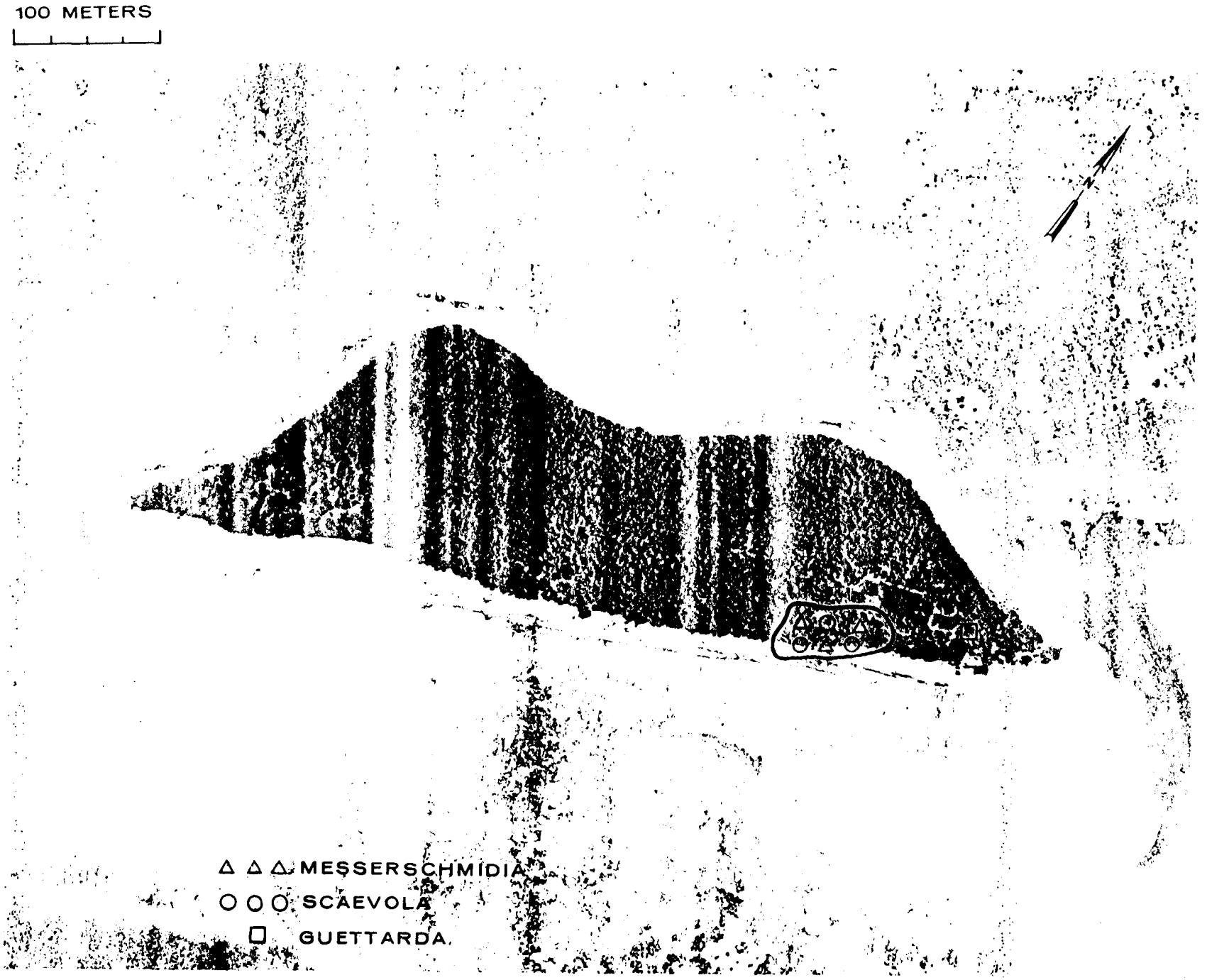

Fig. B.1.1.g. Vegetation sample locations.

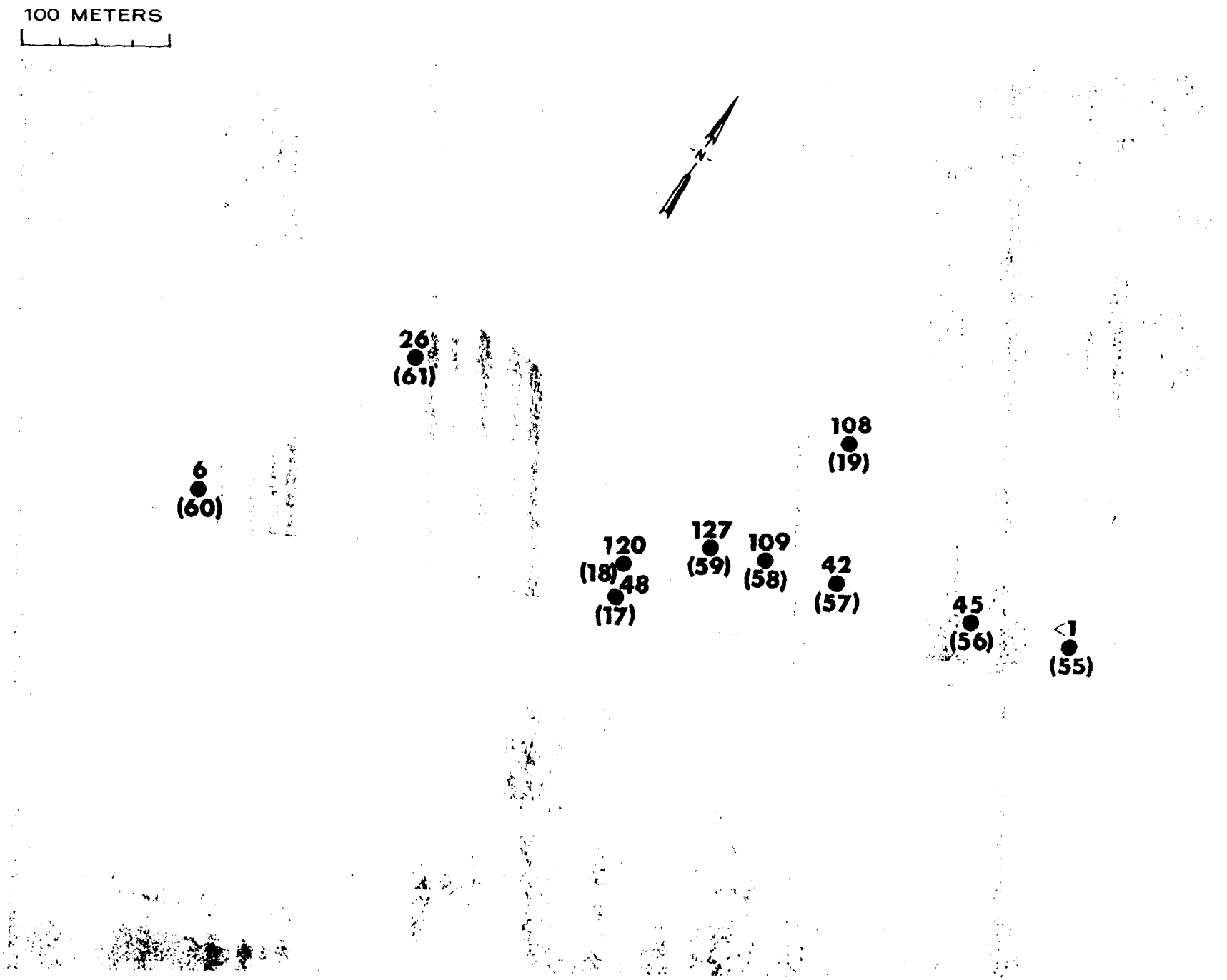

Fig. B.1.1.h. The gamma-ray exposure rates (μR/hr) measured 1 m above the ground by the LiF thermoluminescent dosimeters (TLD). The numbers shown in parentheses denote the location identification numbers.

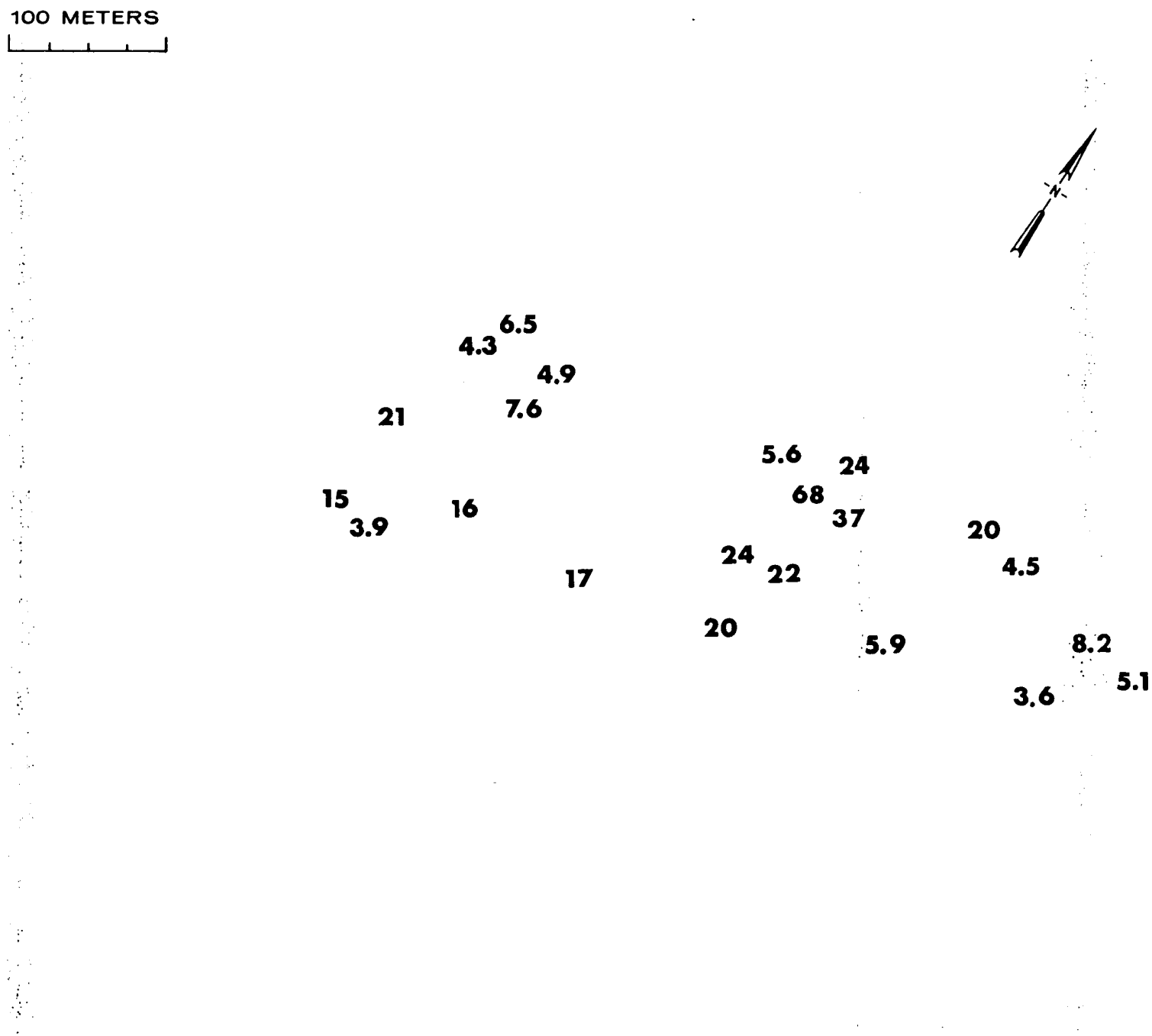

Fig. B.1.1.i. The average ^{239}Pu activities (pCi/g) in soil samples collected to a depth of 15 cm.

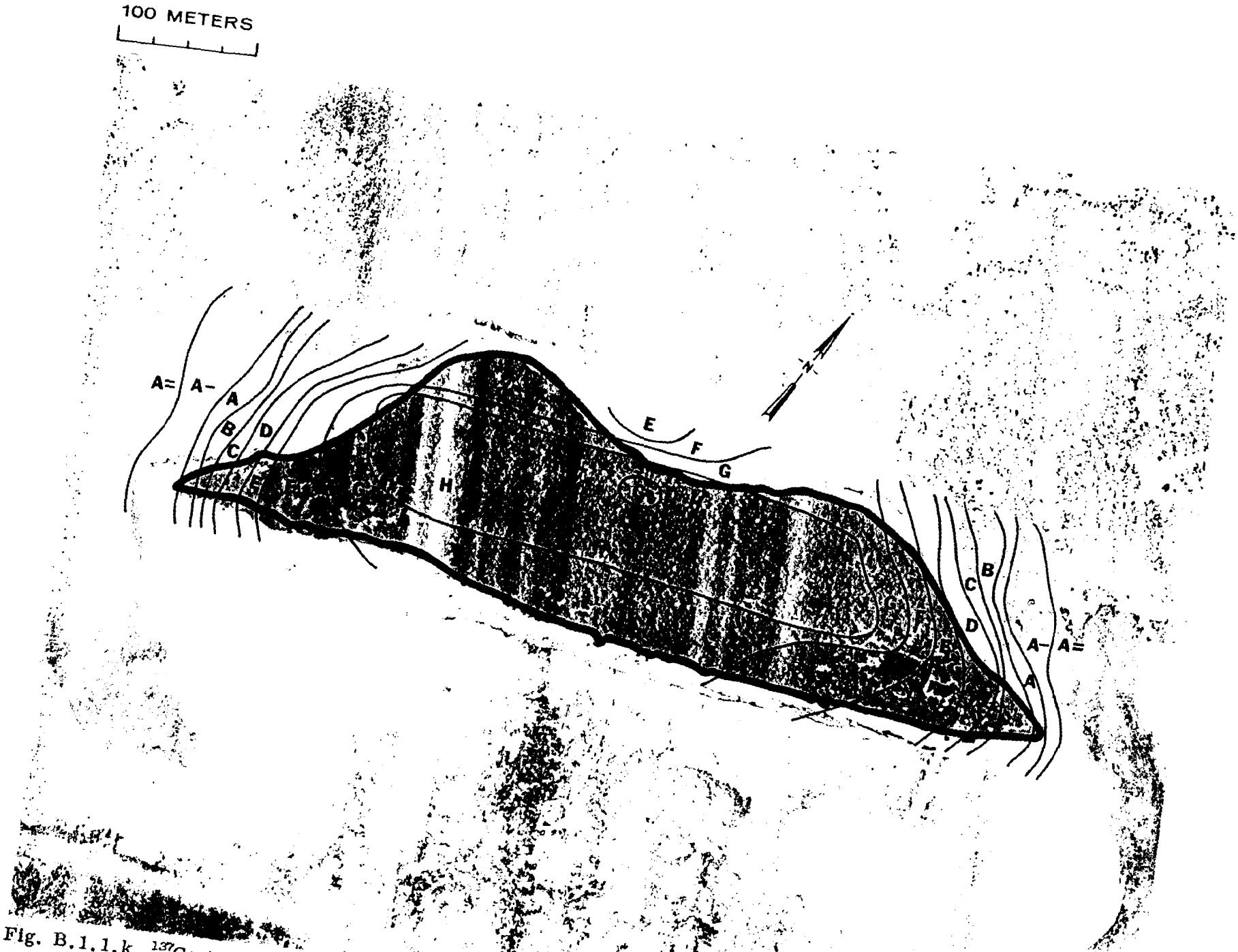

Fig. B.1.1.k. ^{137}Cs isoexposure and isoconcentration contours. (Refer to alph

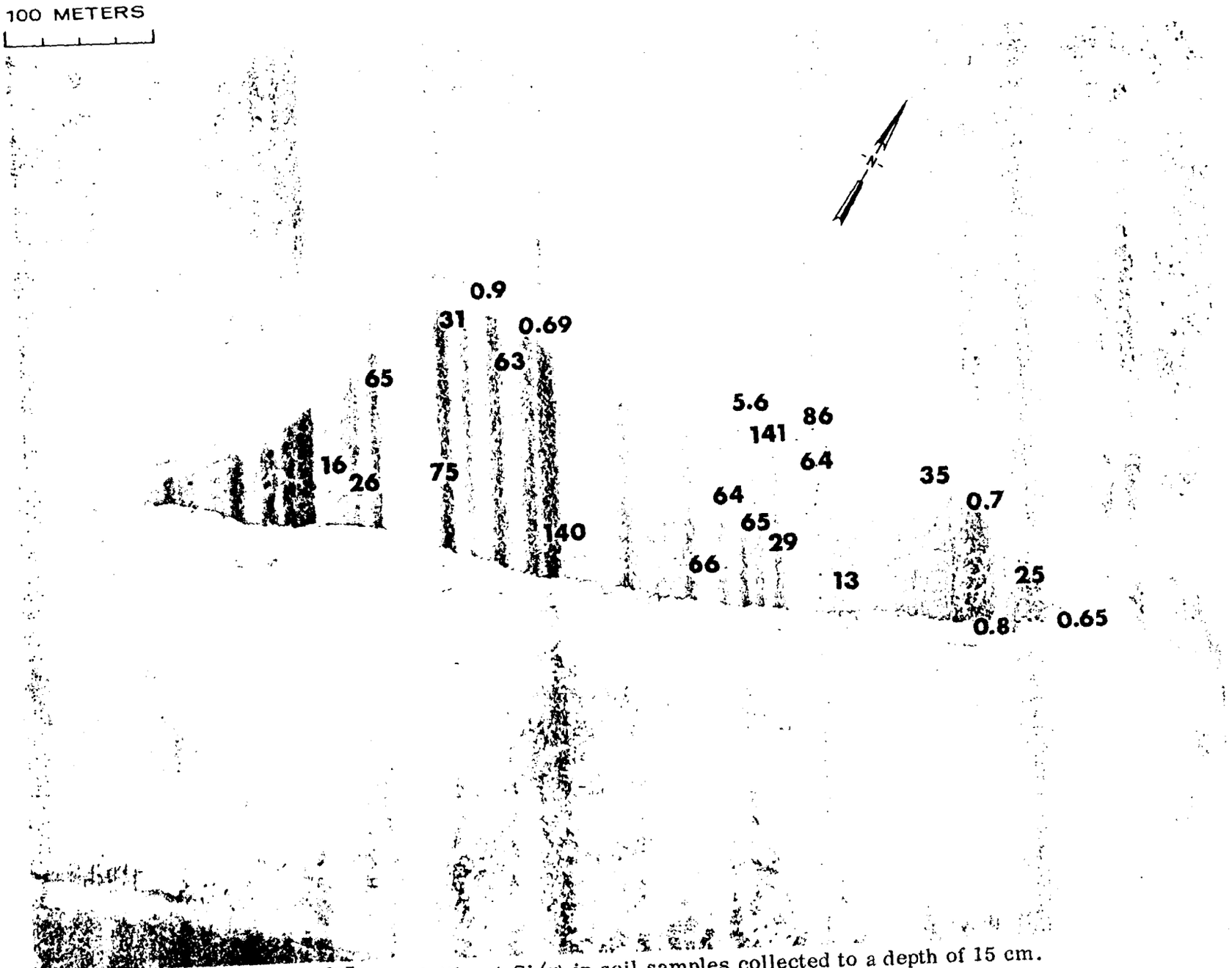

Fig. B.1.1.1. The average ^{137}Cs activities (pCi/g) in soil samples collected to a depth of 15 cm.

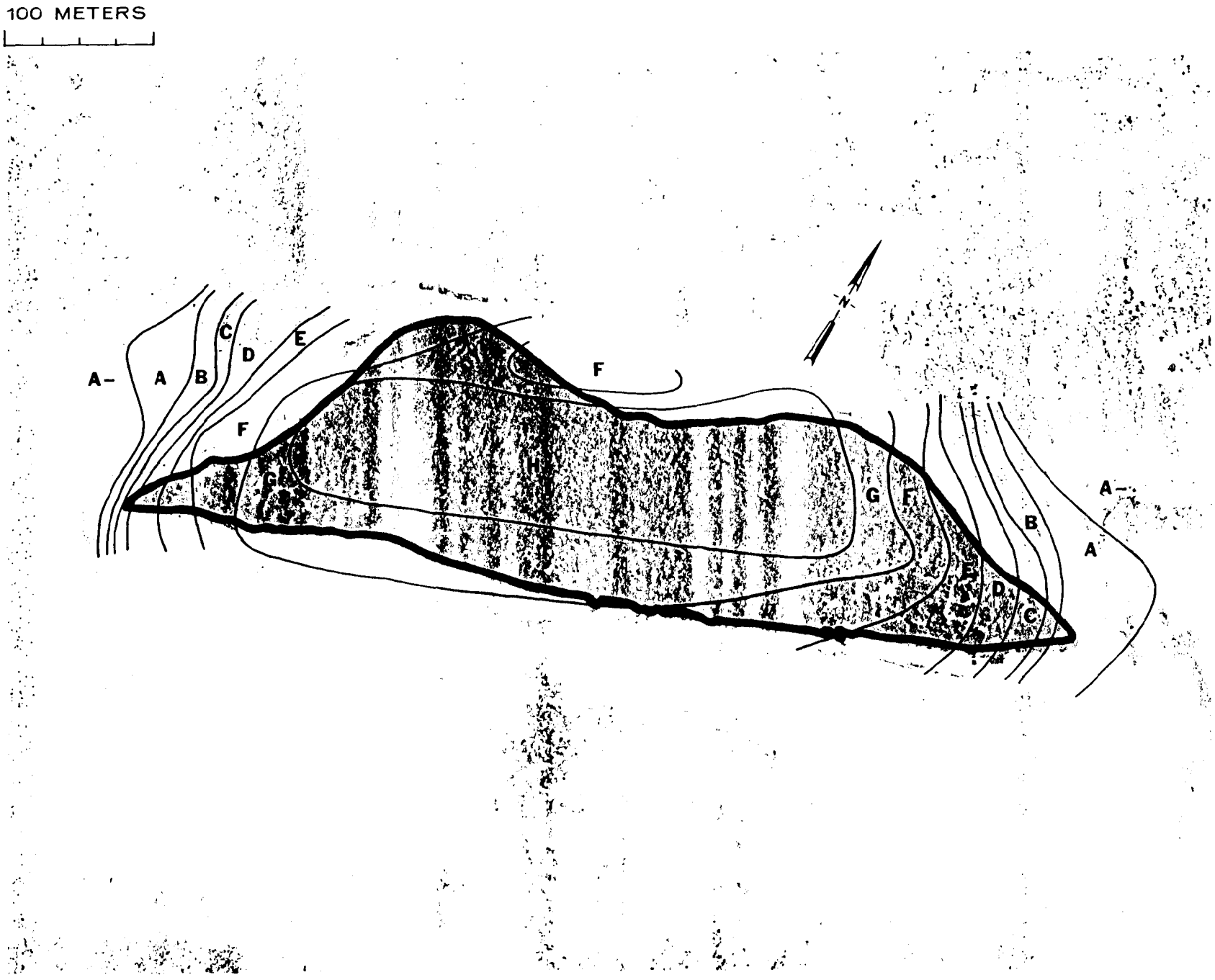

Fig. B.1.1.m. ^{60}Co isoexposure and isoconcentration contours. (Refer to alphabetic symbol key in this appendix.)

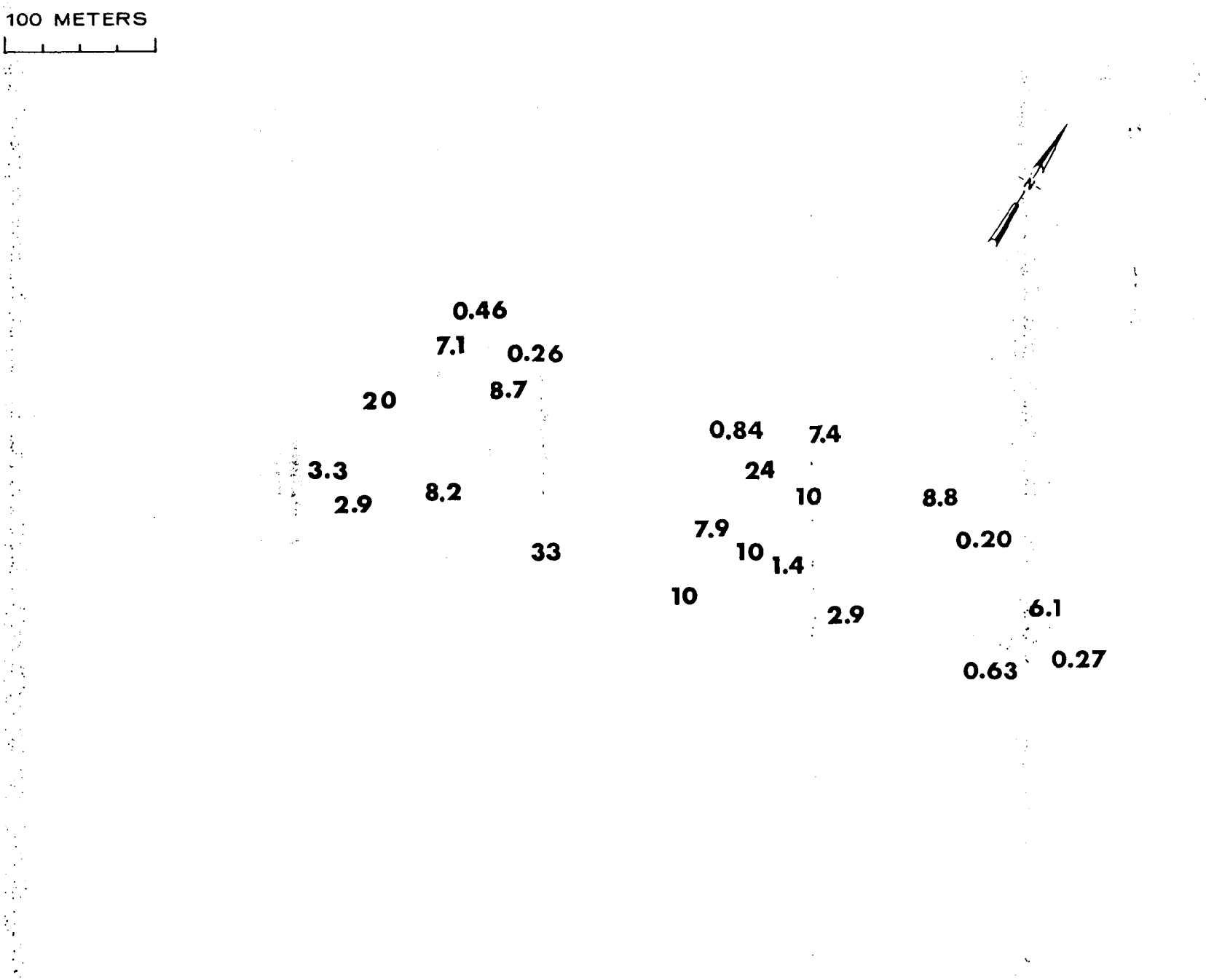

Fig. B.1.1.n. The average ^{60}Co activities (pCi/g) in soil samples collected to a depth of 15 cm.

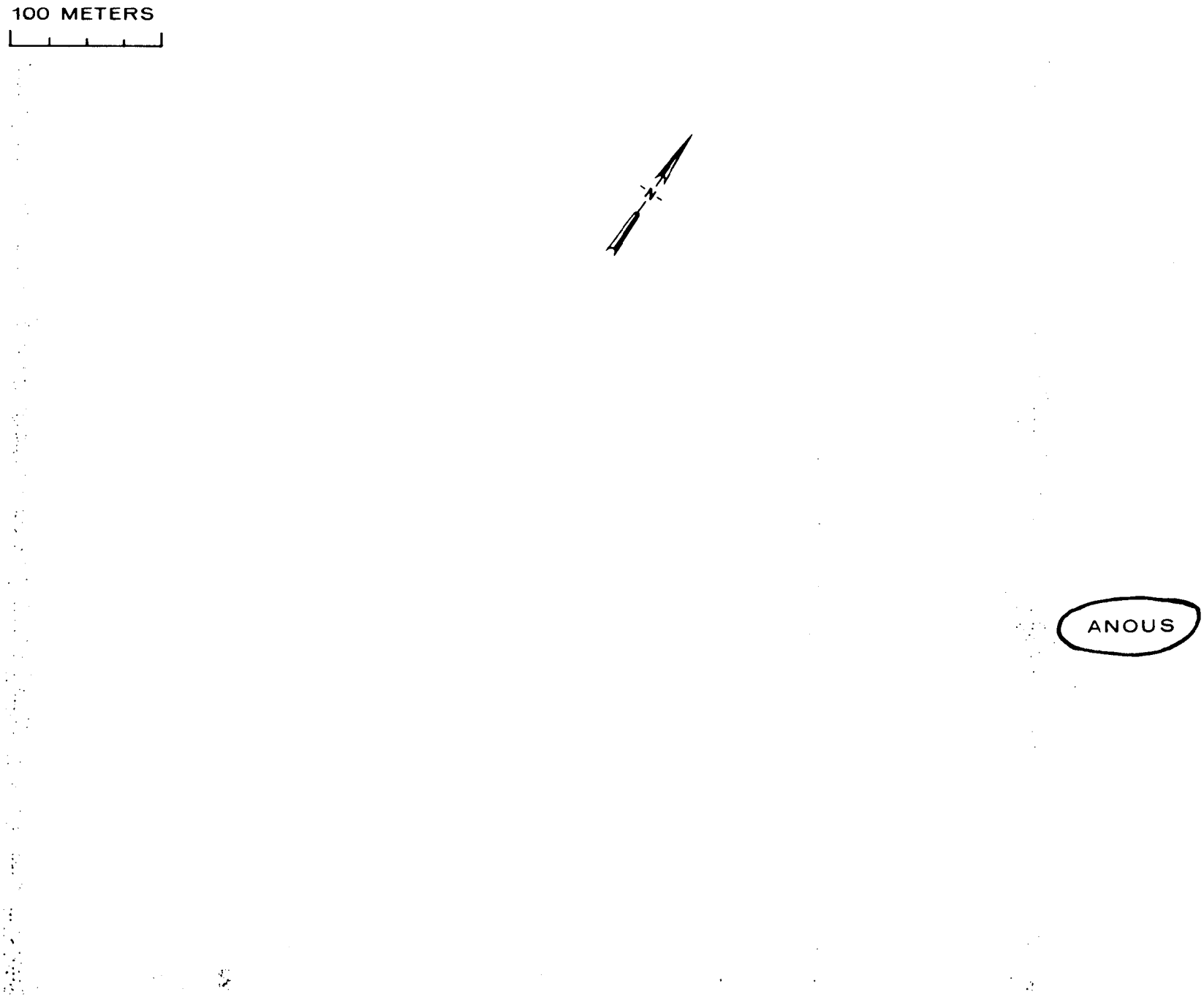

Fig. B.1.1.o. Terrestrial animal sample locations.

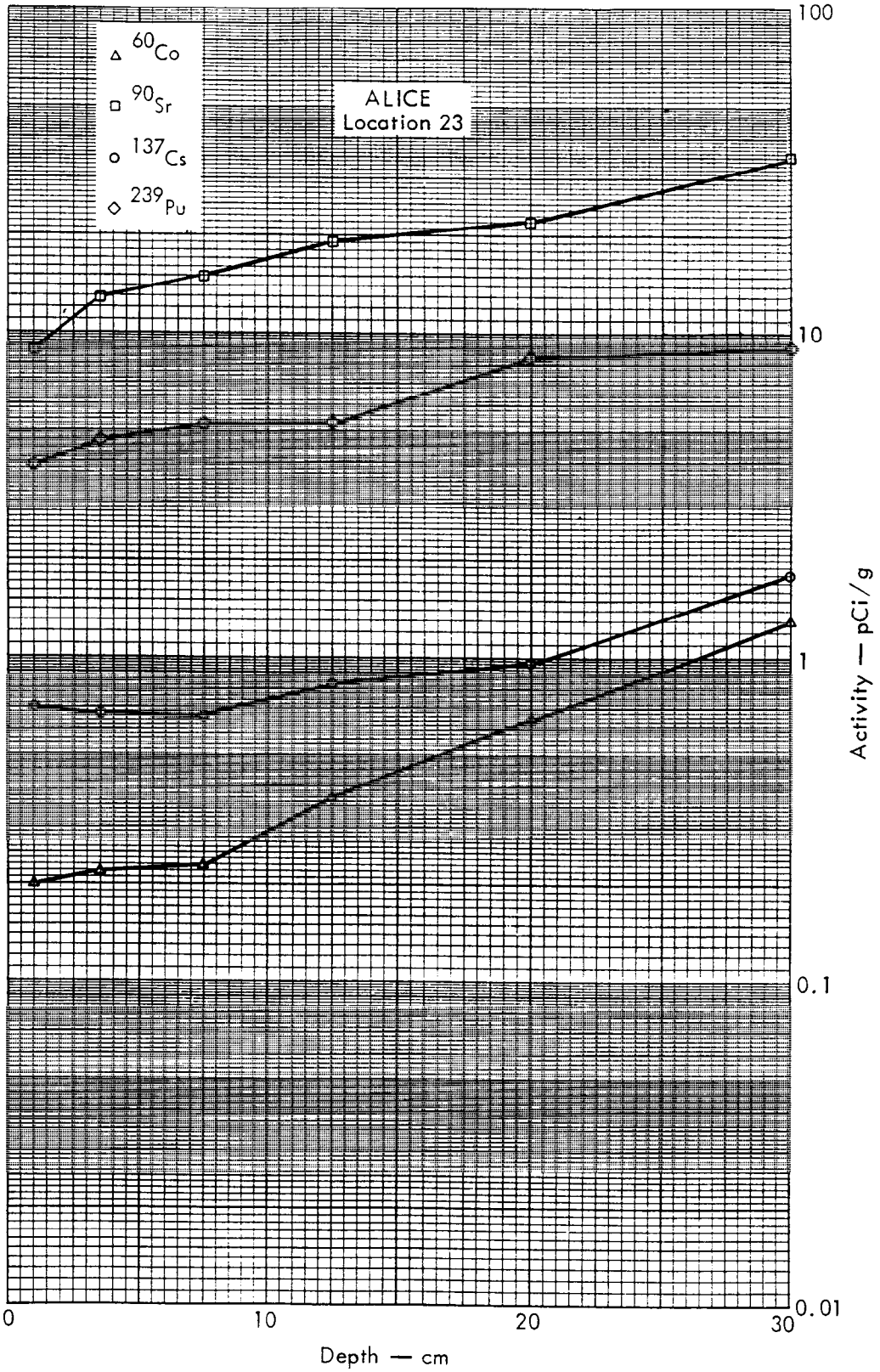

Fig. B. 1. 2a. Activities of selected radionuclides as a function of soil depth.

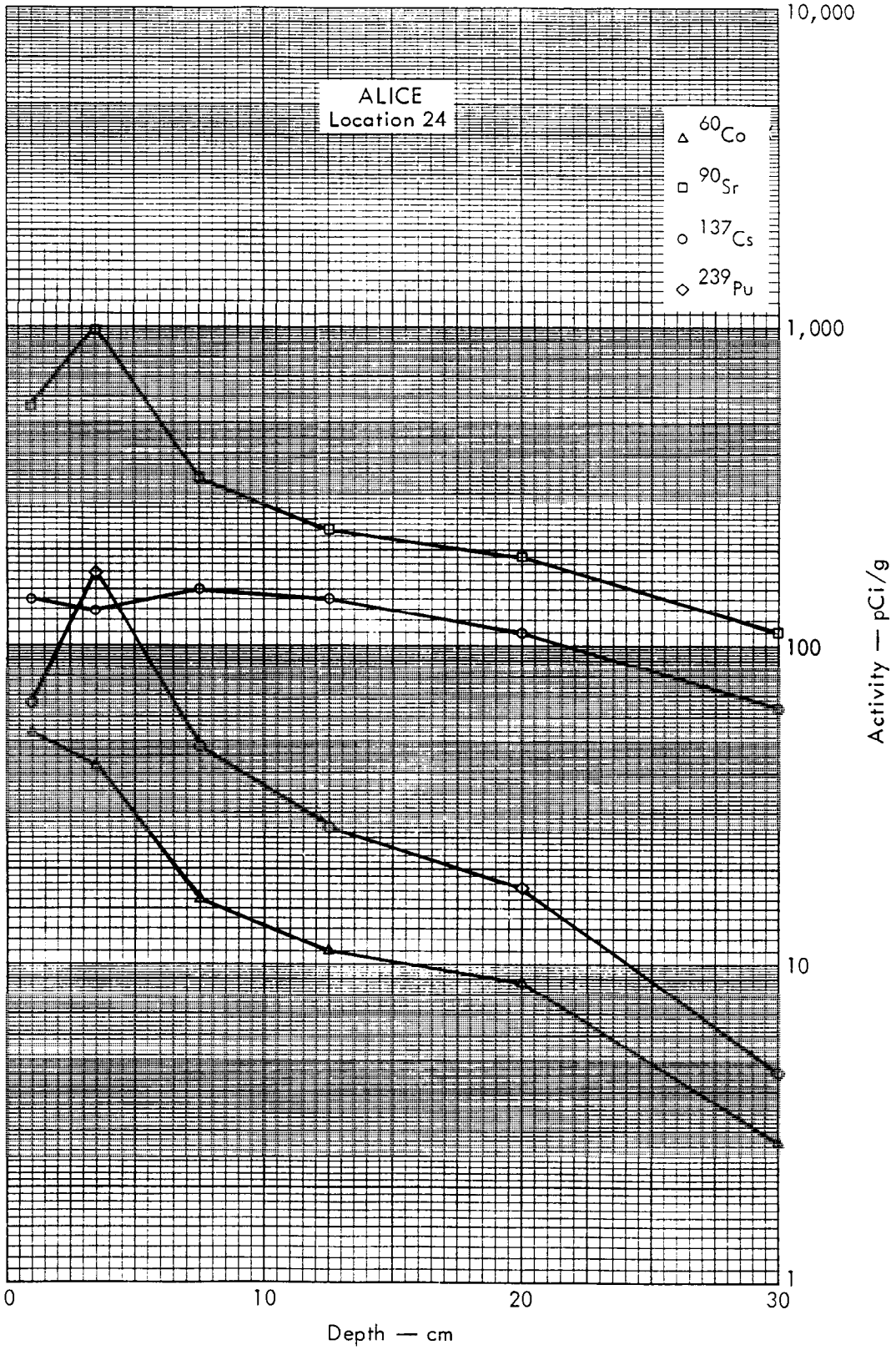

Fig. B. 1. 2b. Activities of selected radionuclides as a function of soil depth.

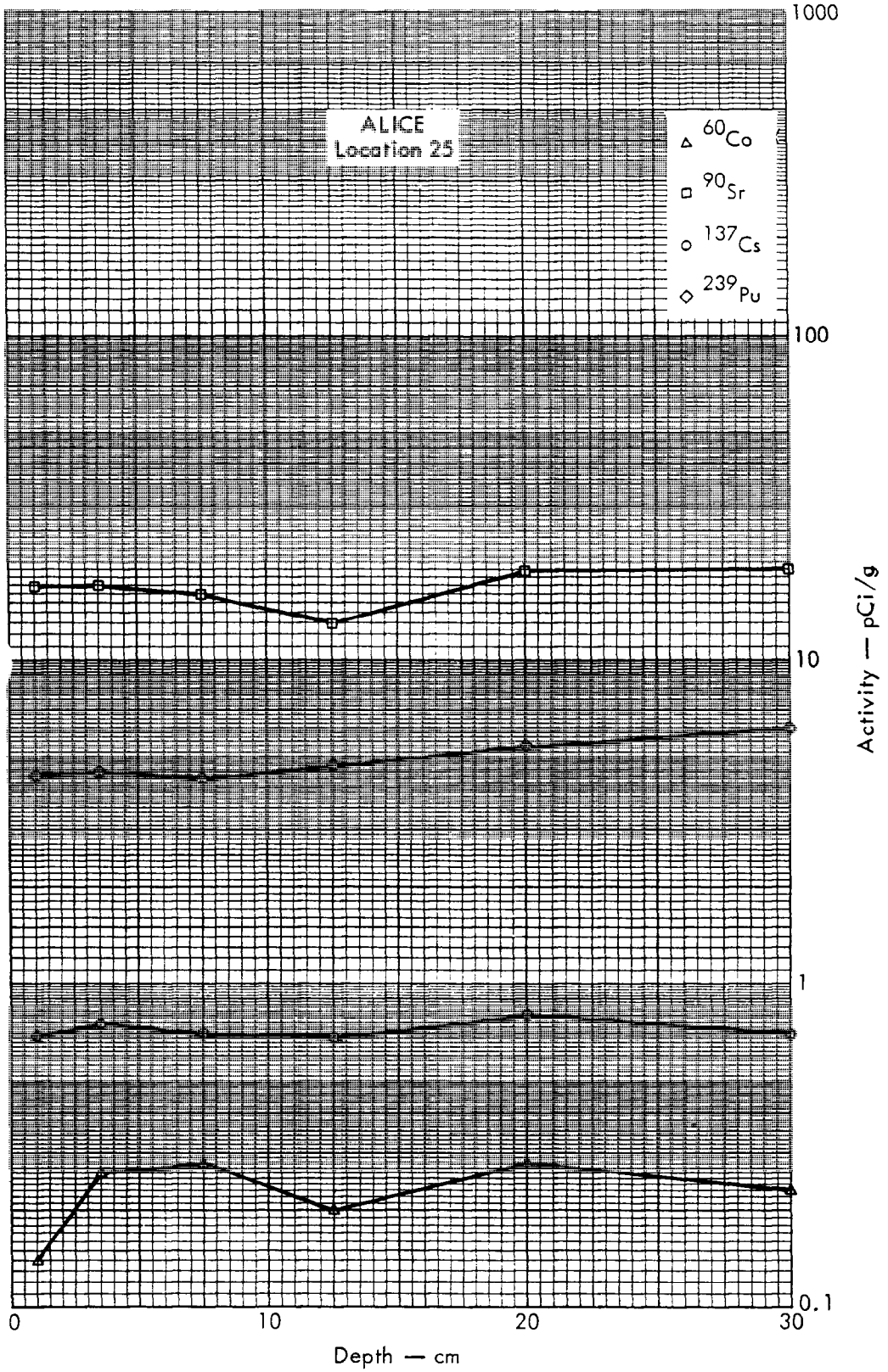

Fig. B.1.2c. Activities of selected radionuclides as a function of soil depth.

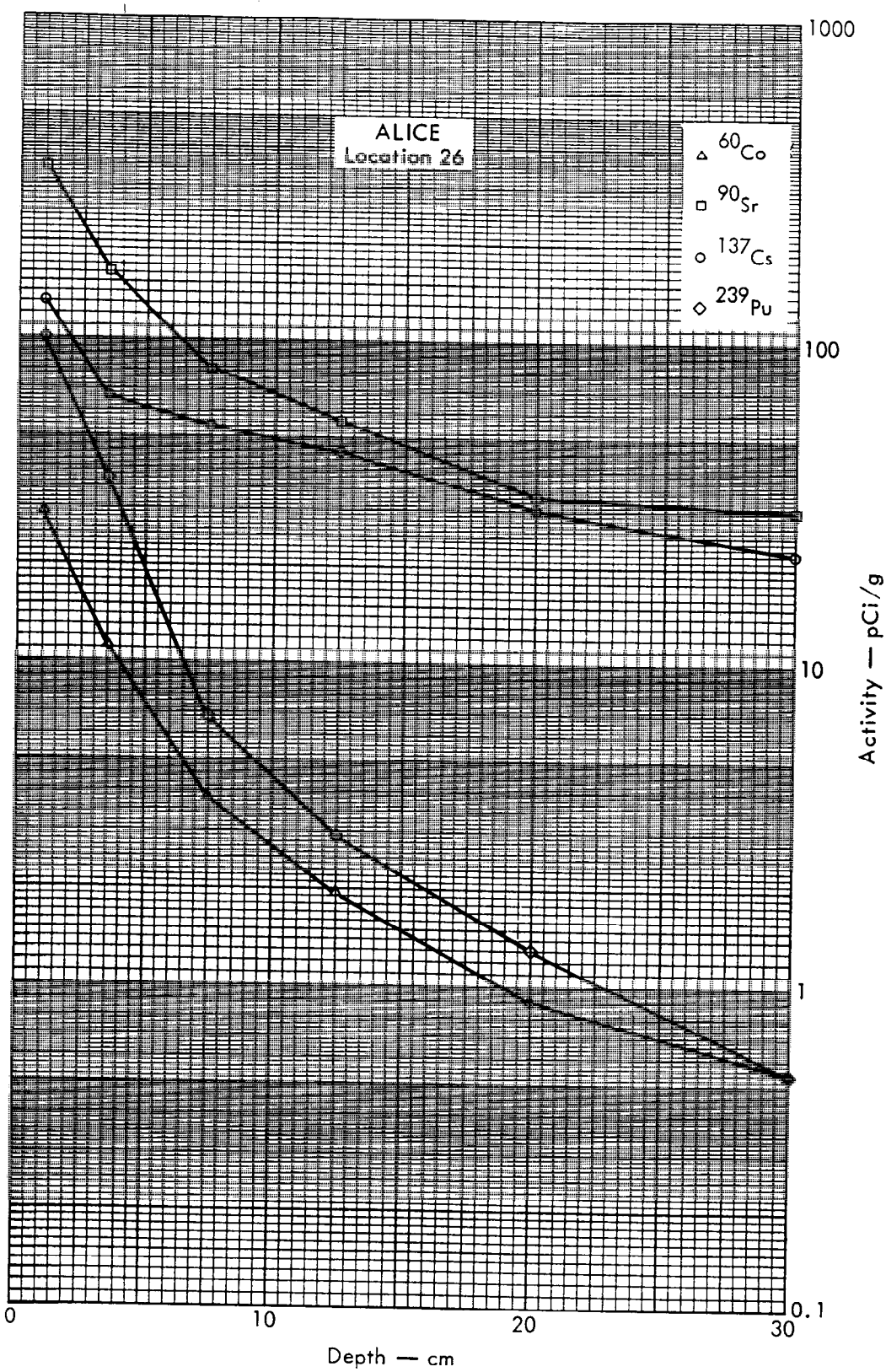

Fig. B.1.2d. Activities of selected radionuclides as a function of soil depth.

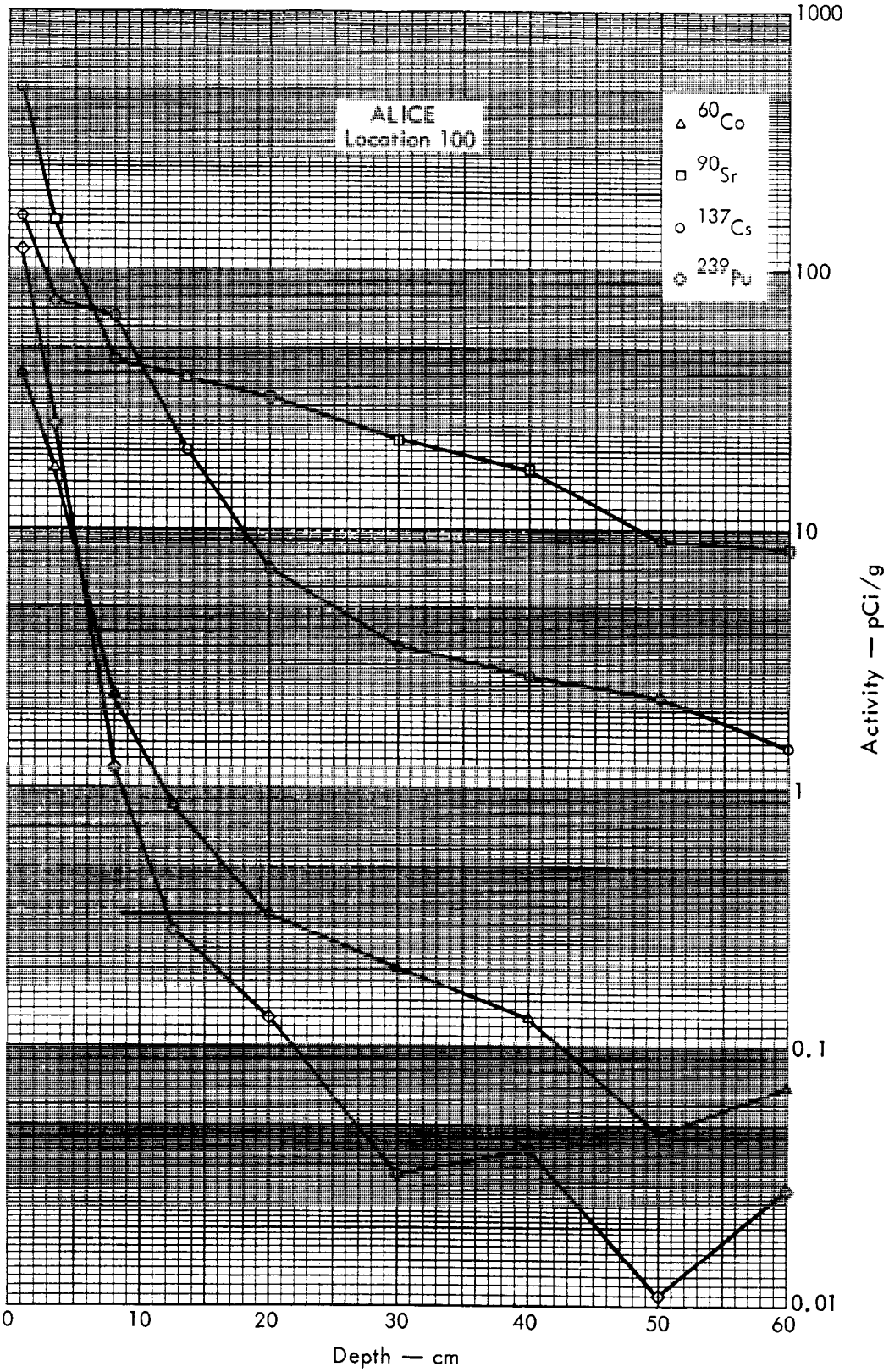

Fig. B. 1. 2e. Activities of selected radionuclides as a function of soil depth.

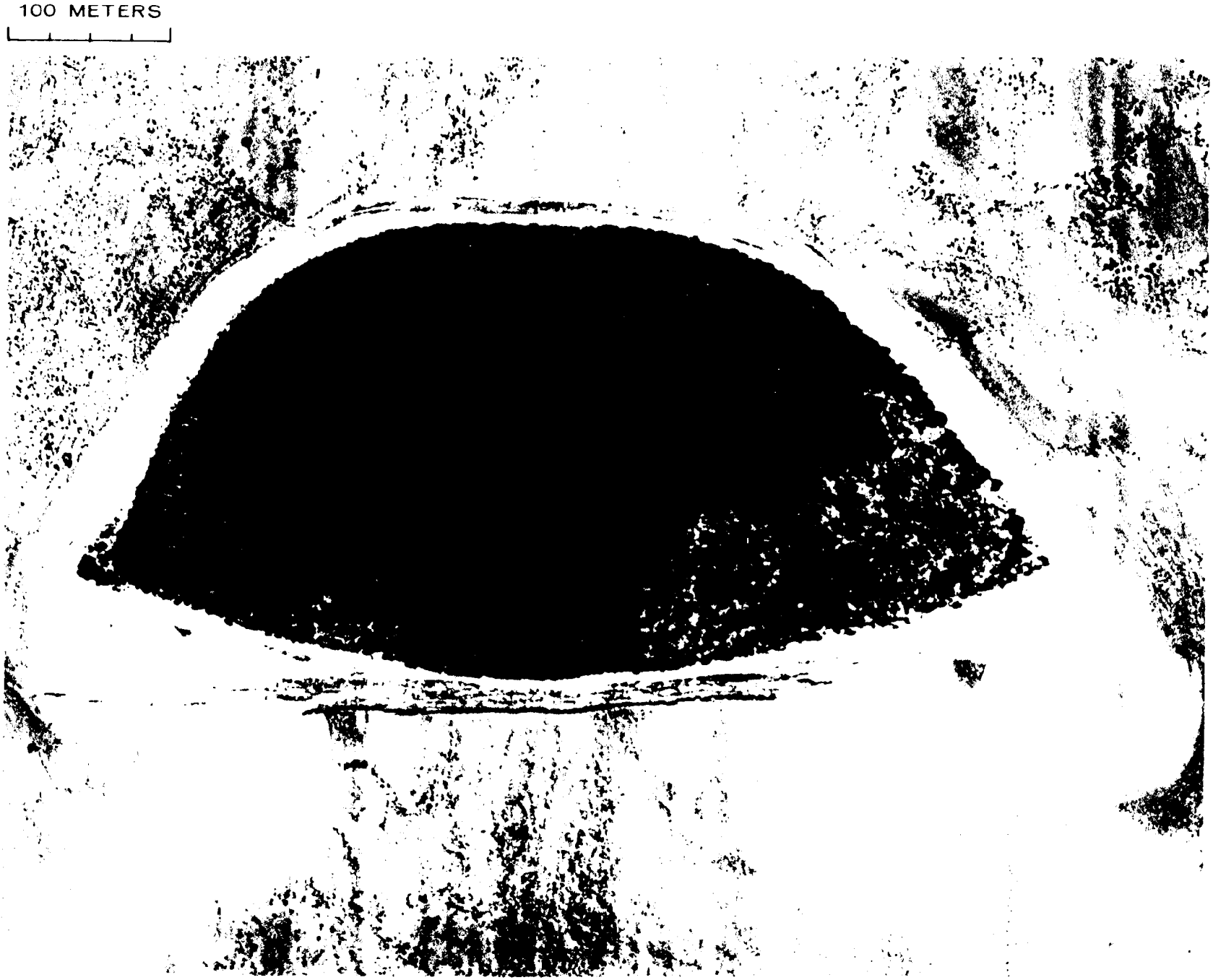

Fig. B.2.1.a.

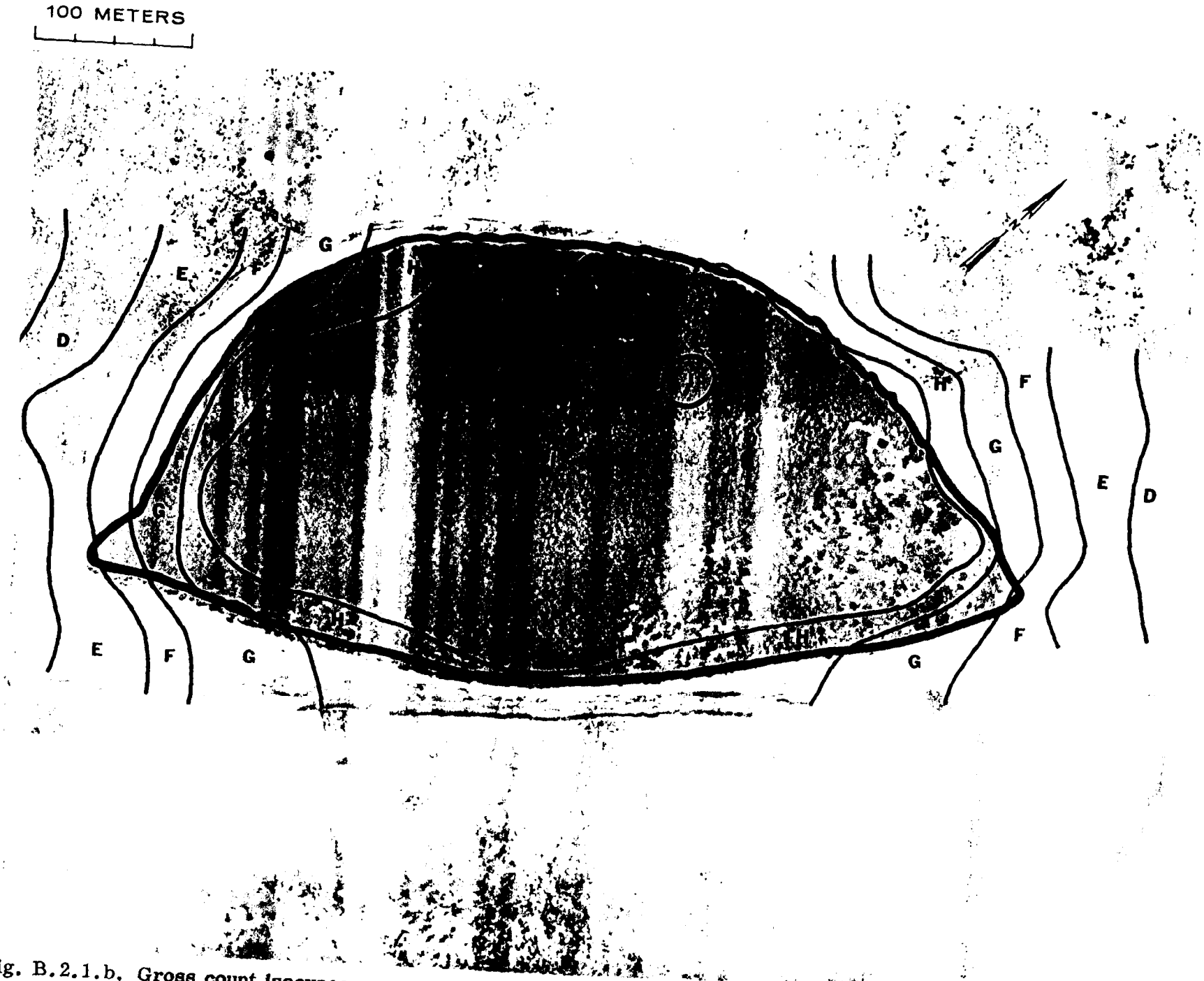

Fig. B.2.1.b. Gross count isoexposure contours. (Refer to alphabetic symbol key in this appendix.)

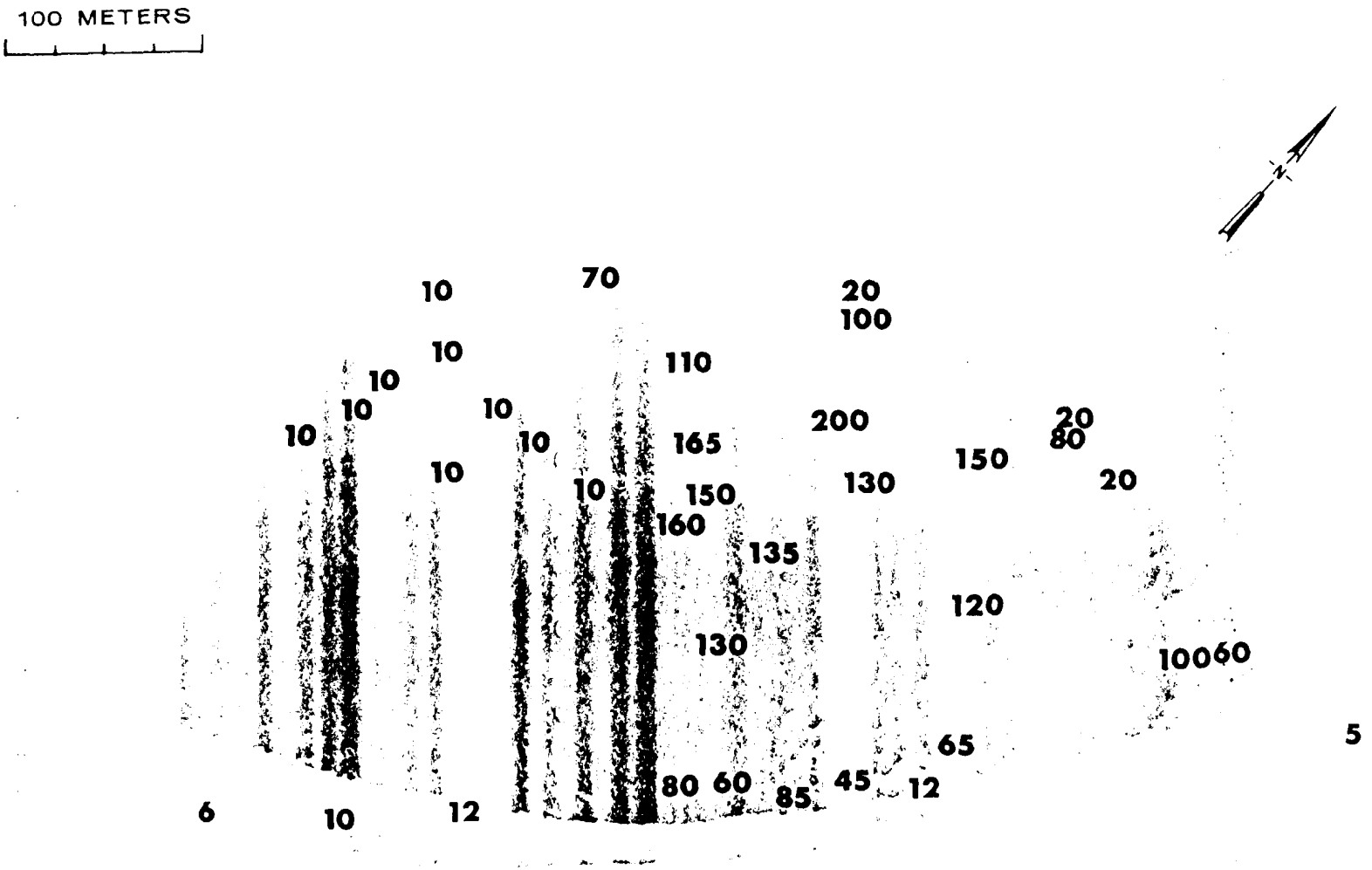

Fig. B.2.1.d. The gamma background exposure rate (μR/hr) at 1 m above the ground, measured with a portable NaI scintillation counter.

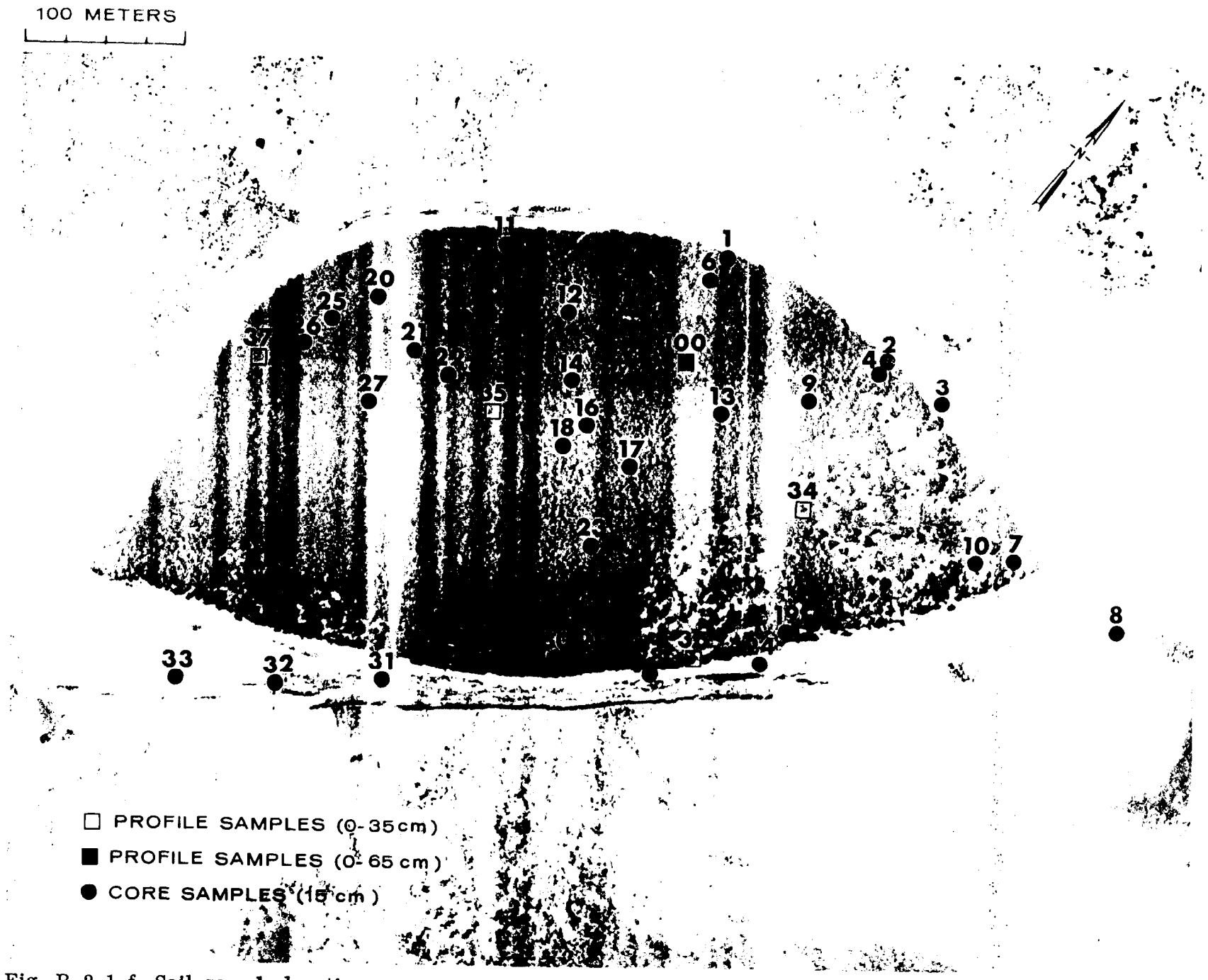

Fig. B.2.1.f. Soil-sample locations.

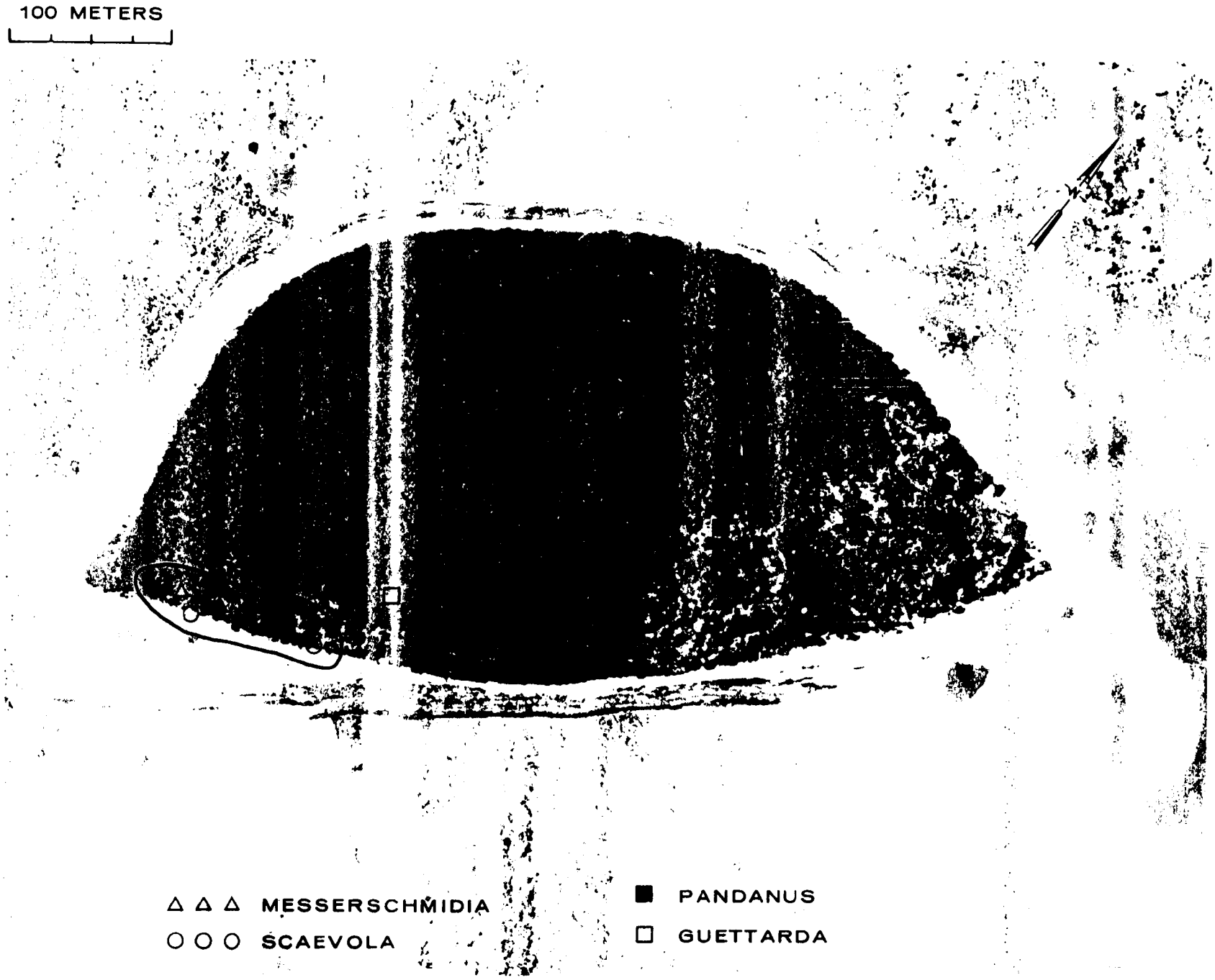

Fig. B.2.1.g. Vegetation sample locations.

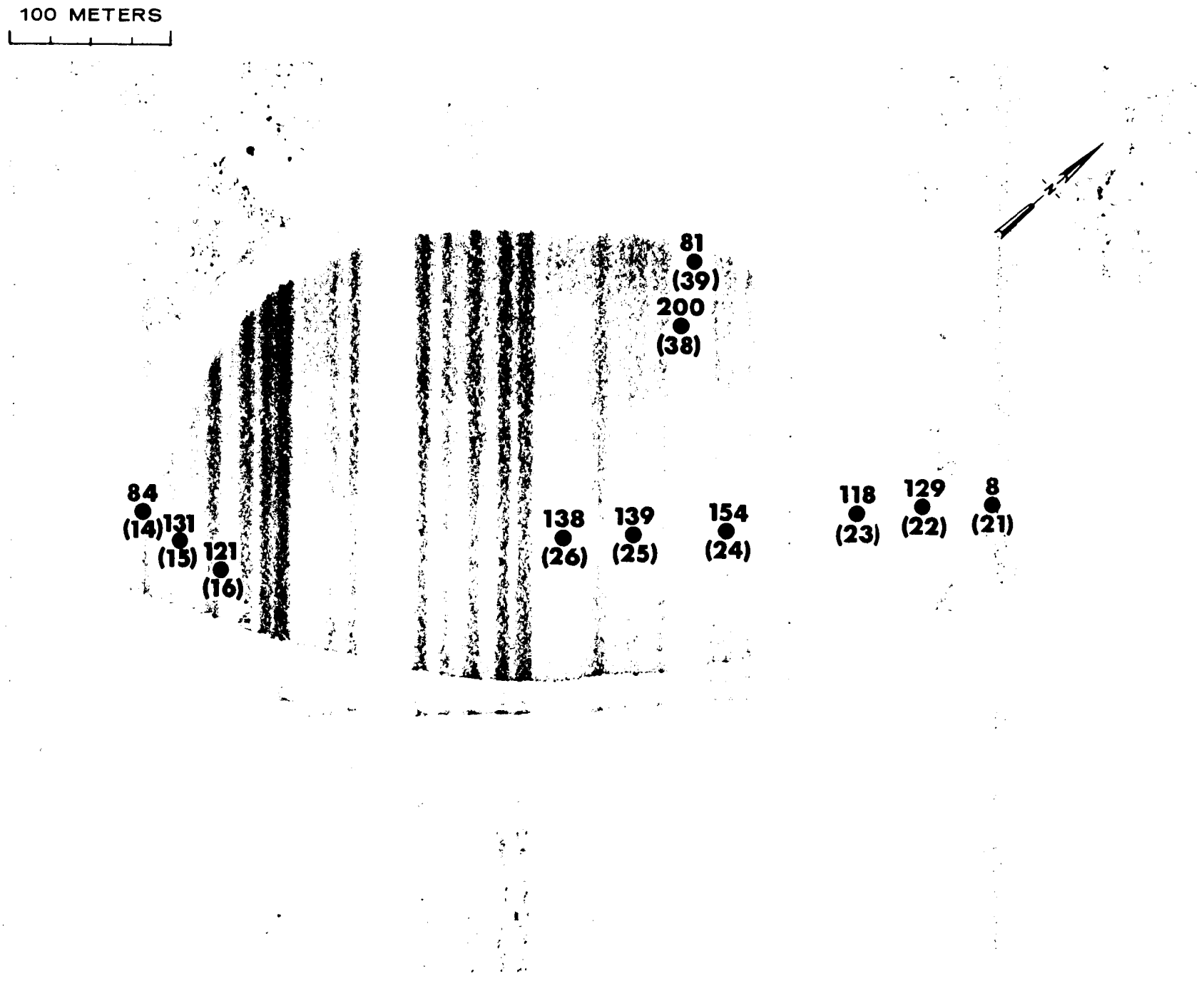

Fig. B.2.1.h. The gamma-ray exposure rates (μR/hr) measured 1 m above the ground by the LiF thermoluminescent dosimeters (TLD). The numbers shown in parentheses denote the location identification numbers.

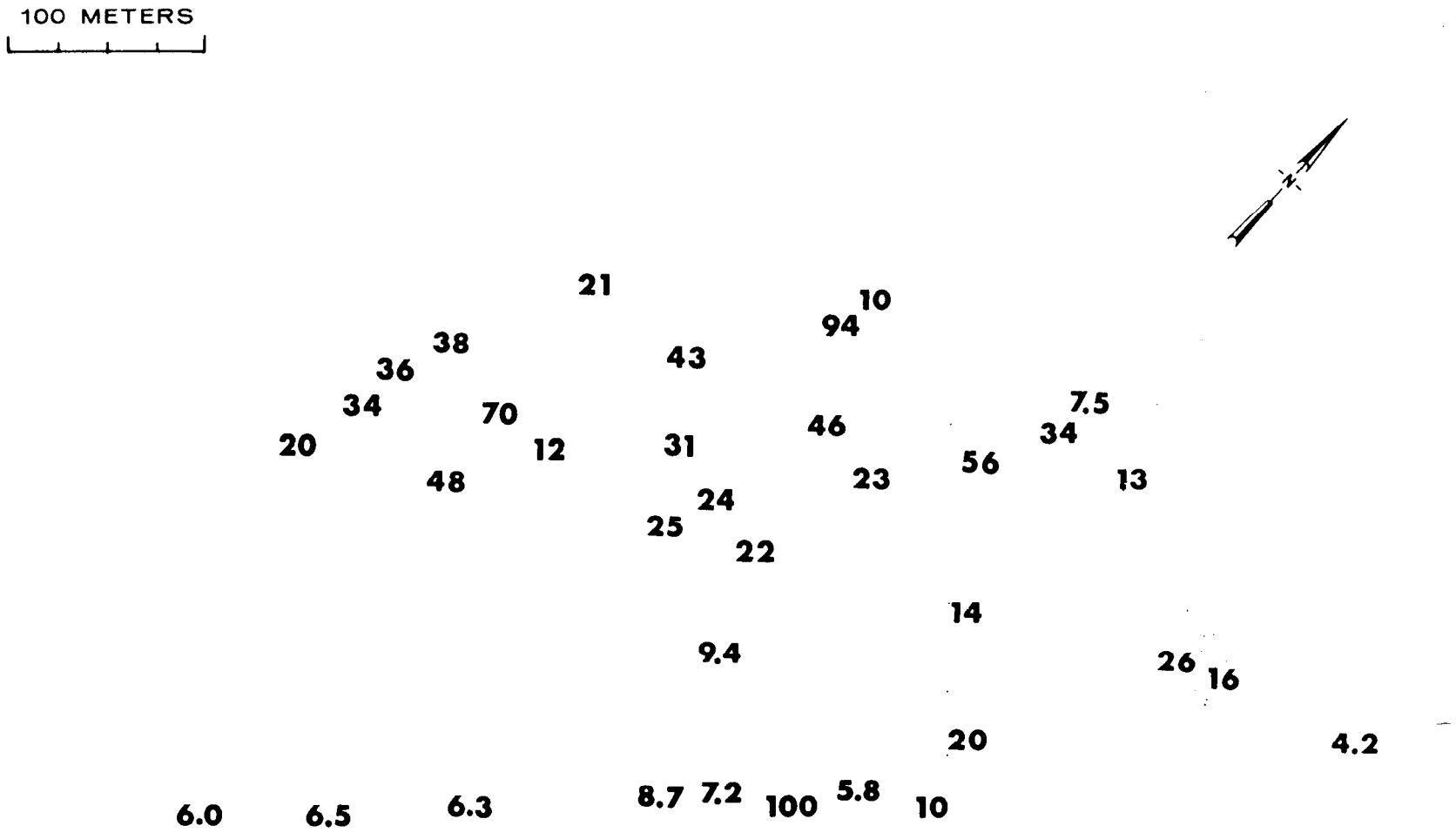

Fig. B.2.1.i. The average ^{239}Pu activities (pCi/g) in soil samples collected to a depth of 15 cm.

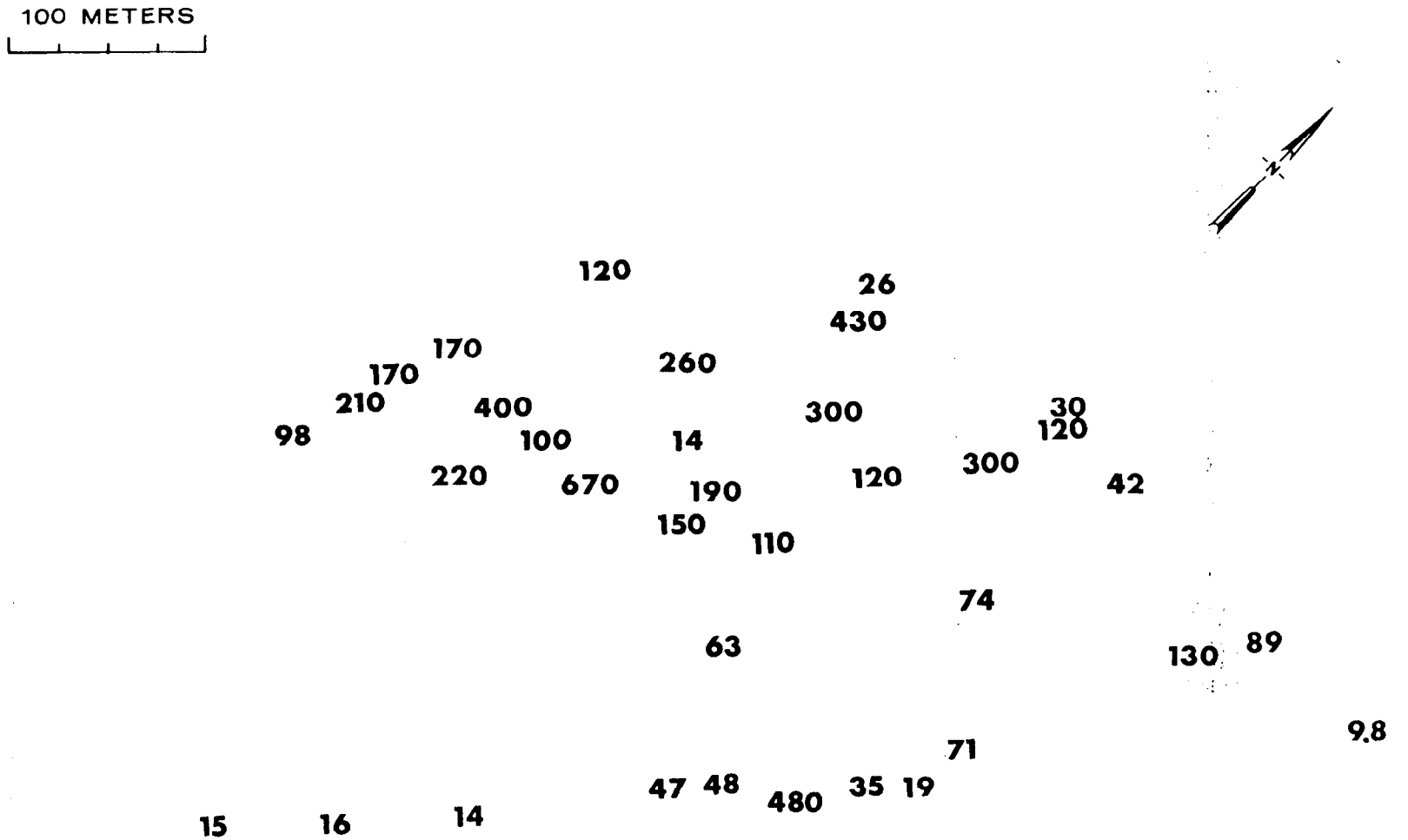

Fig. B.2.1.j. The average ^{90}Sr activities (pCi/g) in soil samples collected to a depth of 15 cm.

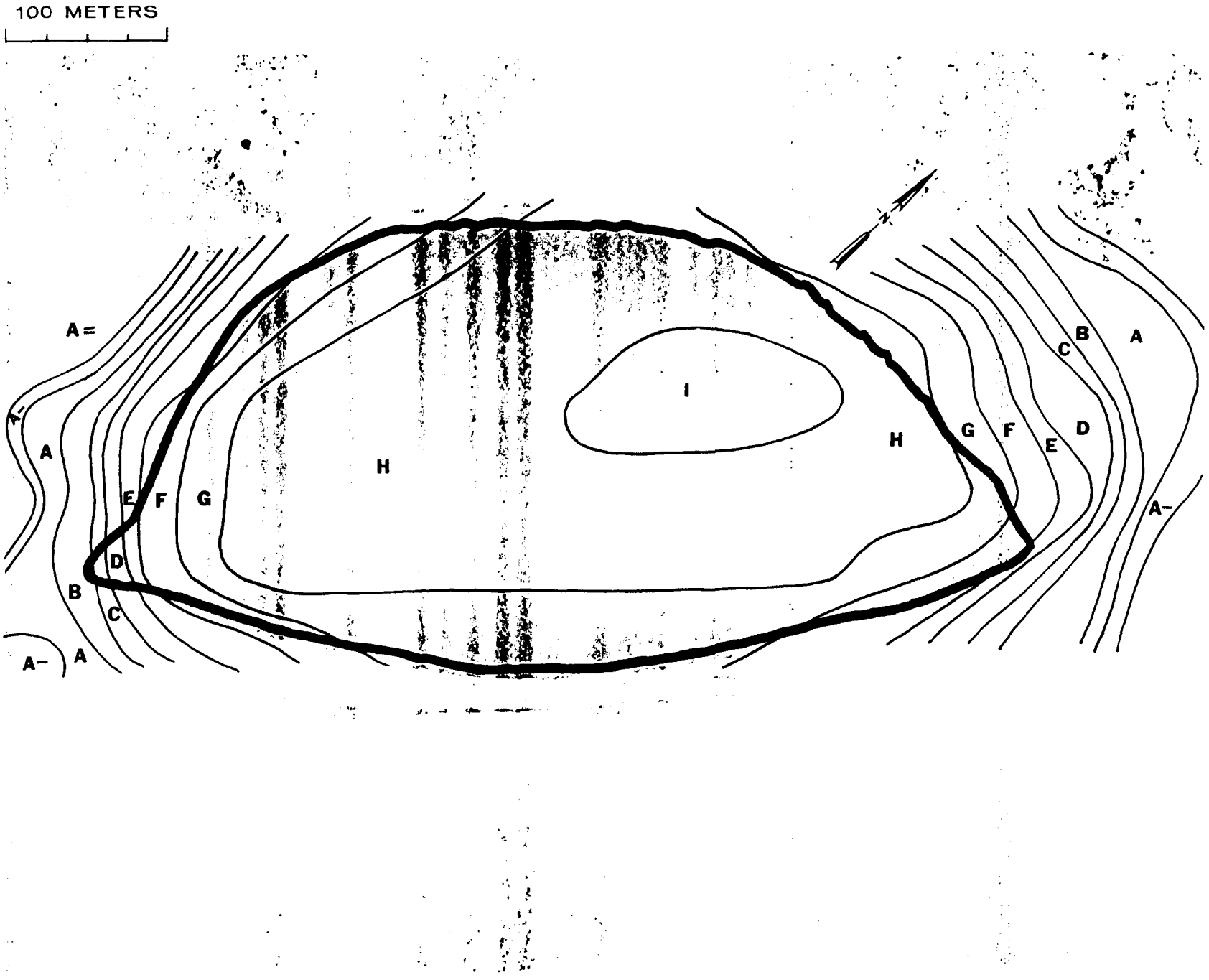

Fig. B.2.1.k. ^{137}Cs isoexposure and isoconcentration contours. (Refer to alphabetic symbol key in this appendix.)

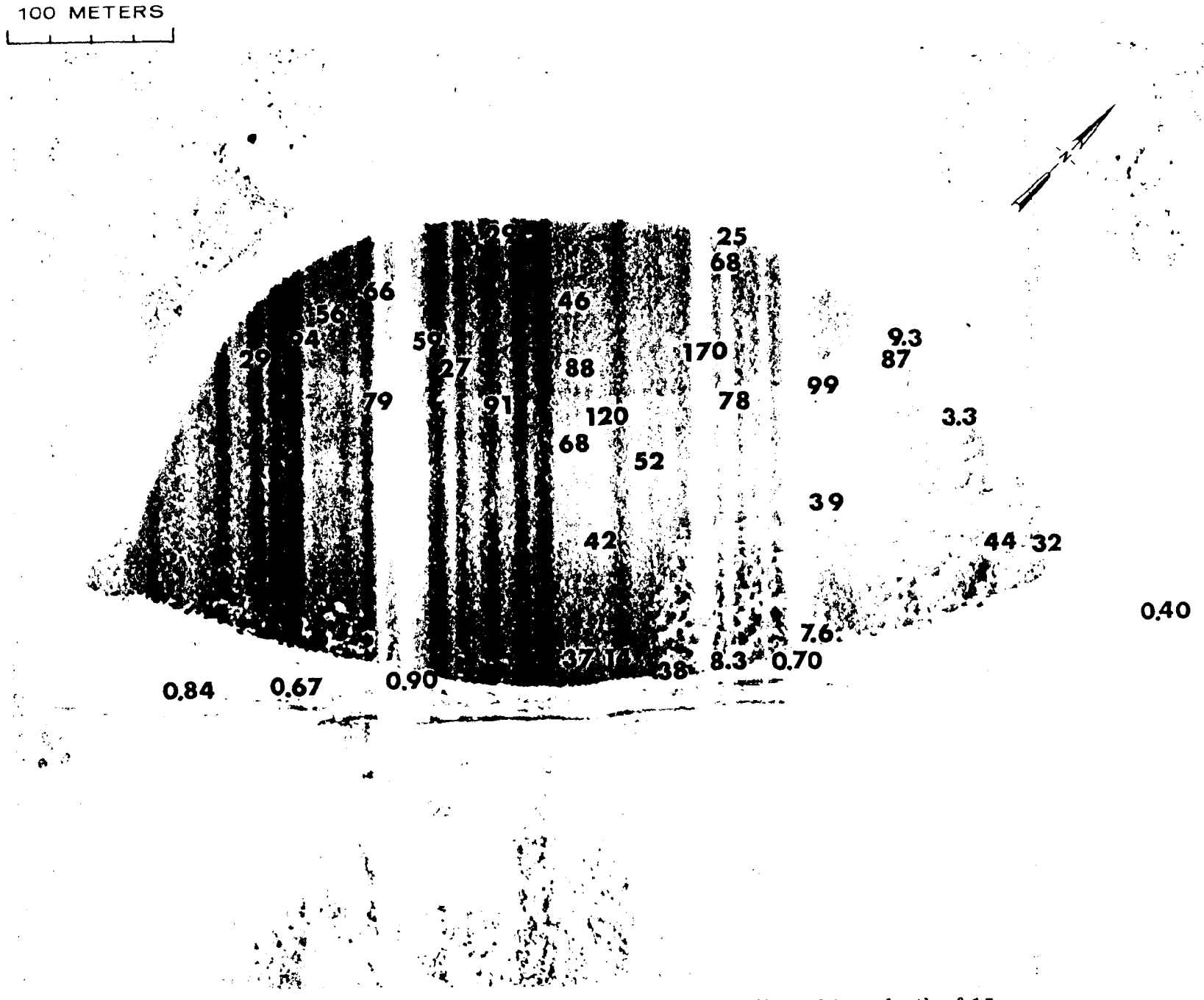

Fig. B.2.1.1. The average ^{137}Cs activities (pCi/g) in soil samples collected to a depth of 15 cm.

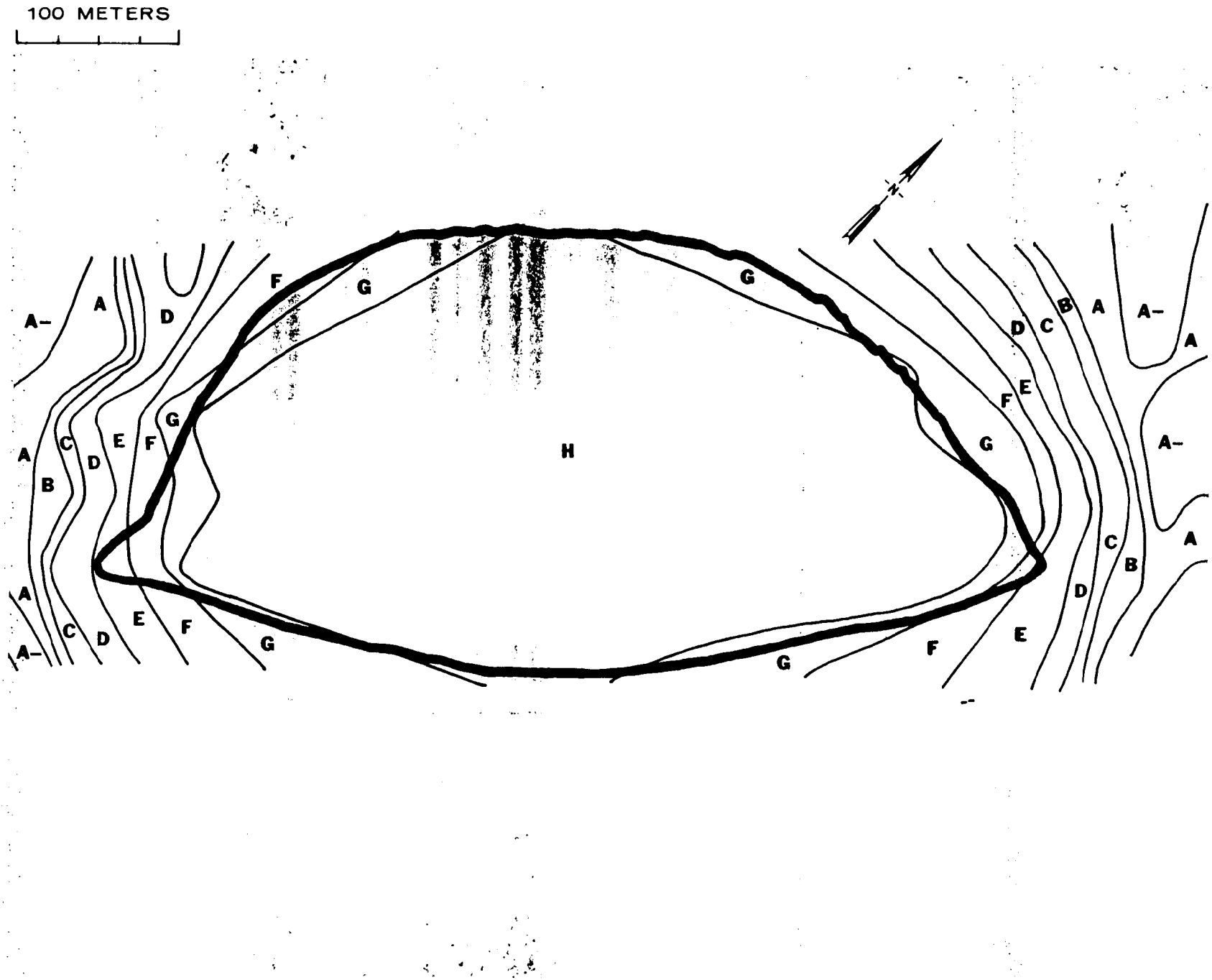

Fig. B.2.1.m. ^{60}Co isoexposure and isoconcentration contours. (Refer to alphabetic symbol key in this appendix.)

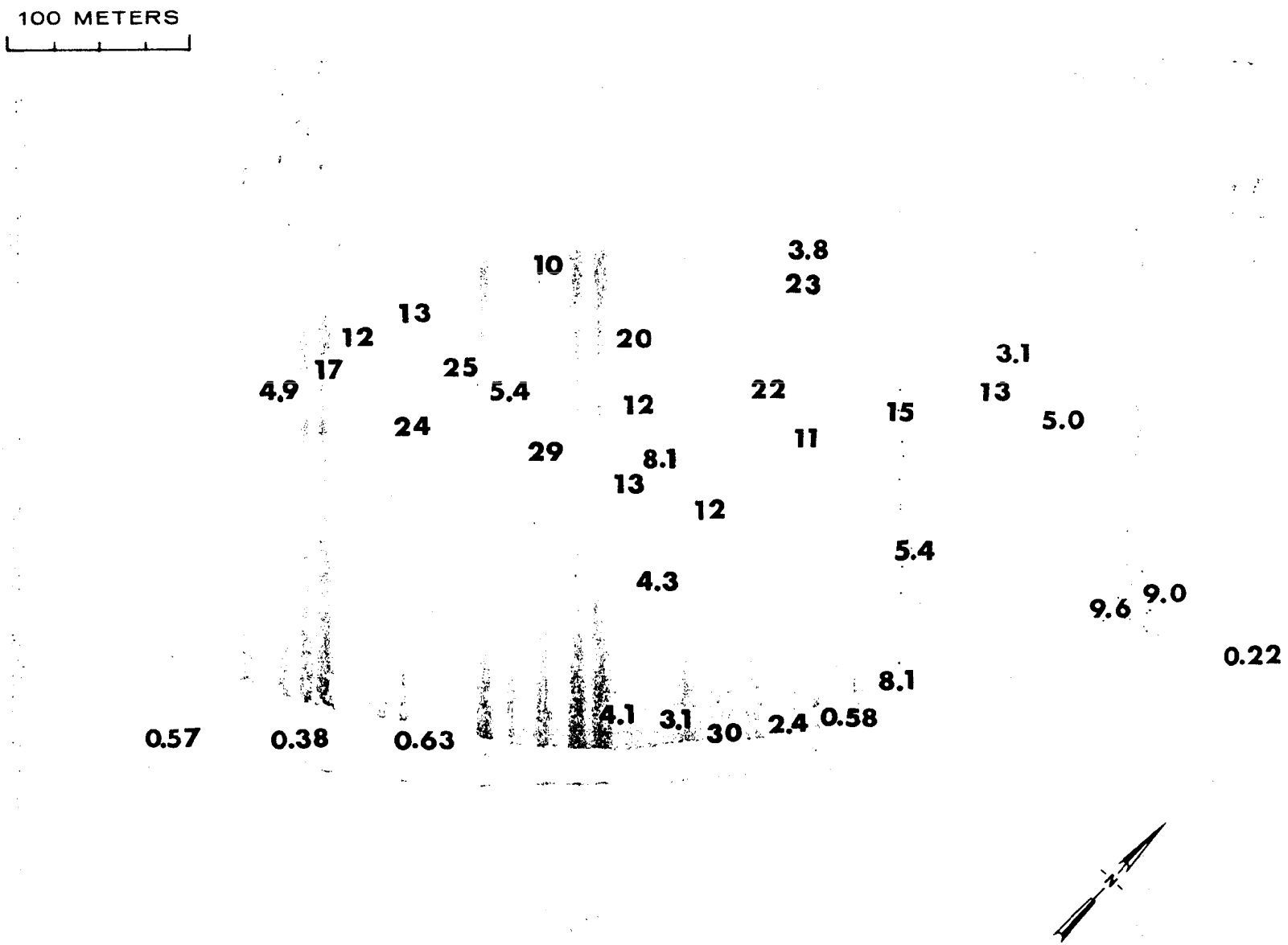

Fig. B.2.1.n. The average ^{60}Co activities (pCi/g) in soil samples collected to a depth of 15 cm.

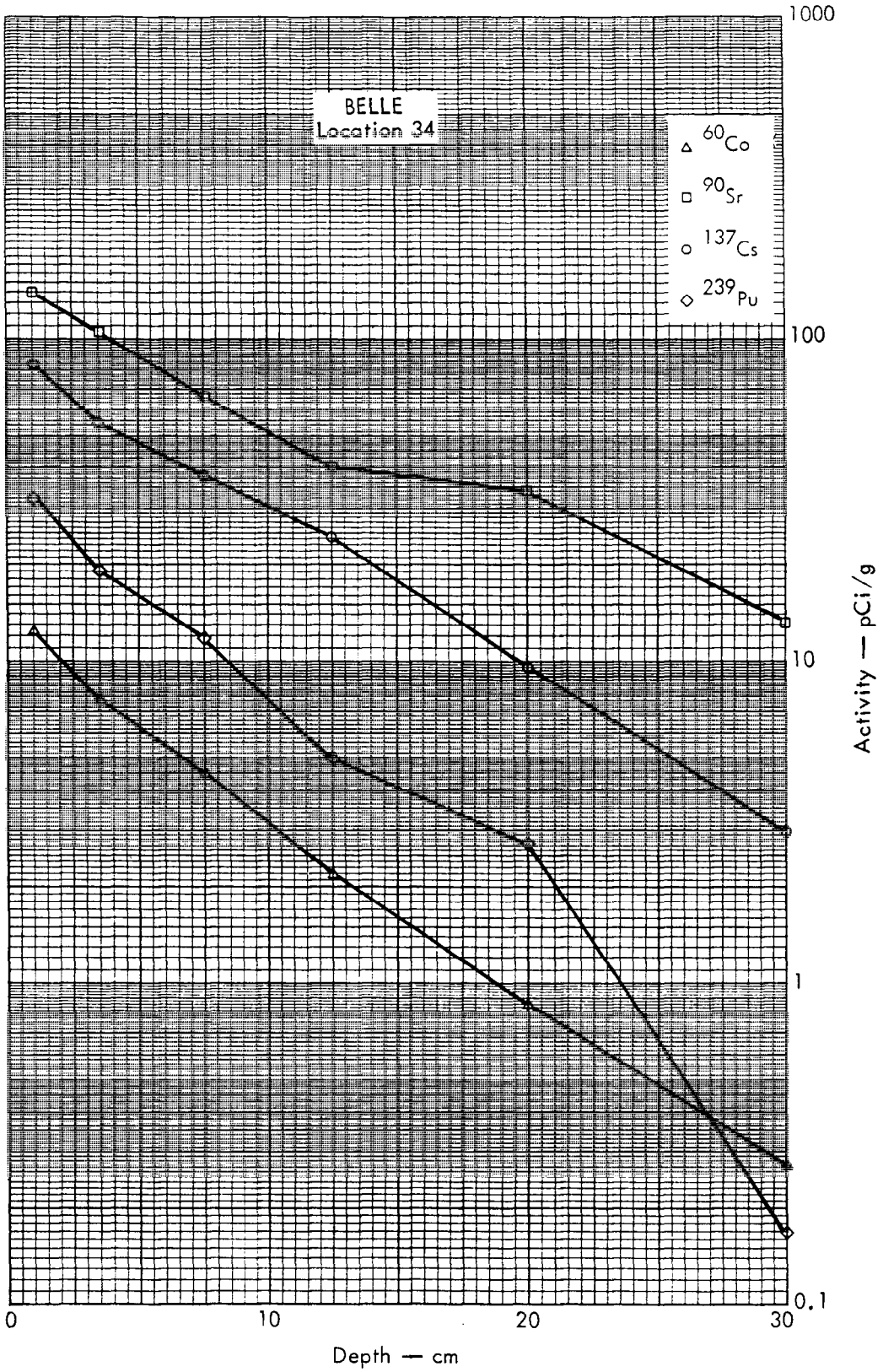

Fig. B. 2. 2a. Activities of selected radionuclides as a function of soil depth.

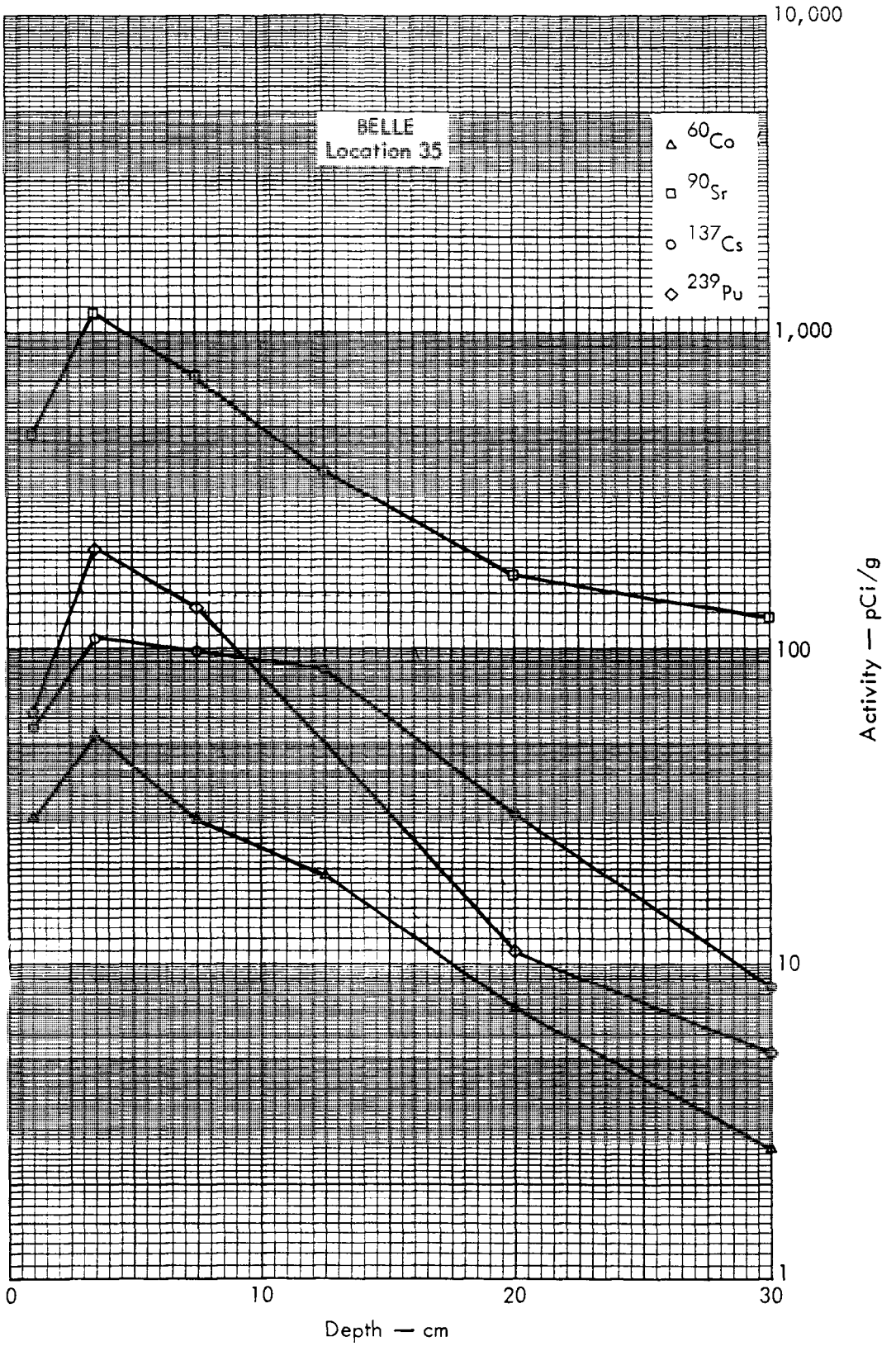

Fig. B. 2. 2b. Activities of selected radionuclides as a function of soil depth.

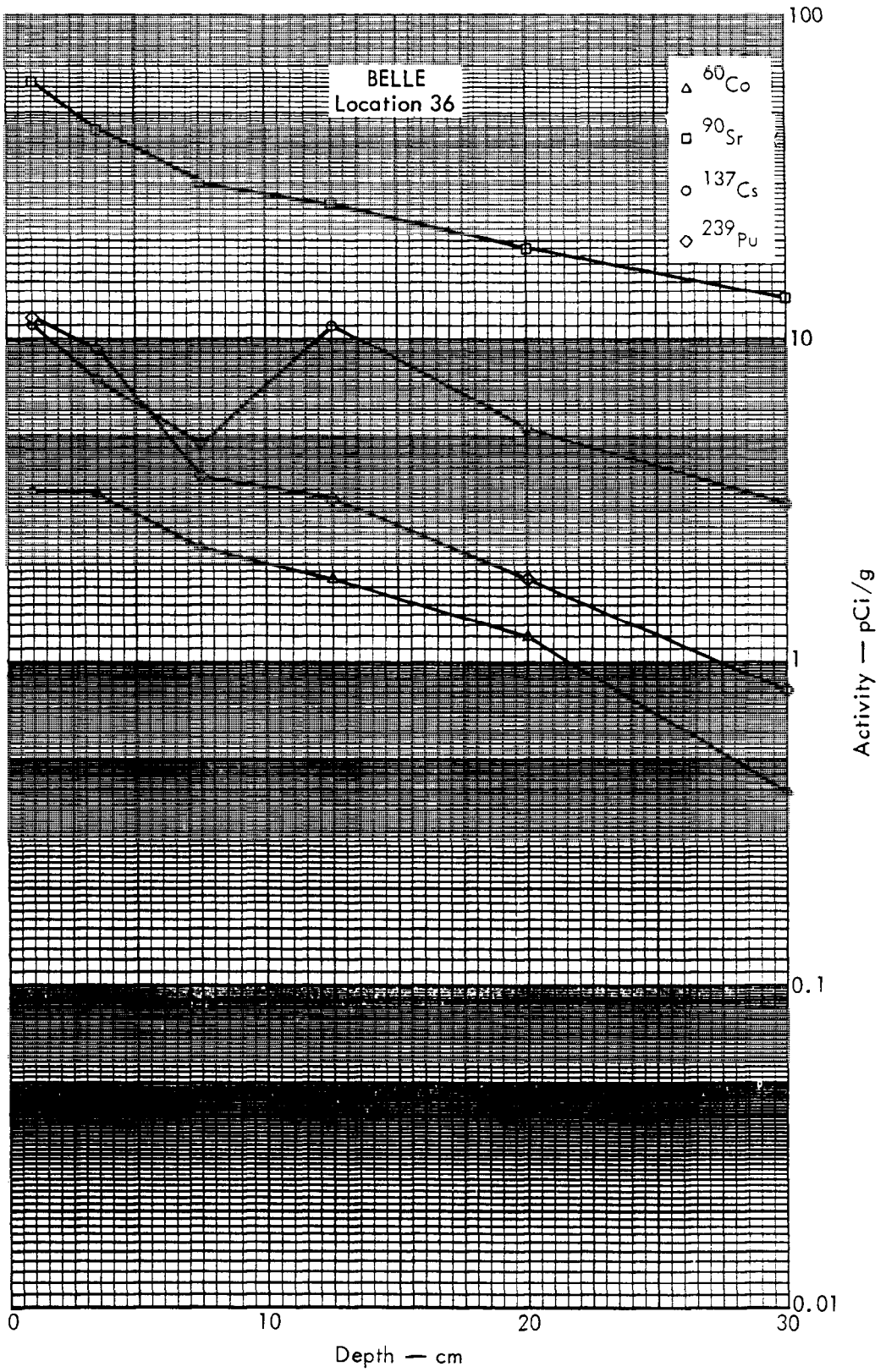

Fig. B.2.2c. Activities of selected radionuclides as a function of soil depth.

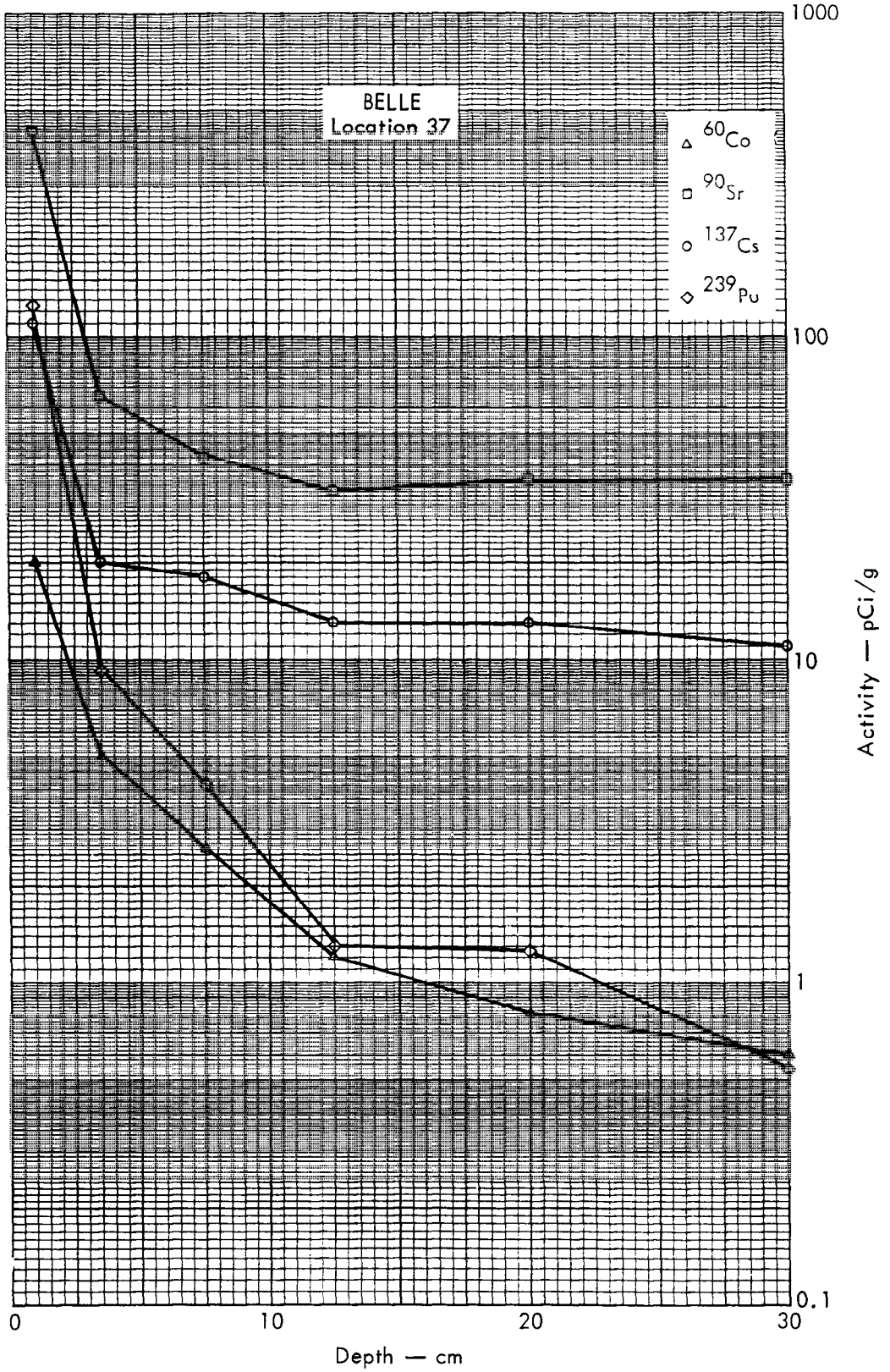

Fig. B. 2. 2d. Activities of selected radionuclides as a function of soil depth.

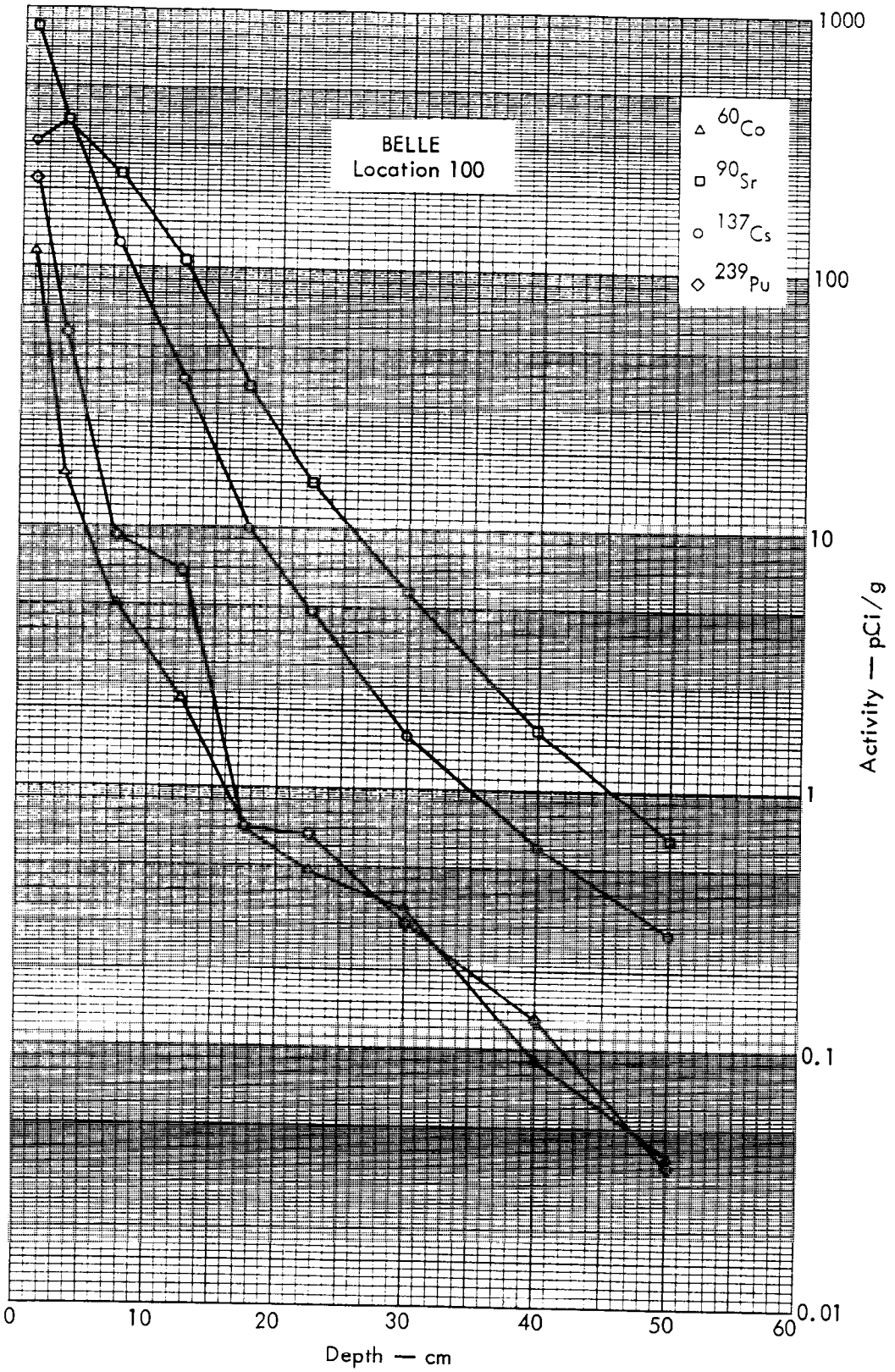

Fig. B. 2. 2e. Activities of selected radionuclides as a function of soil depth.

Fig. B.3.1.a.

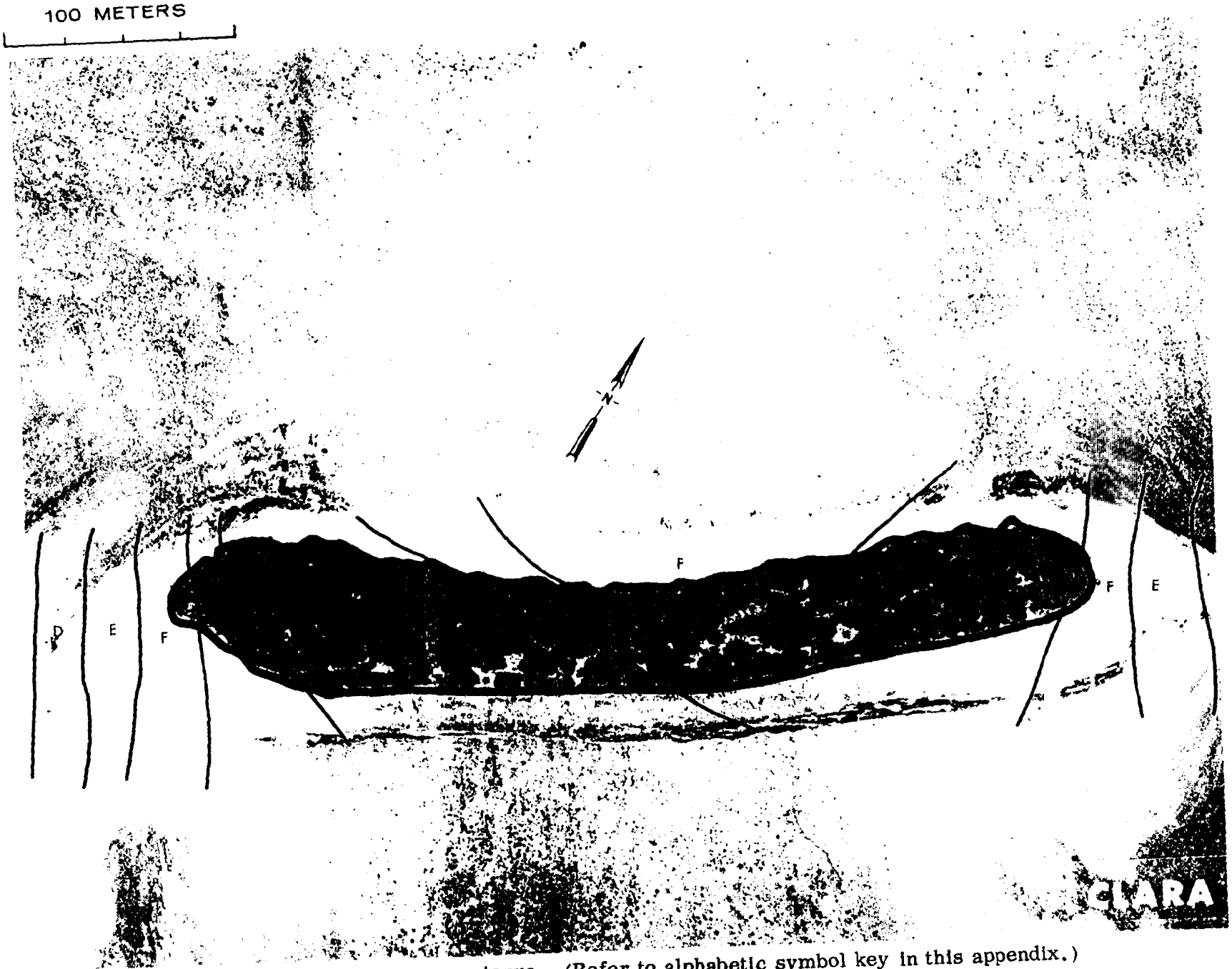

Fig. B.3.1.b. Gross count isoexposure contours. (Refer to alphabetic symbol key in this appendix.)

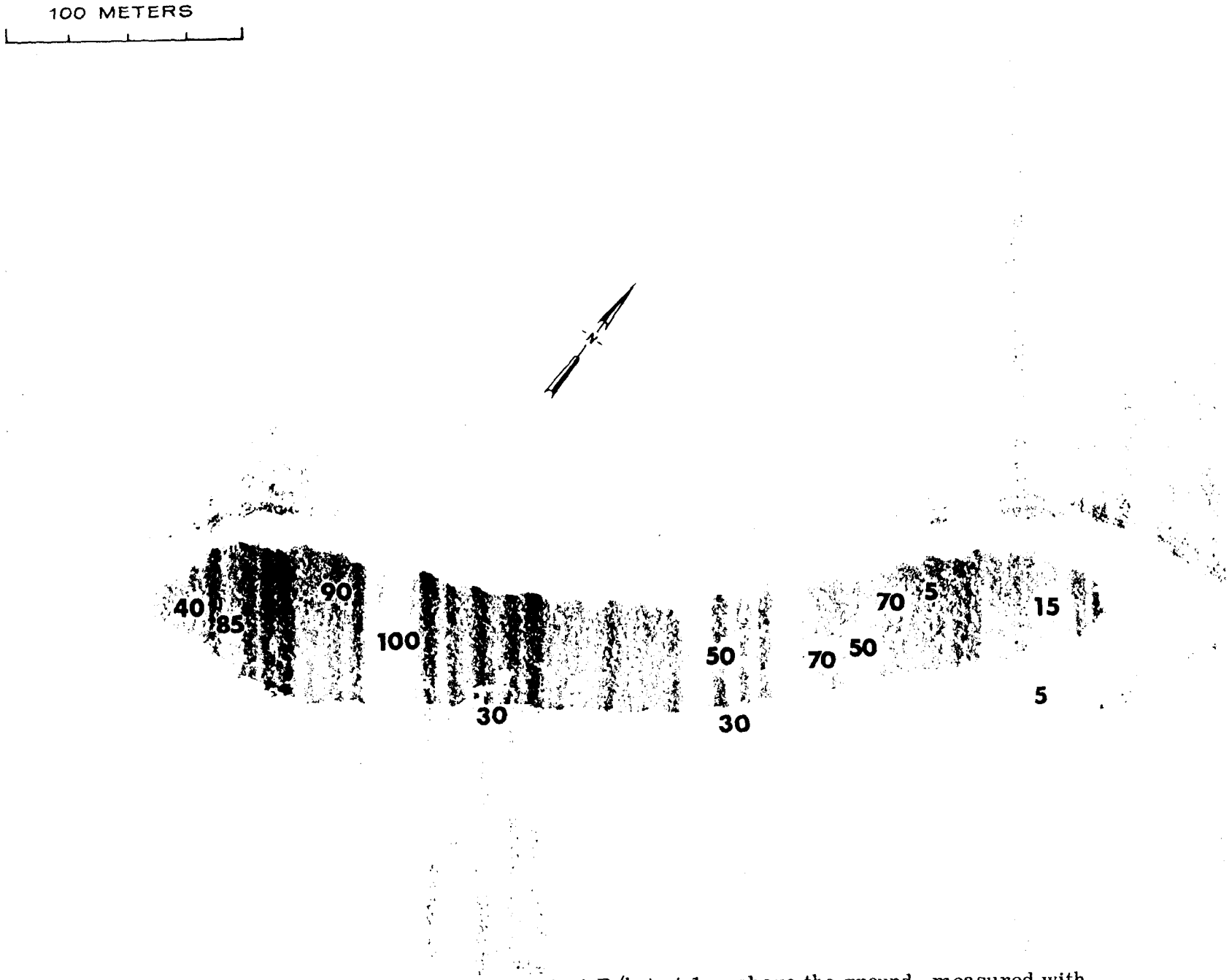

Fig. B.3.1.d. The gamma background exposure rate (μR/hr) at 1 m above the ground, measured with a portable NaI scintillation counter.

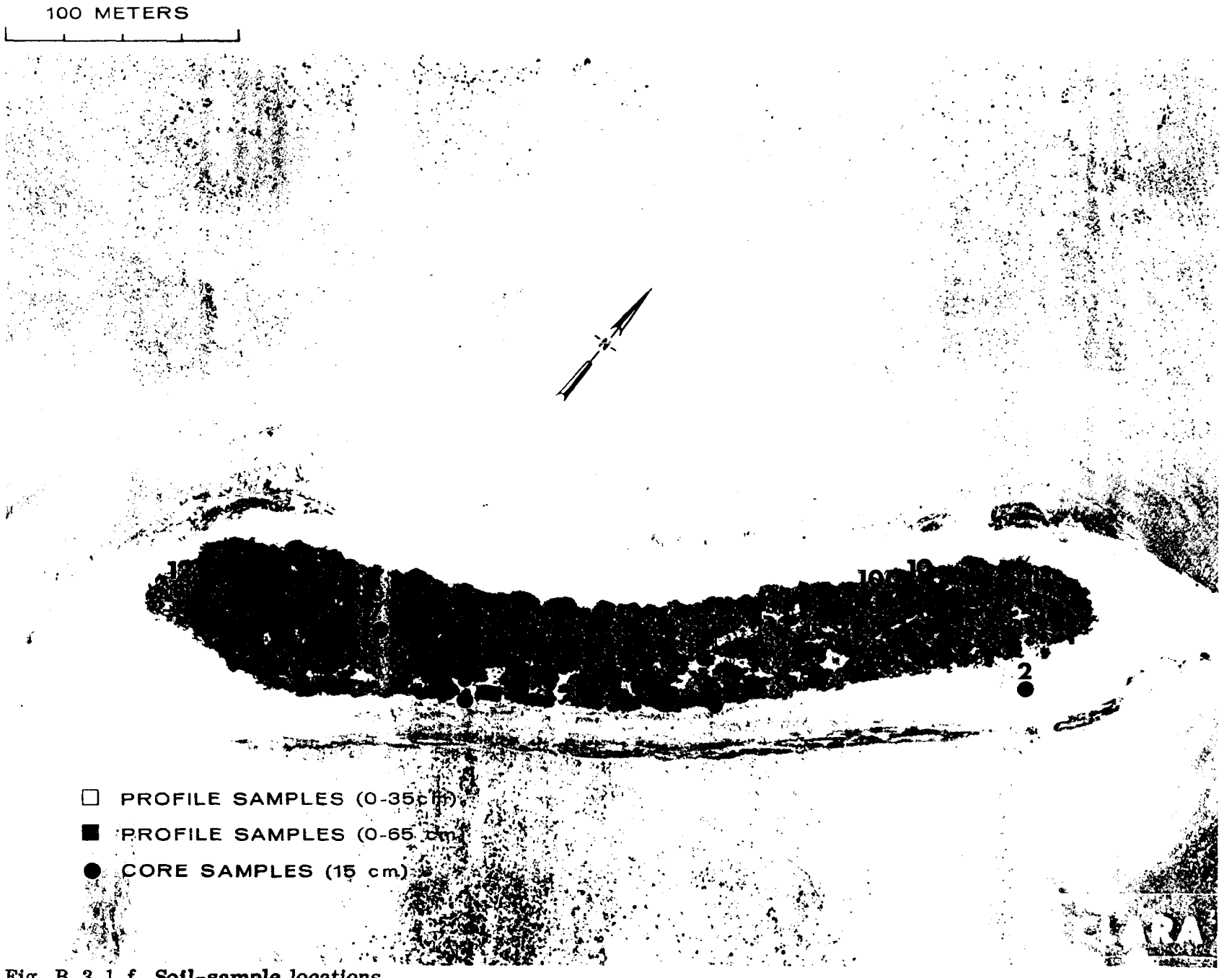

Fig. B.3.1.f. Soil-sample locations.

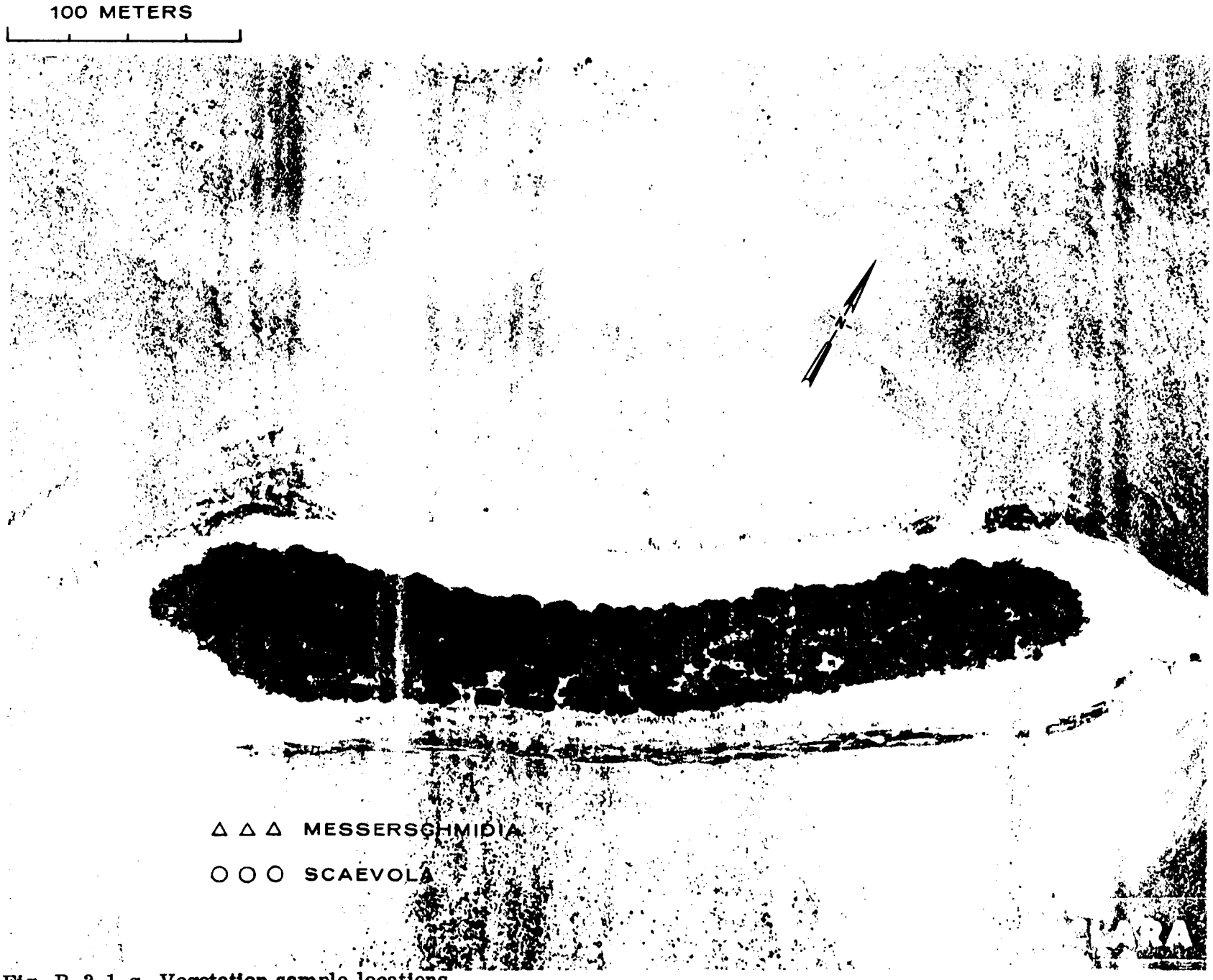

Fig. B.3.1.g. Vegetation sample locations.

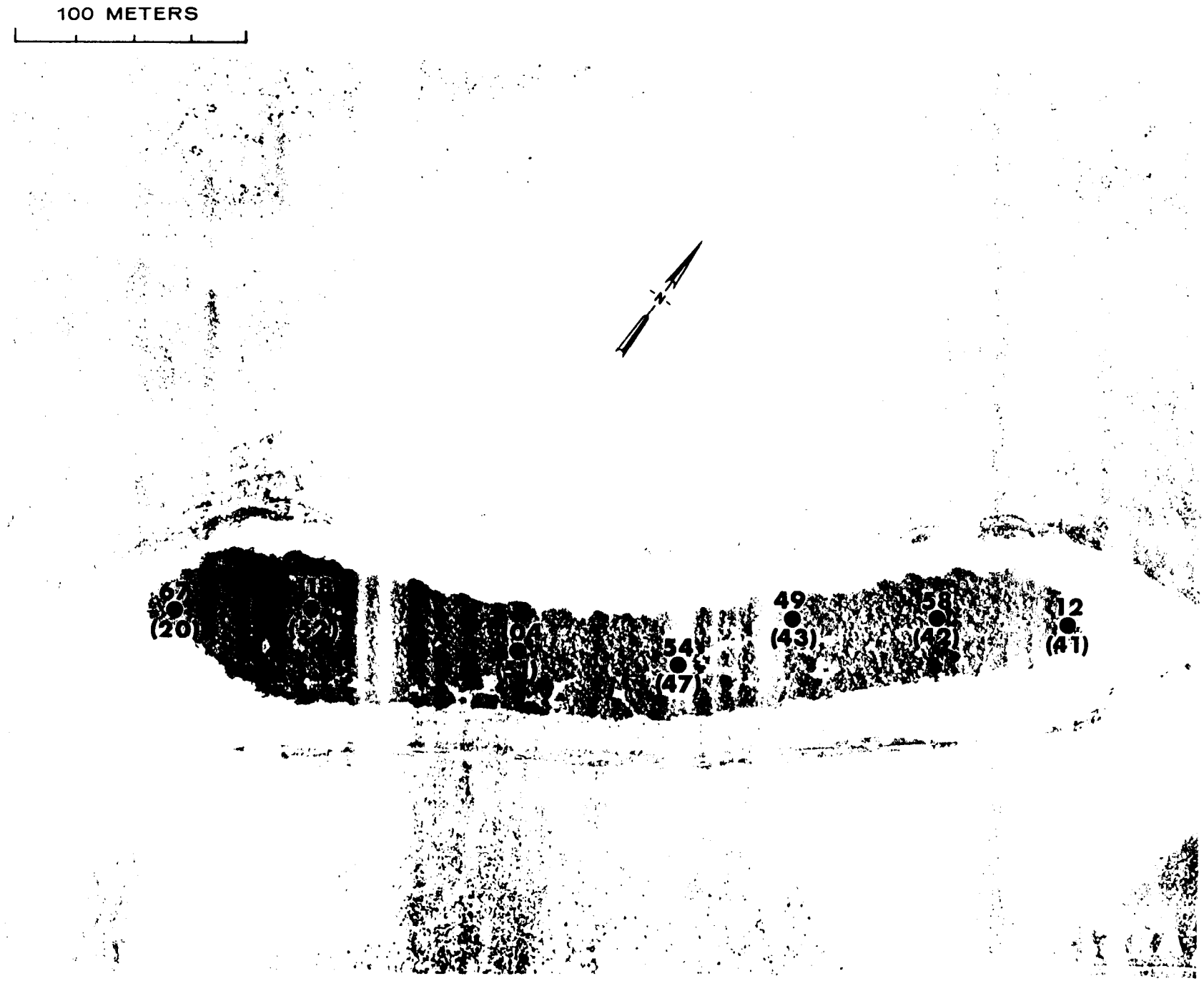

Fig. B.3.1.h. The gamma-ray exposure rates (μR/hr) measured 1 m above the ground by the LiF thermoluminescent dosimeters (TLD). The numbers shown in parentheses denote the location identification numbers.

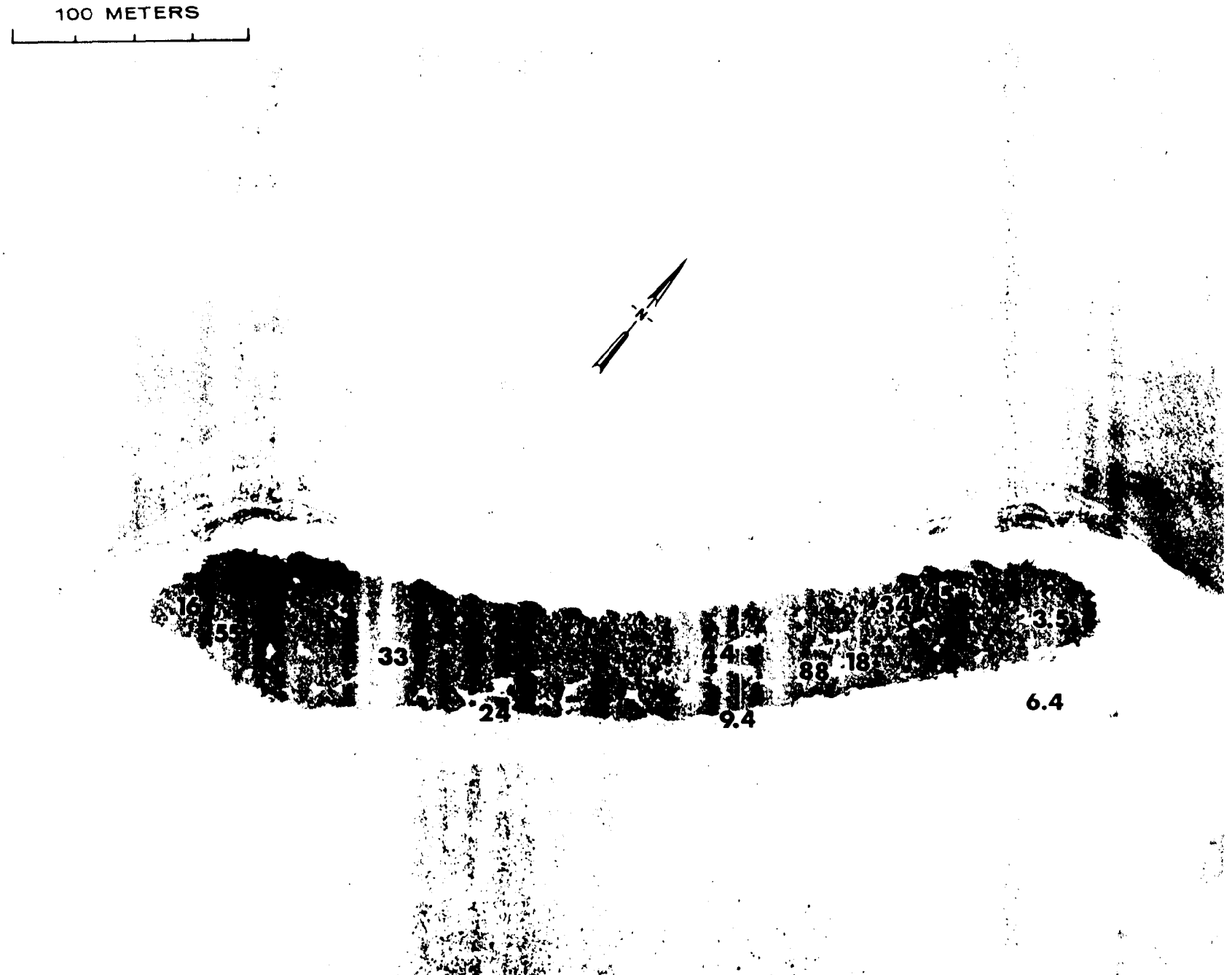

Fig. B.3.1.i. The average ^{239}Pu activities (pCi/g) in soil samples collected to a depth of 15 cm.

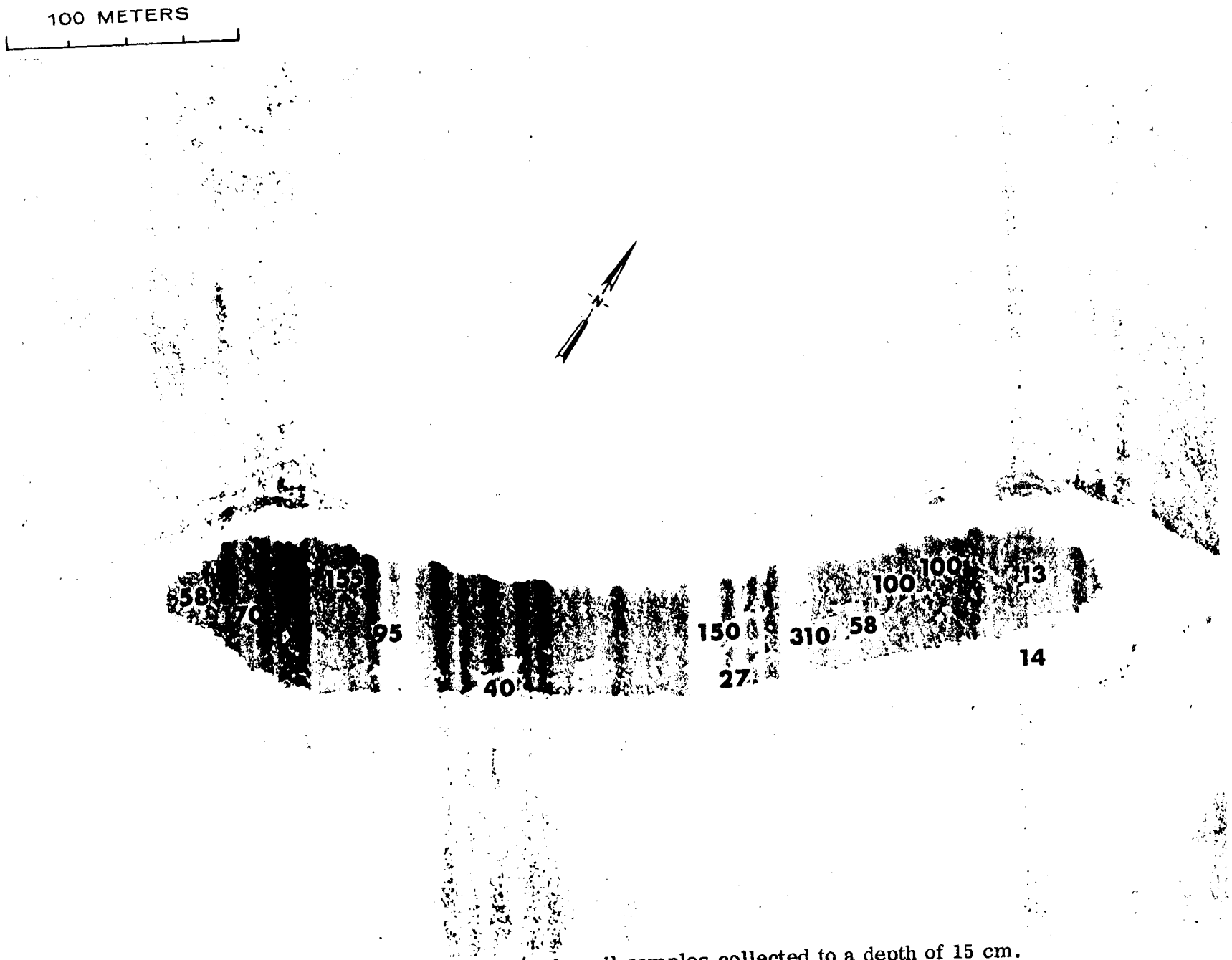

Fig. B.3.1.j. The average ^{90}Sr activities (pCi/g) in soil samples collected to a depth of 15 cm.

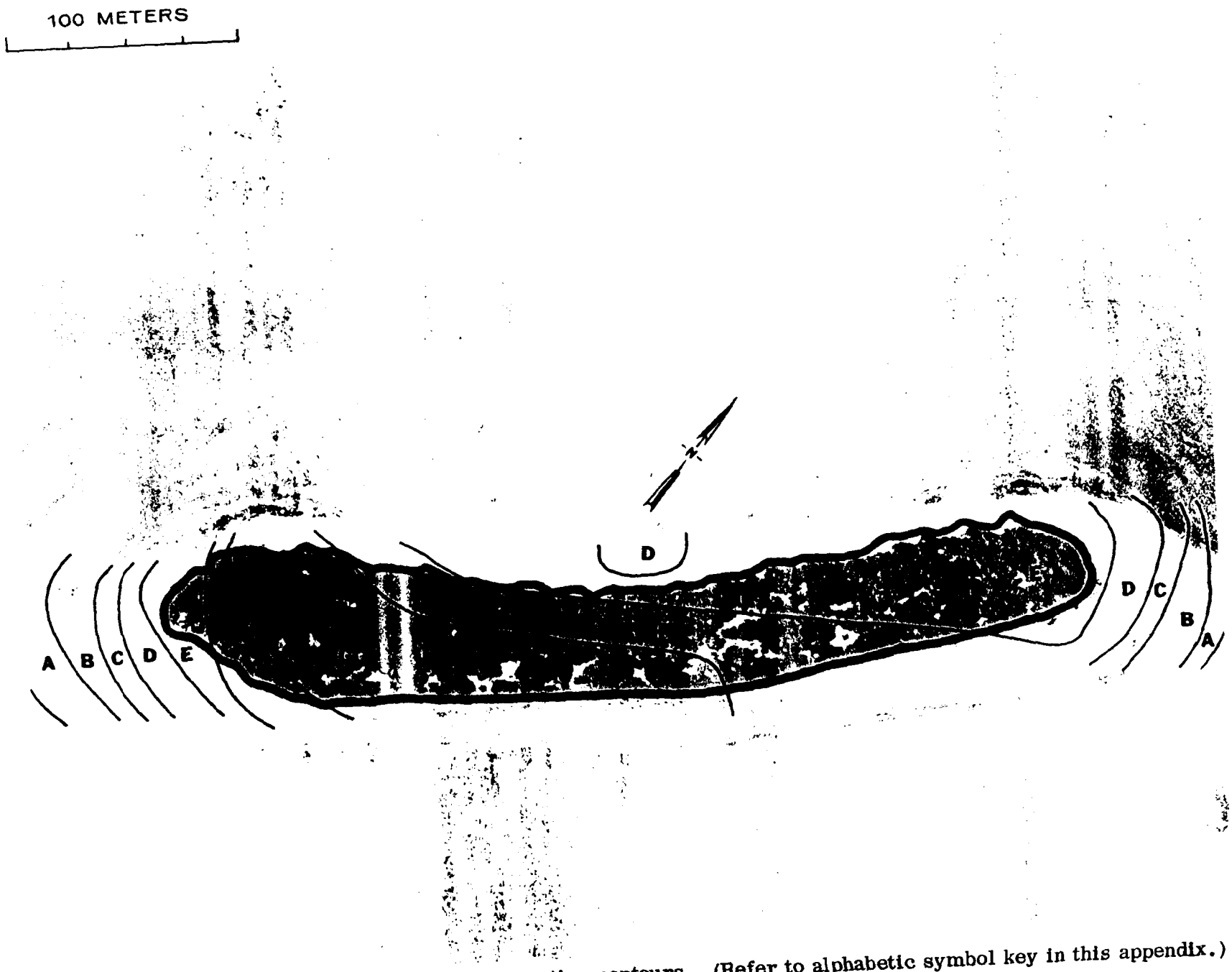

Fig. B.3.1.k. ^{137}Cs isoexposure and isoconcentration contours. (Refer to alphabetic symbol key in this appendix.)

Fig. B.3.1.1. The average ^{137}Cs activities (pCi/g) in soil samples collected to a depth of 15 cm.

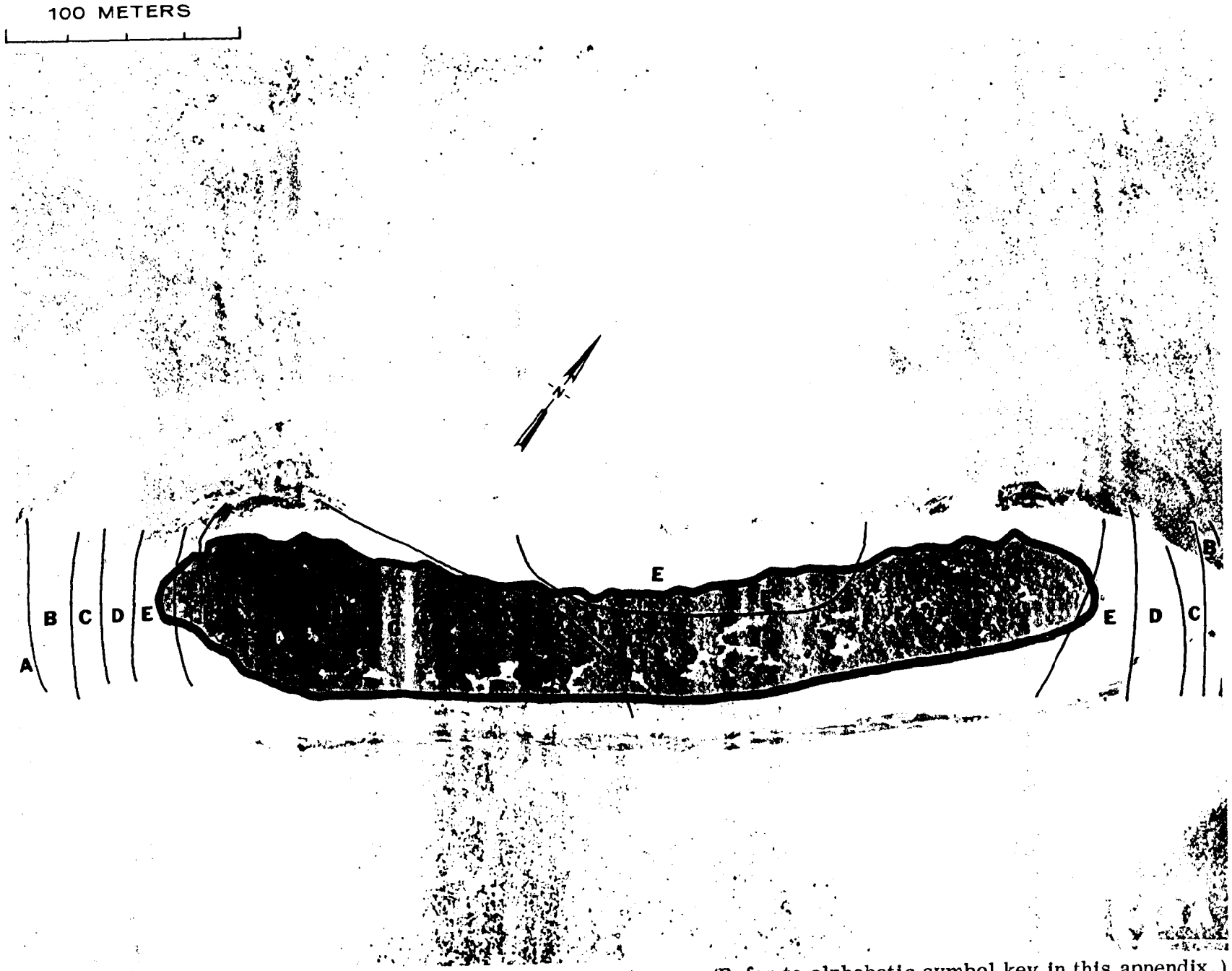

Fig. B.3.1.m. ^{60}Co isoexposure and isoconcentration contours. (Refer to alphabetic symbol key in this appendix.)

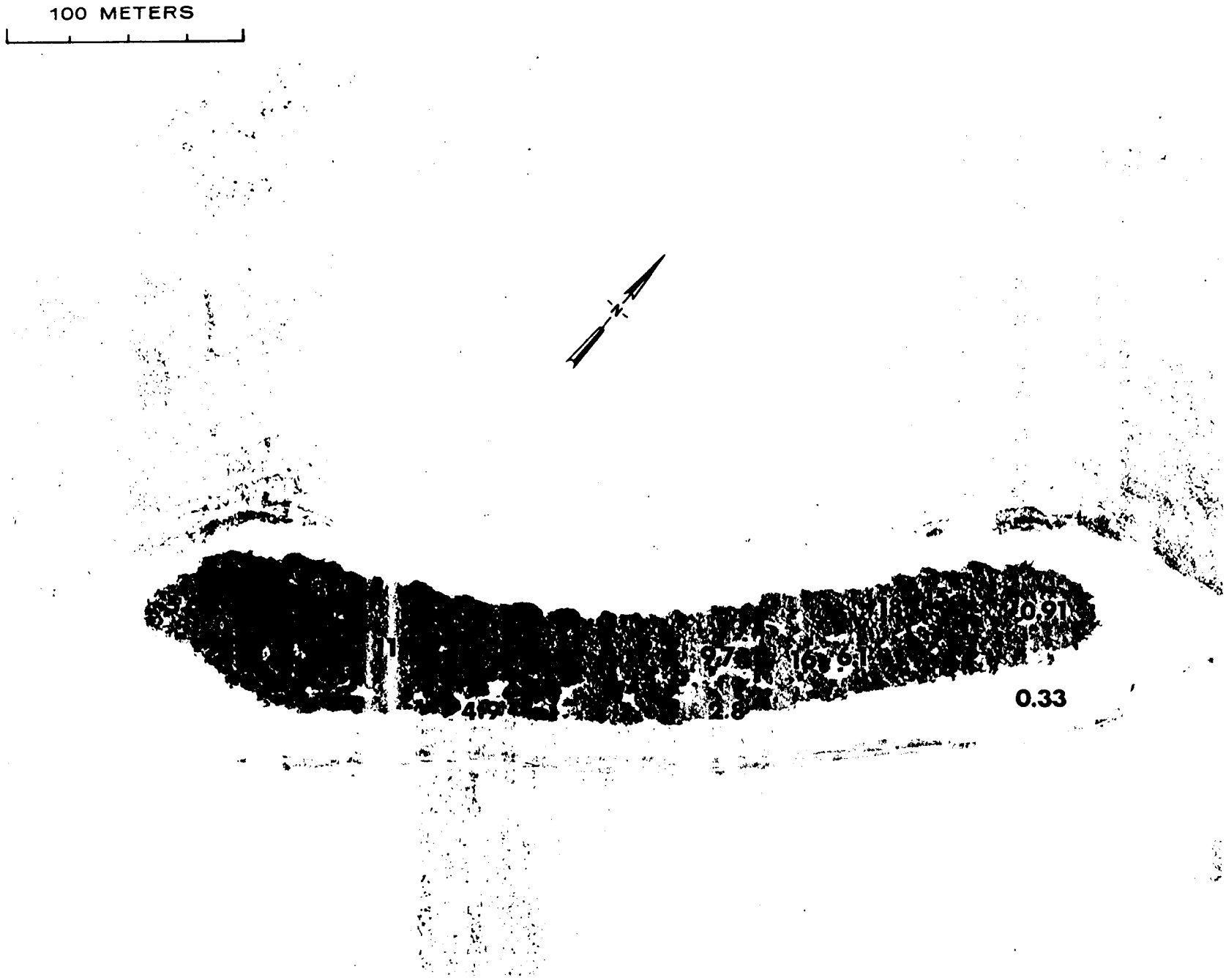

Fig. B.3.1.n. The average ^{60}Co activities (pCi/g) in soil samples collected to a depth of 15 cm.

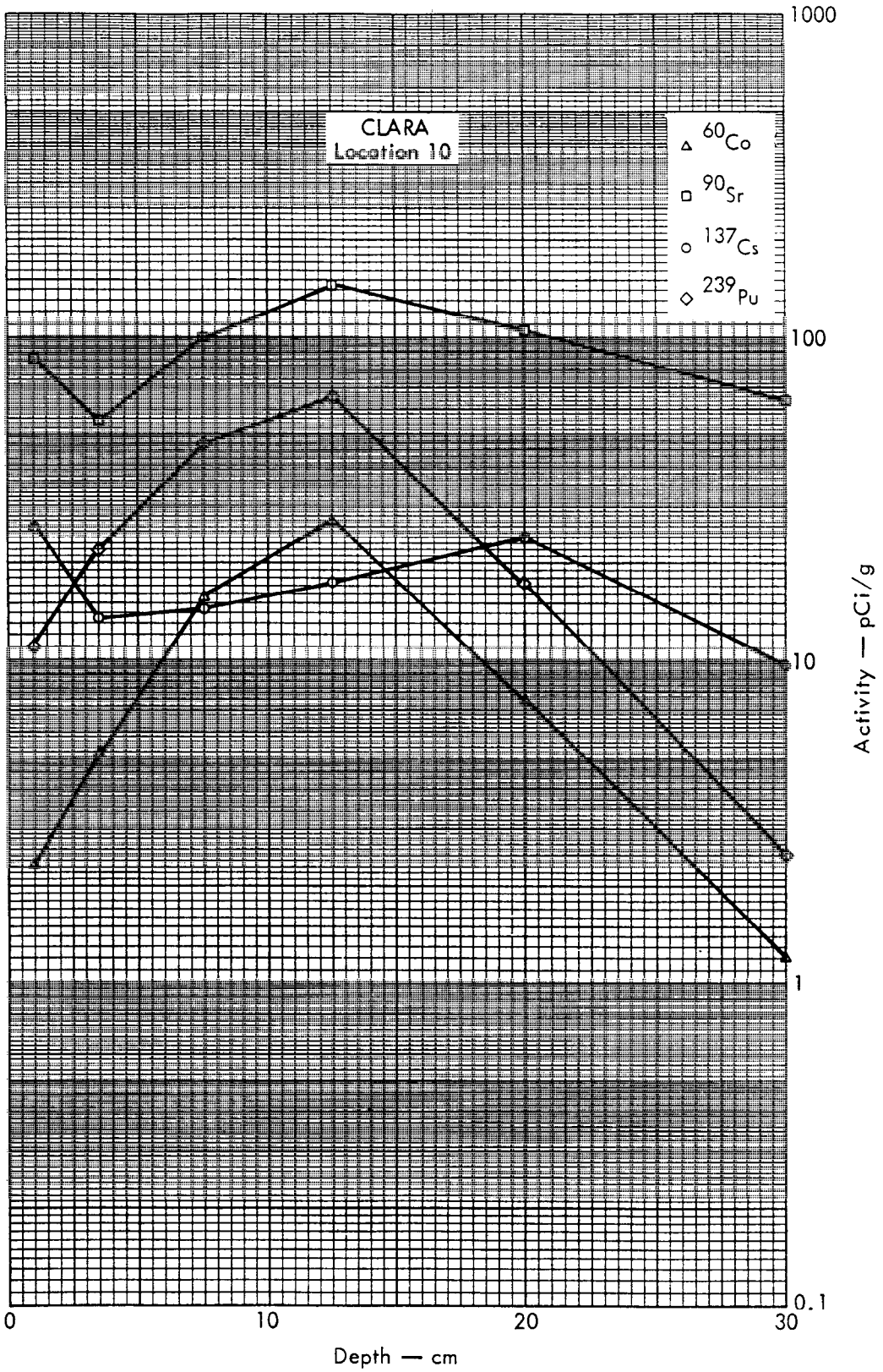

Fig. B.3.2a. Activities of selected radionuclides as a function of soil depth.

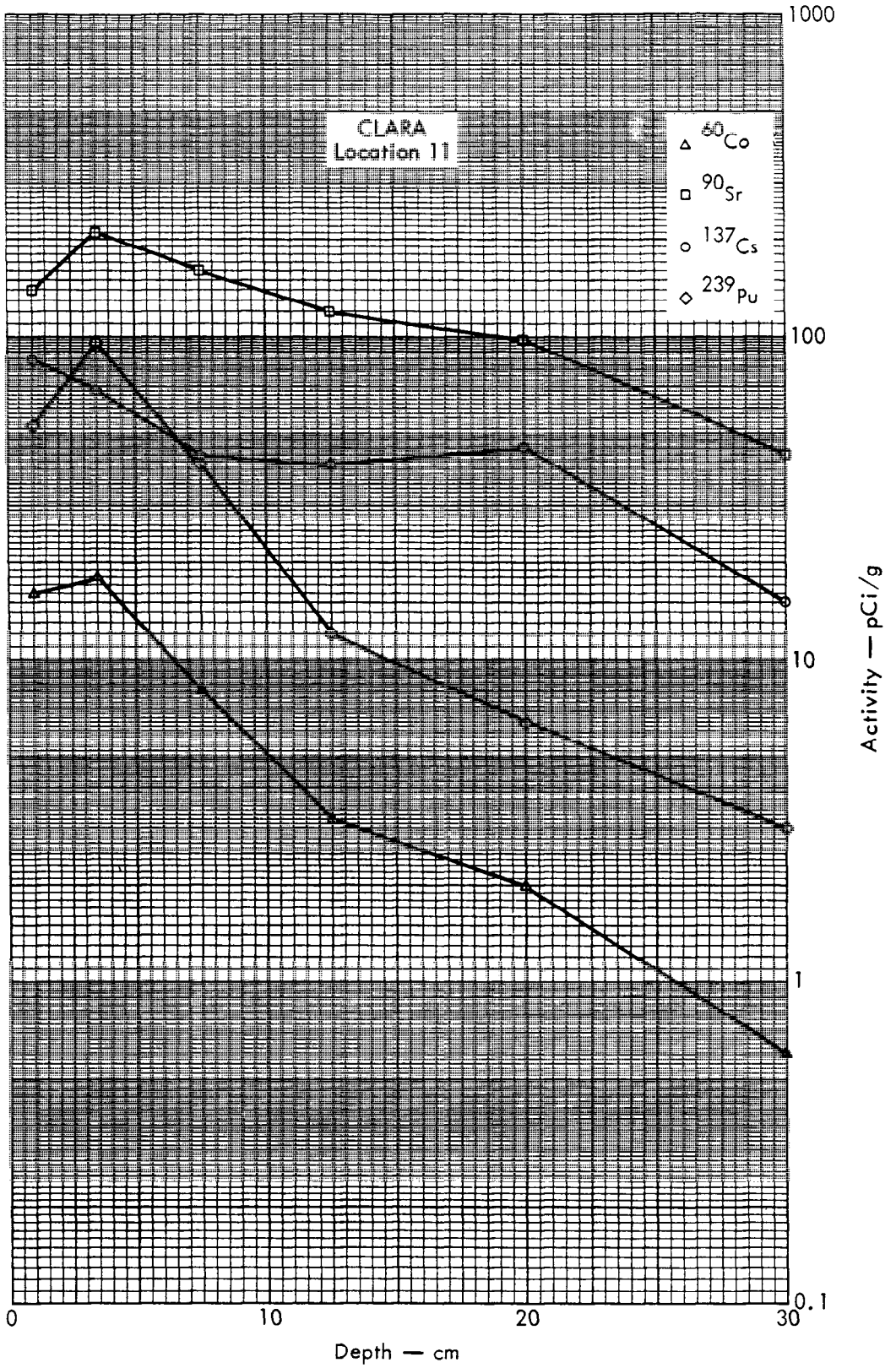

Fig. B. 3. 2b. Activities of selected radionuclides as a function of soil depth.

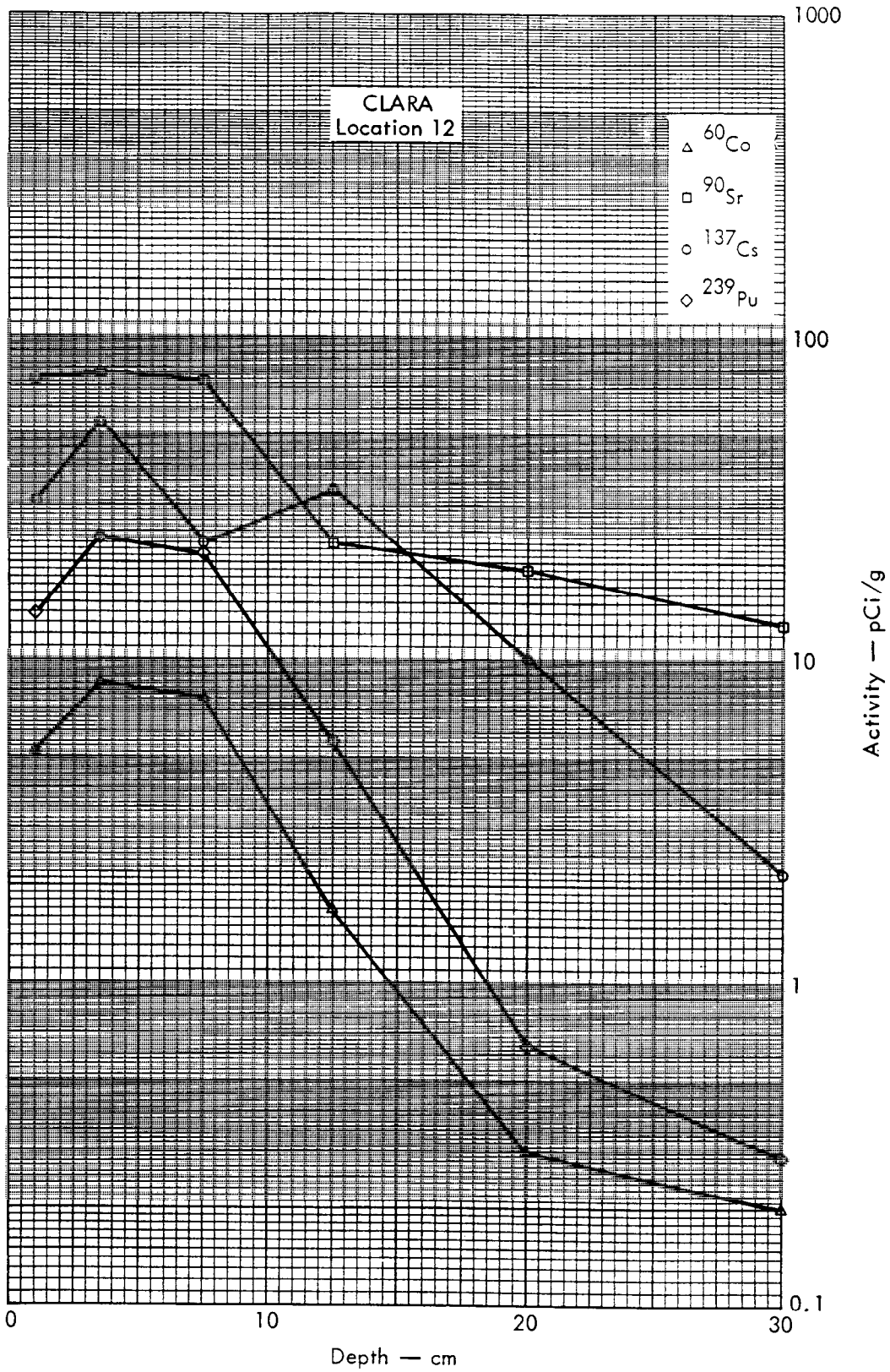

Fig. B.3.2c. Activities of selected radionuclides as a function of soil depth.

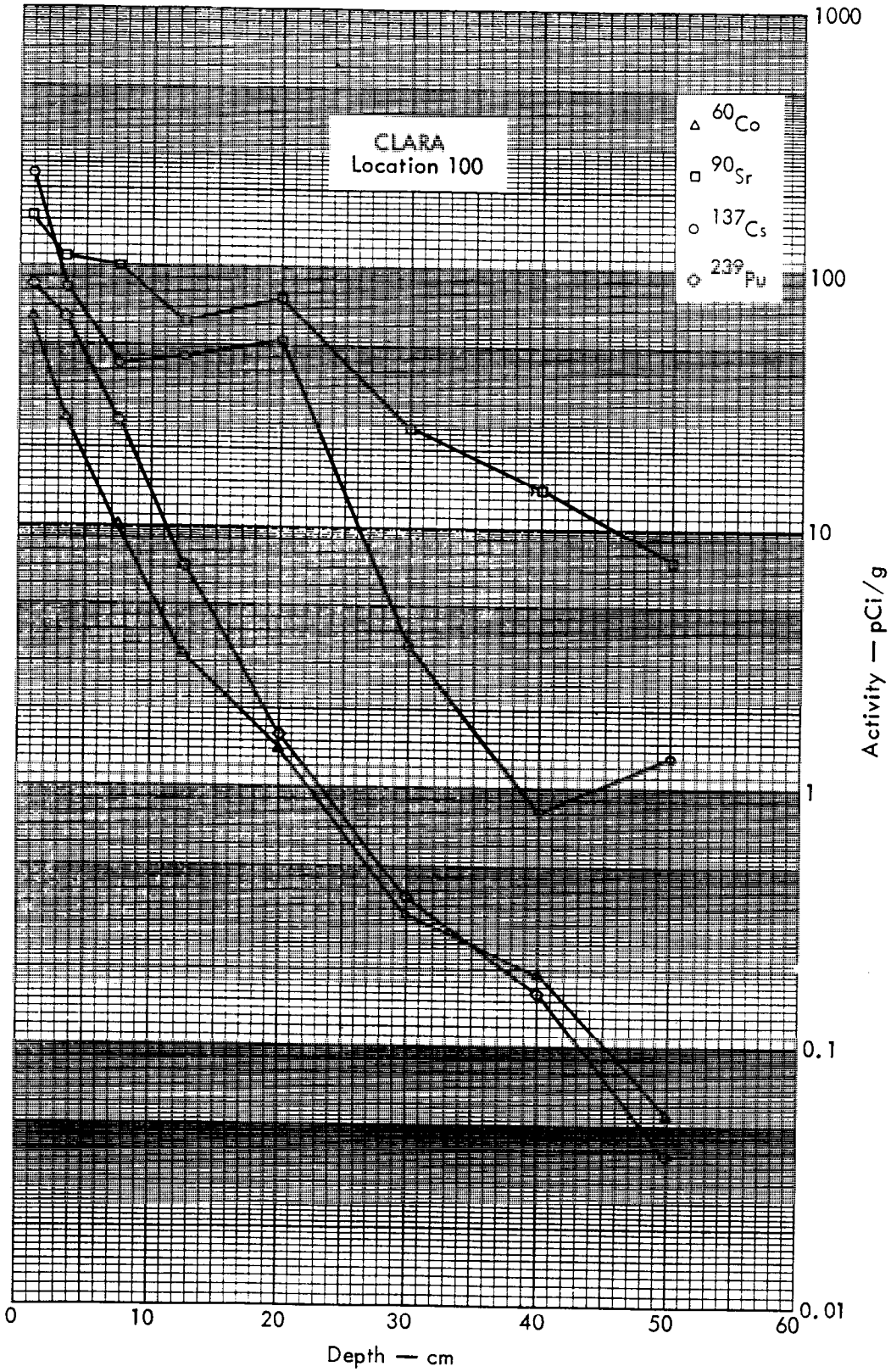

Fig. B. 3. 2d. Activities of selected radionuclides as a function of soil depth.

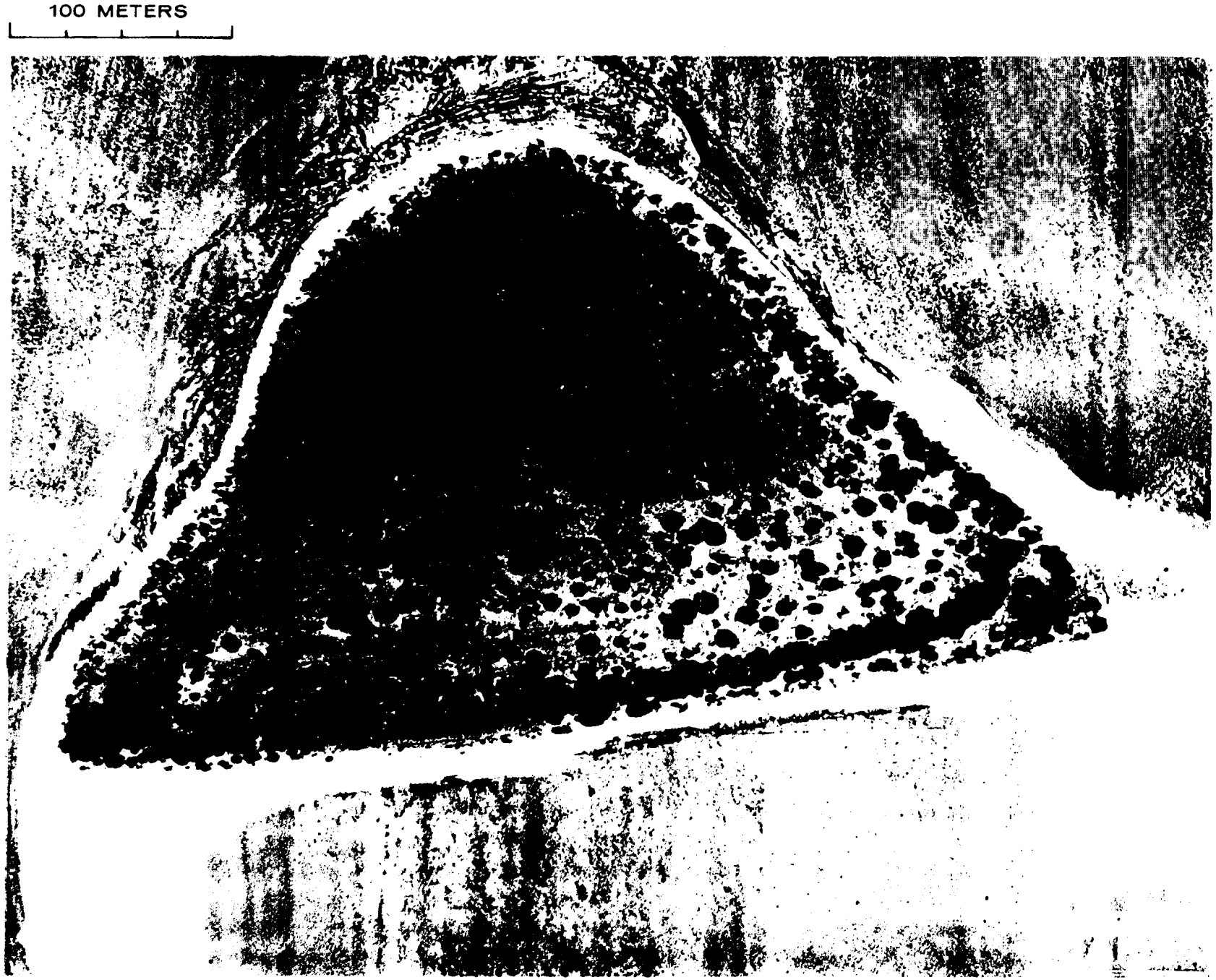

Fig. B.4.1.a.

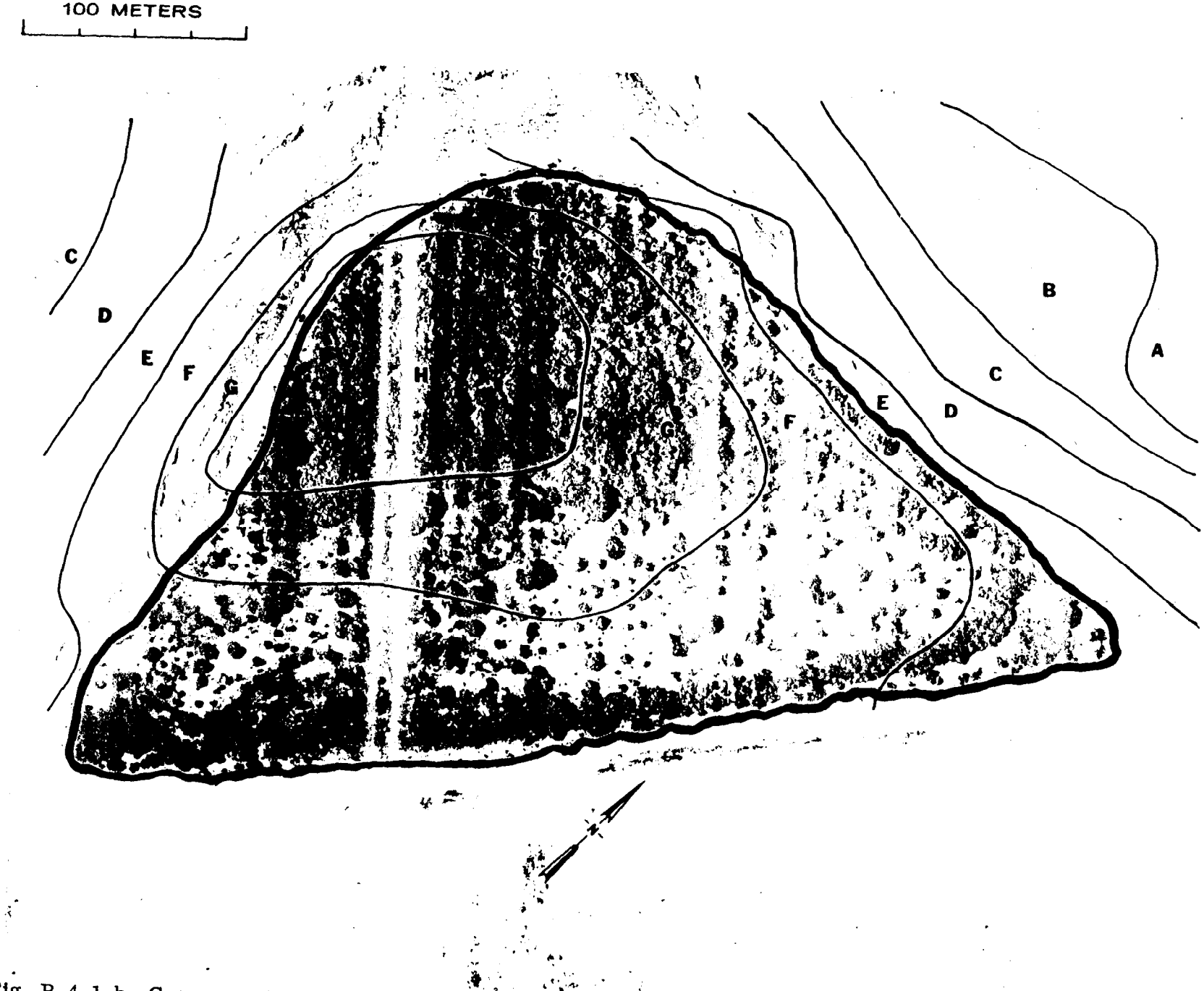

Fig. B.4.1.b. Gross count isoexposure contours. (Refer to alphabetic symbol key in this appendix.)

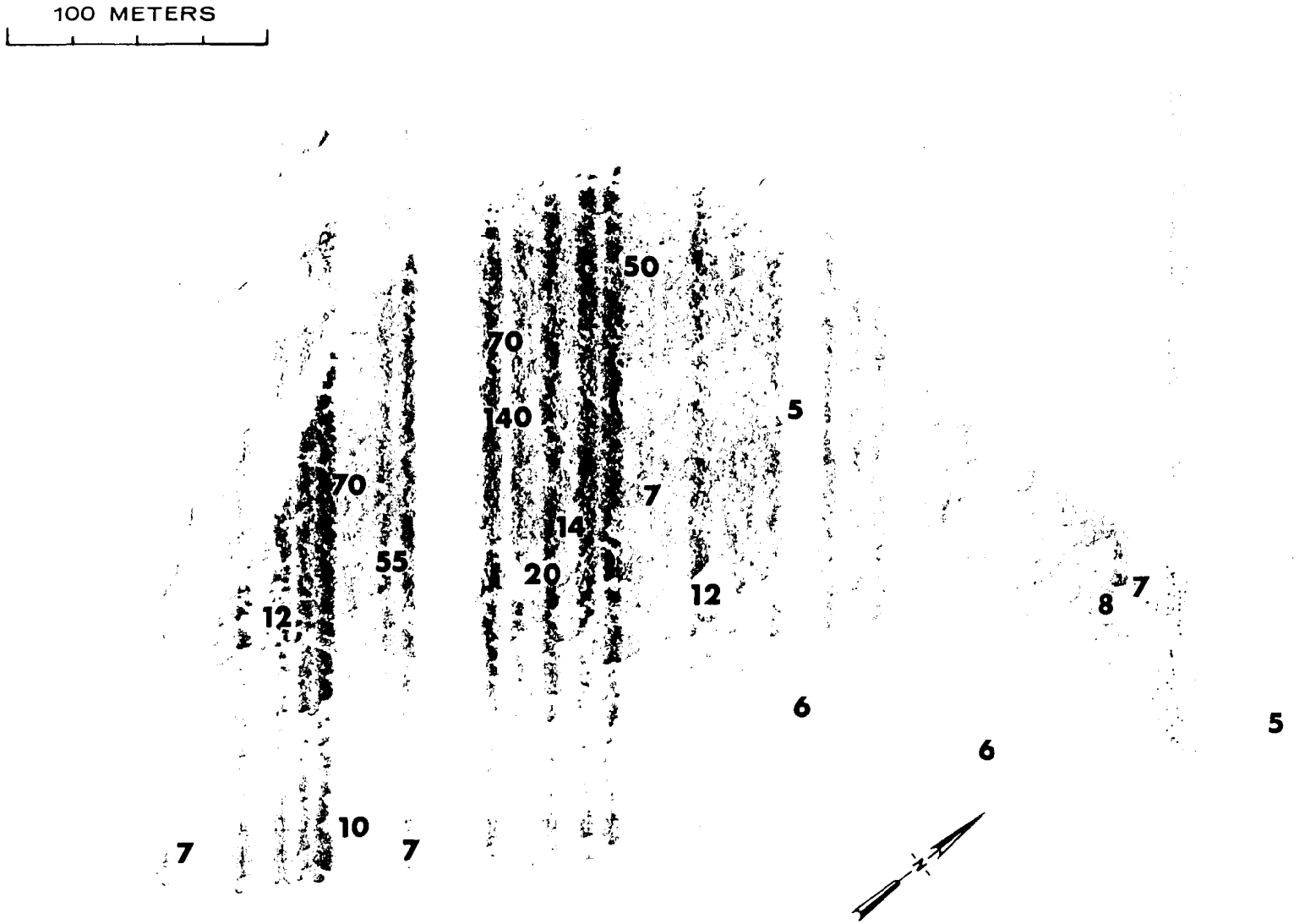

Fig. B.4.1.d. The gamma background exposure rate (μR/hr) at 1 m above the ground, measured with a portable NaI scintillation counter.

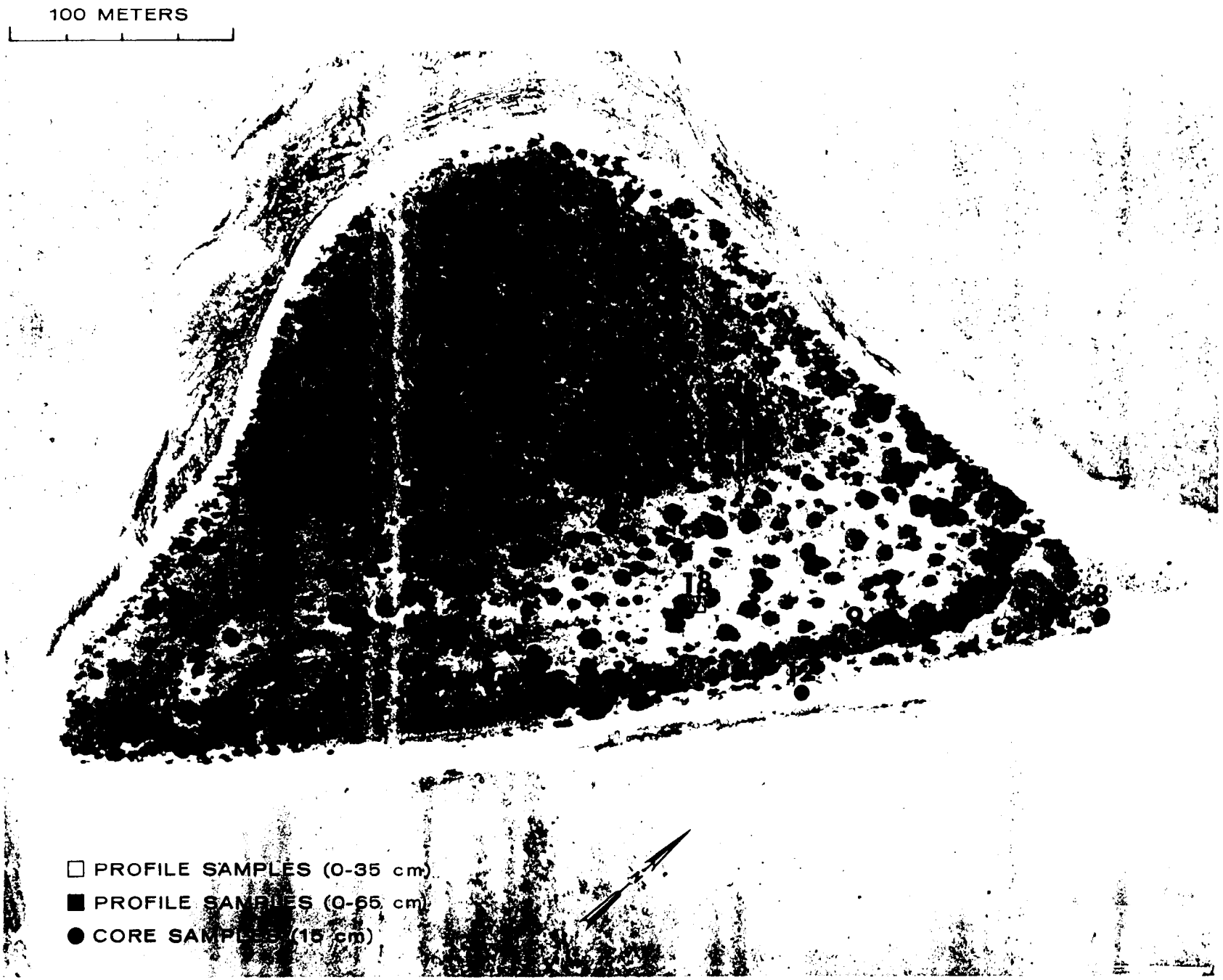

Fig. B.4.1.f. Soil-sample locations.

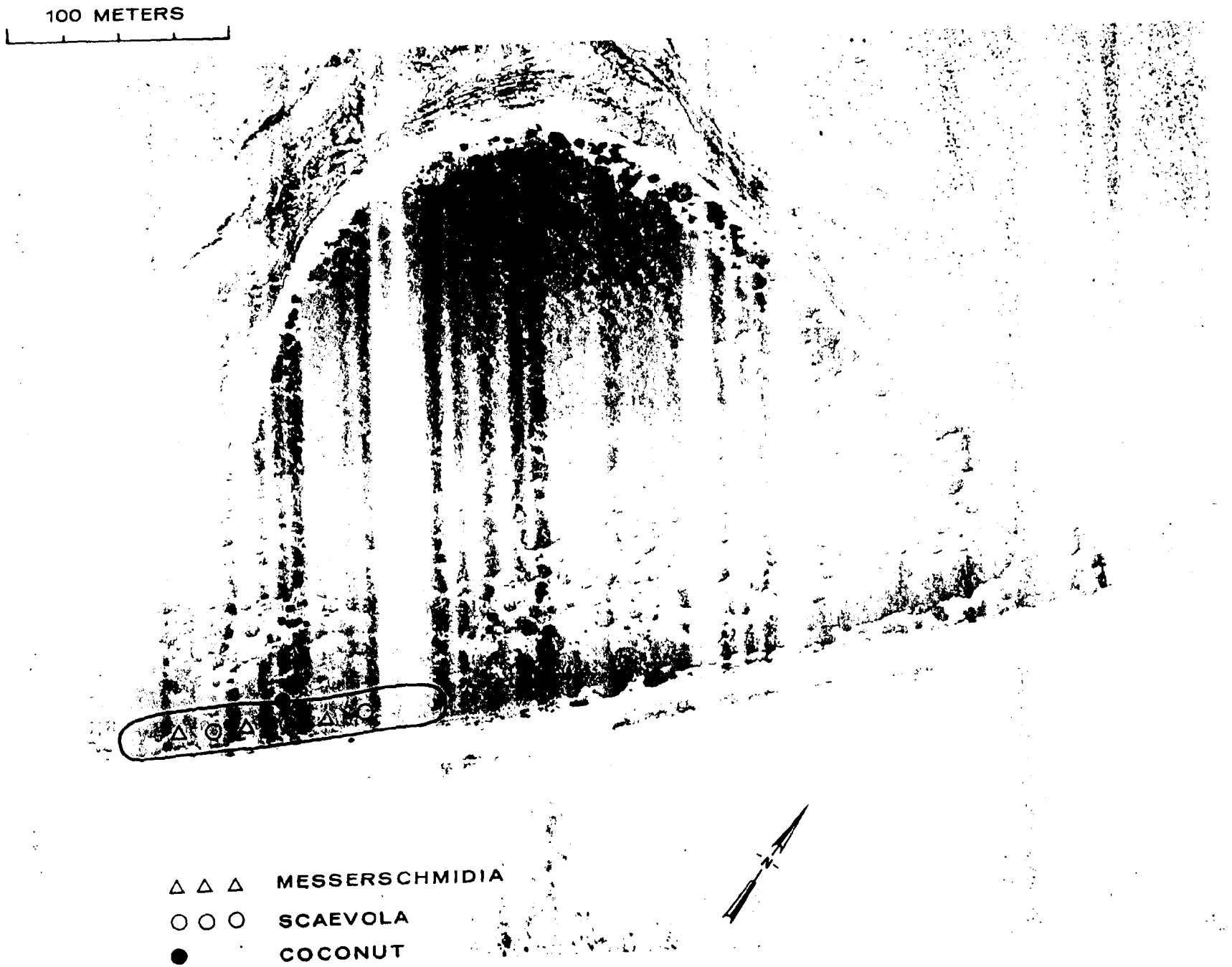

Fig. B.4.1.g. Vegetation sample locations.

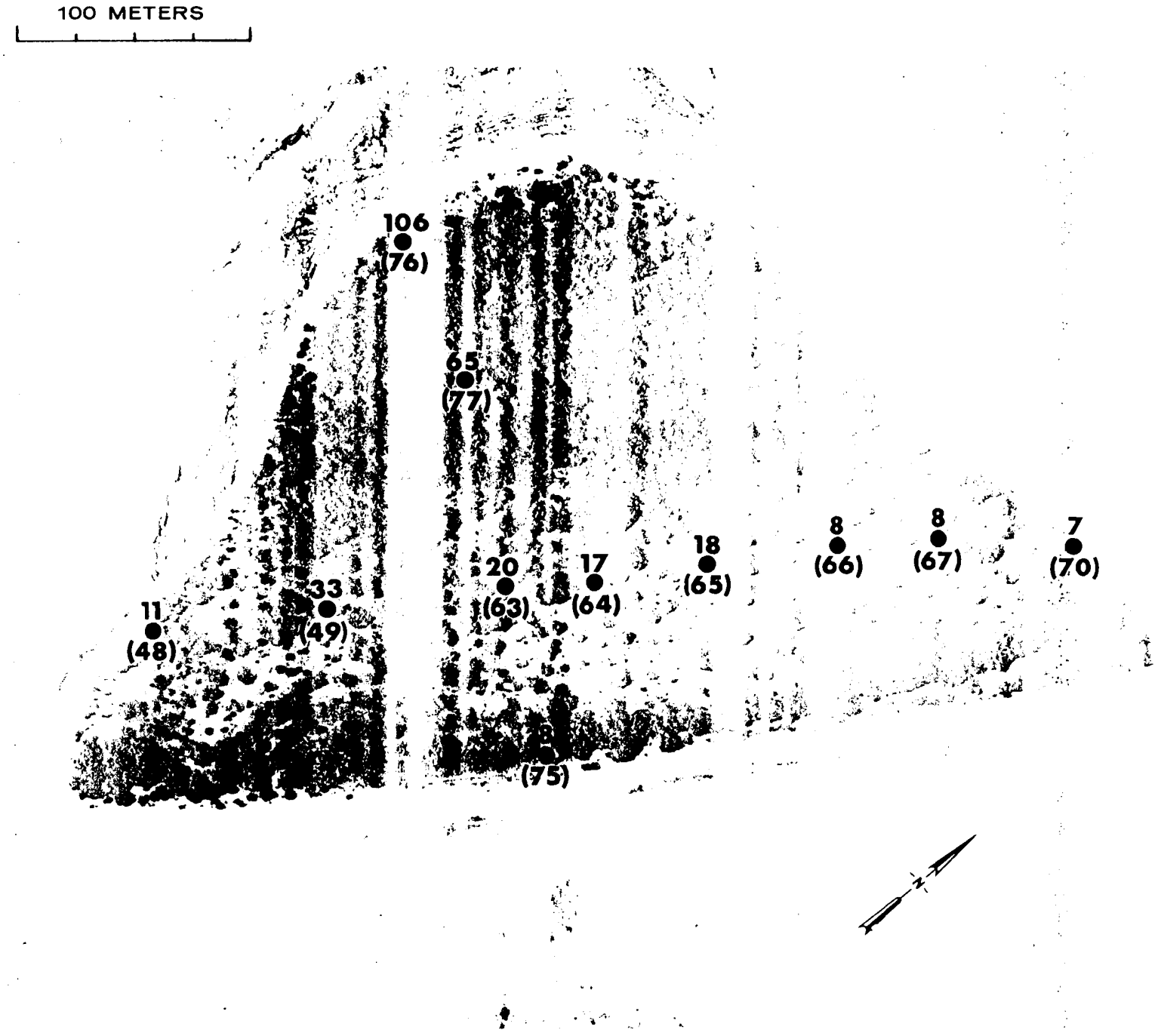

Fig. B.4.1.h. The gamma-ray exposure rates (μR/hr) measured 1 m above the ground by the LiF thermoluminescent dosimeters (TLD). The numbers shown in parentheses denote the location identification numbers.

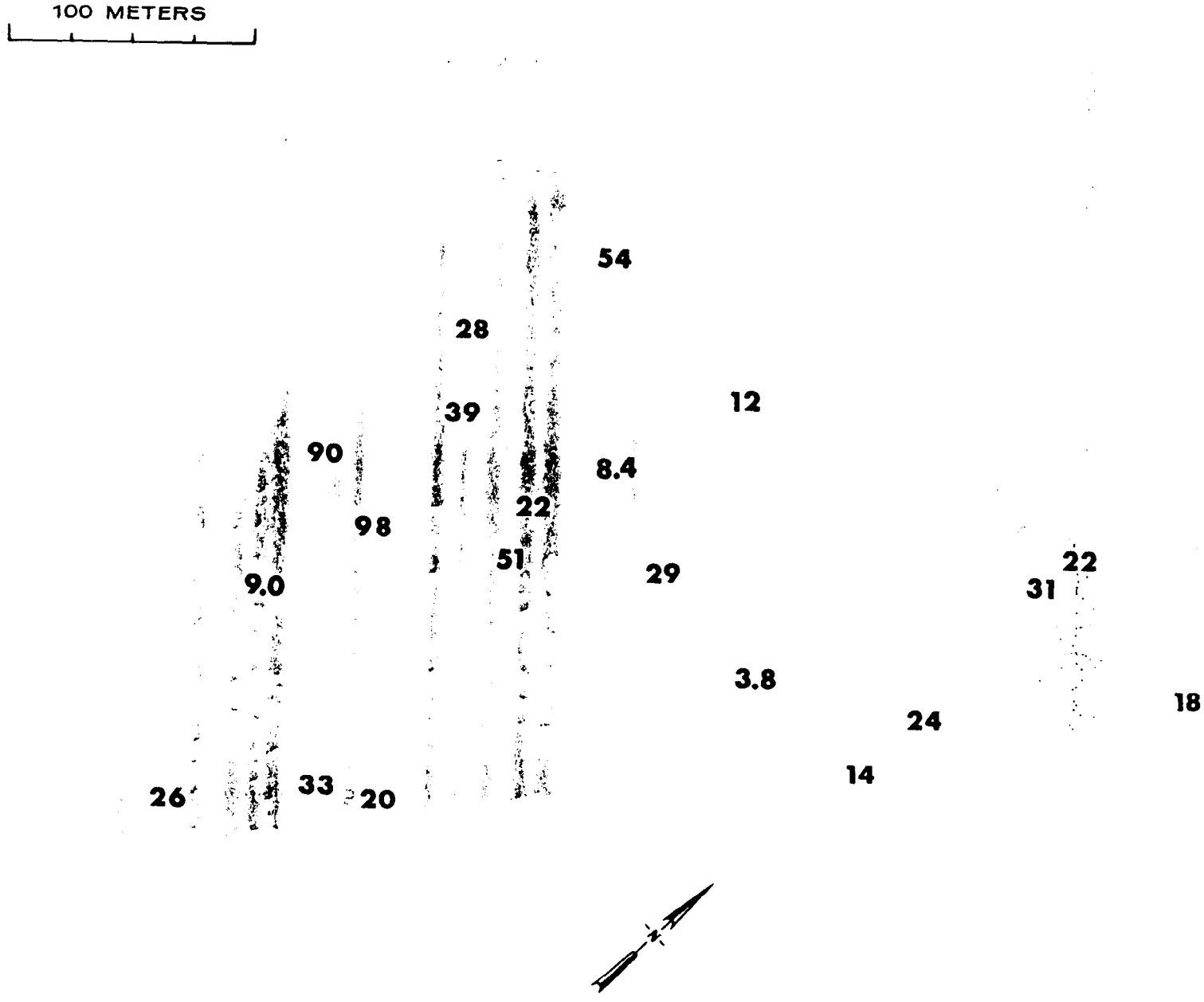

Fig. B.4.1.i. The average ^{239}Pu activities (pCi/g) in soil samples collected to a depth of 15 cm.

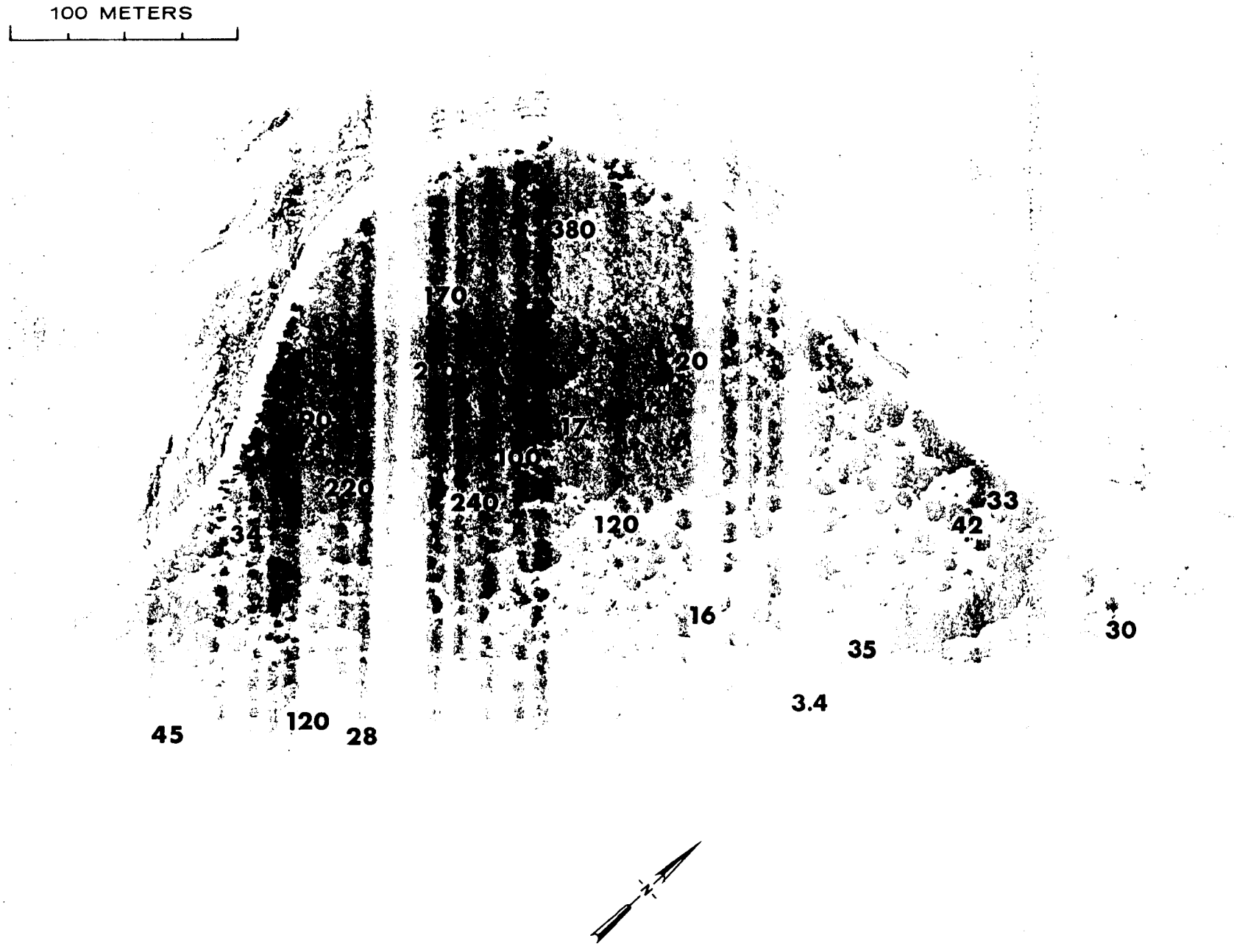

Fig. B.4.1.j. The average ^{90}Sr activities (pCi/g) in soil samples collected to a depth of 15 cm.

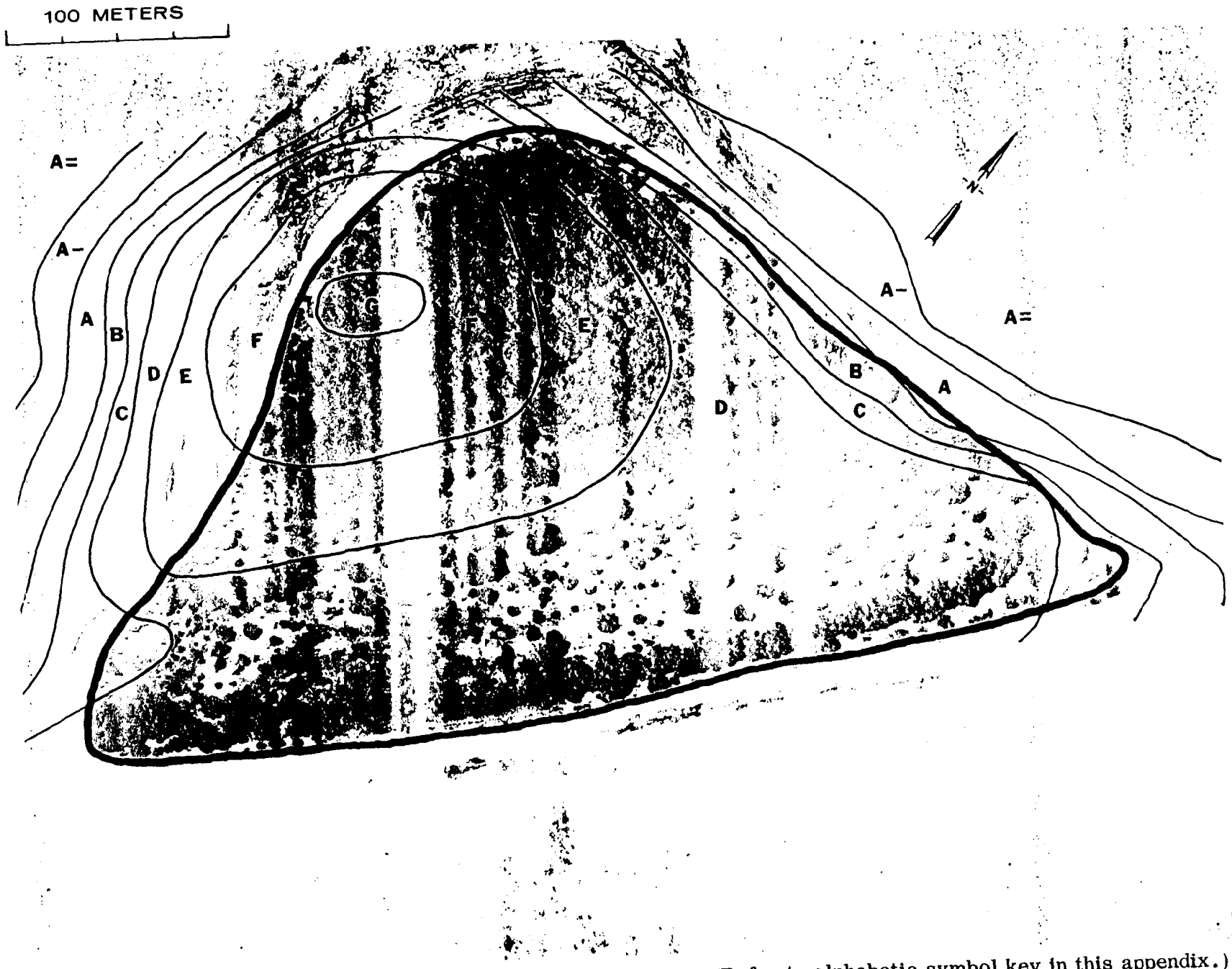

Fig. B.4.1.k. ^{137}Cs isoexposure and isoconcentration contours. (Refer to alphabetic symbol key in this appendix.)

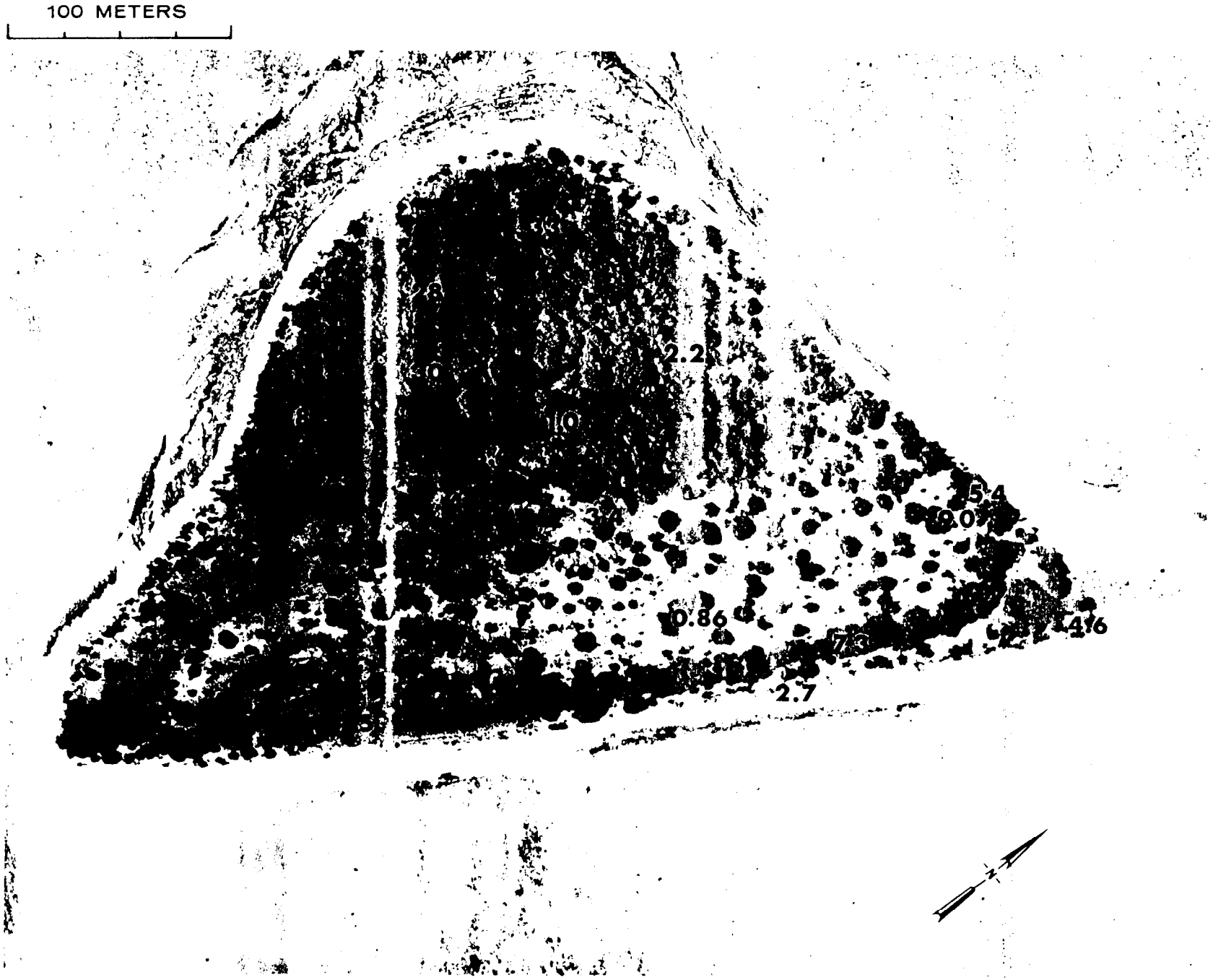

Fig. B.4.1.1. The average ^{137}Cs activities (pCi/g) in soil samples collected to a depth of 15 cm.

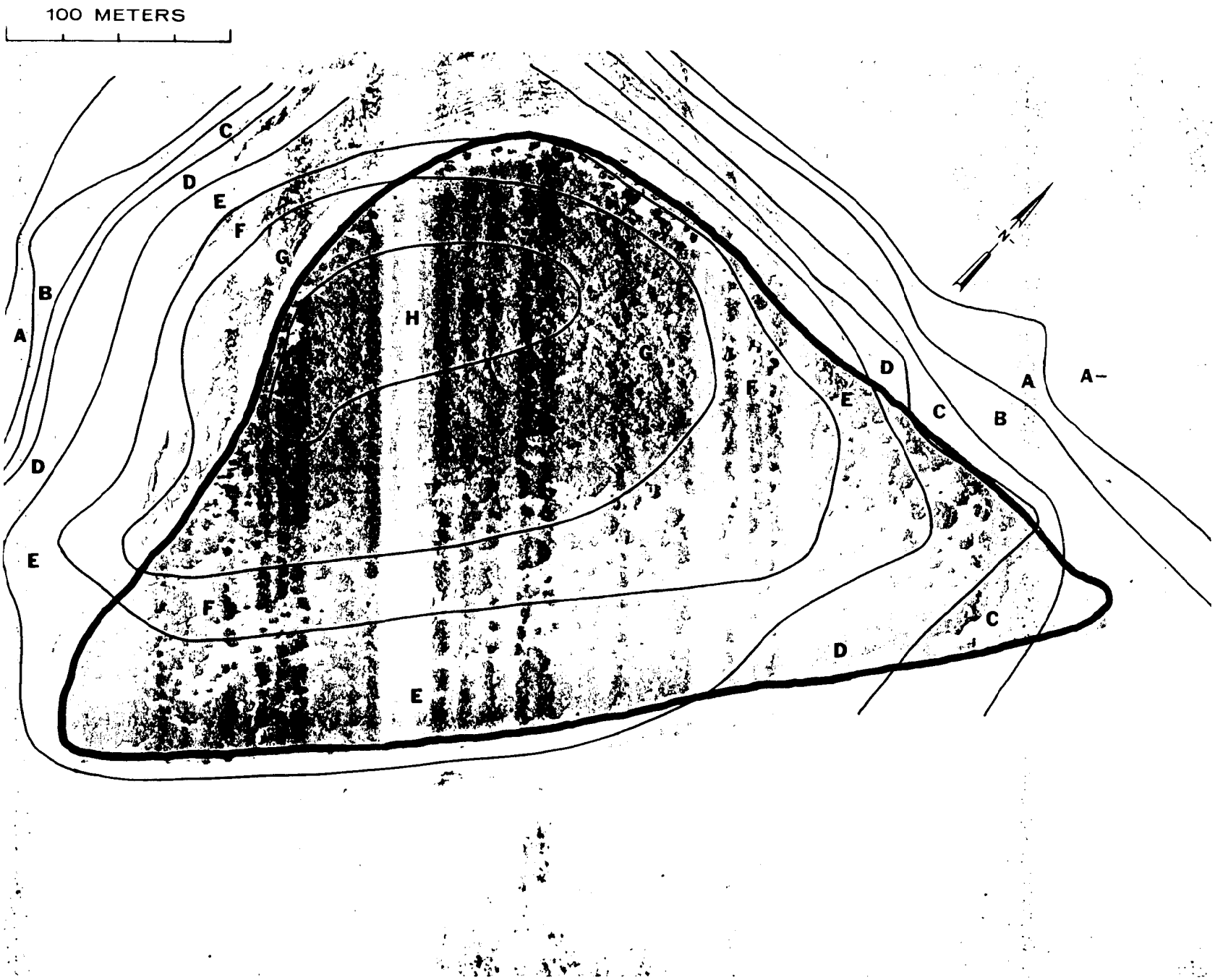

Fig. B.4.1.m. ^{60}Co isoexposure and isoconcentration contours. (Refer to alphabetic symbol key in this appendix.)

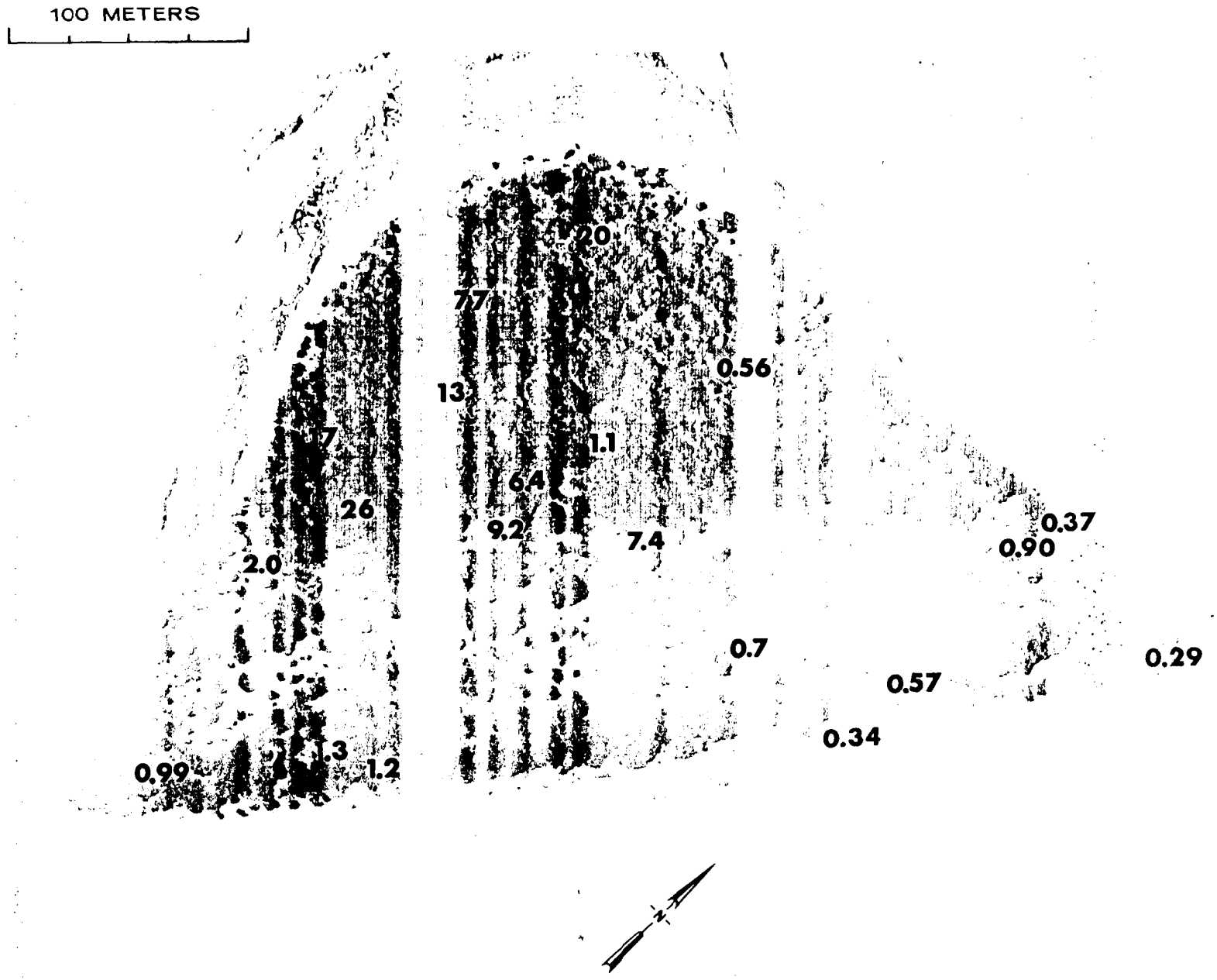

Fig. B.4.1.n. The average ^{60}Co activities (pCi/g) in soil samples collected to a depth of 15 cm.

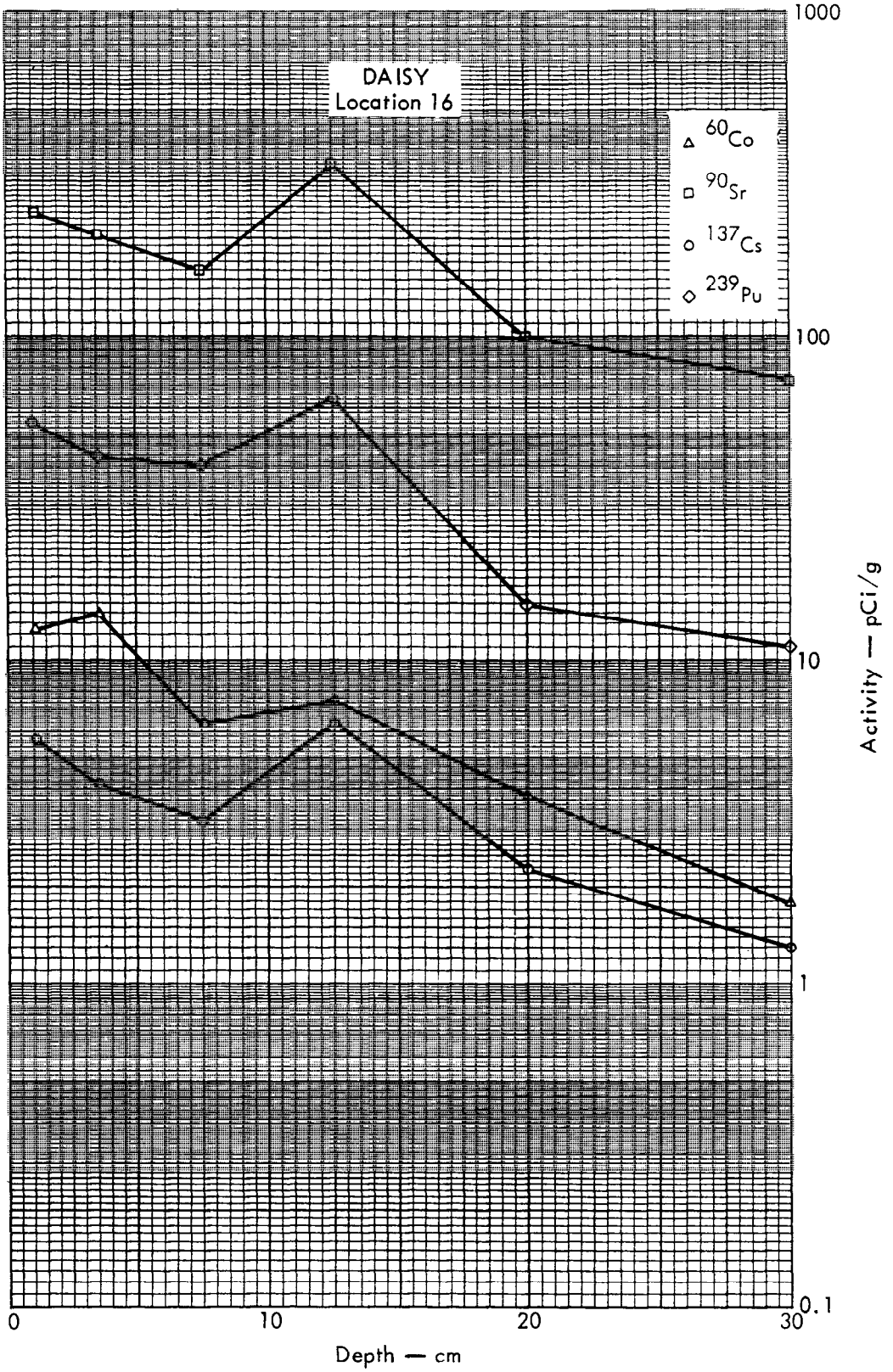

Fig. B.4.2a. Activities of selected radionuclides as a function of soil depth.

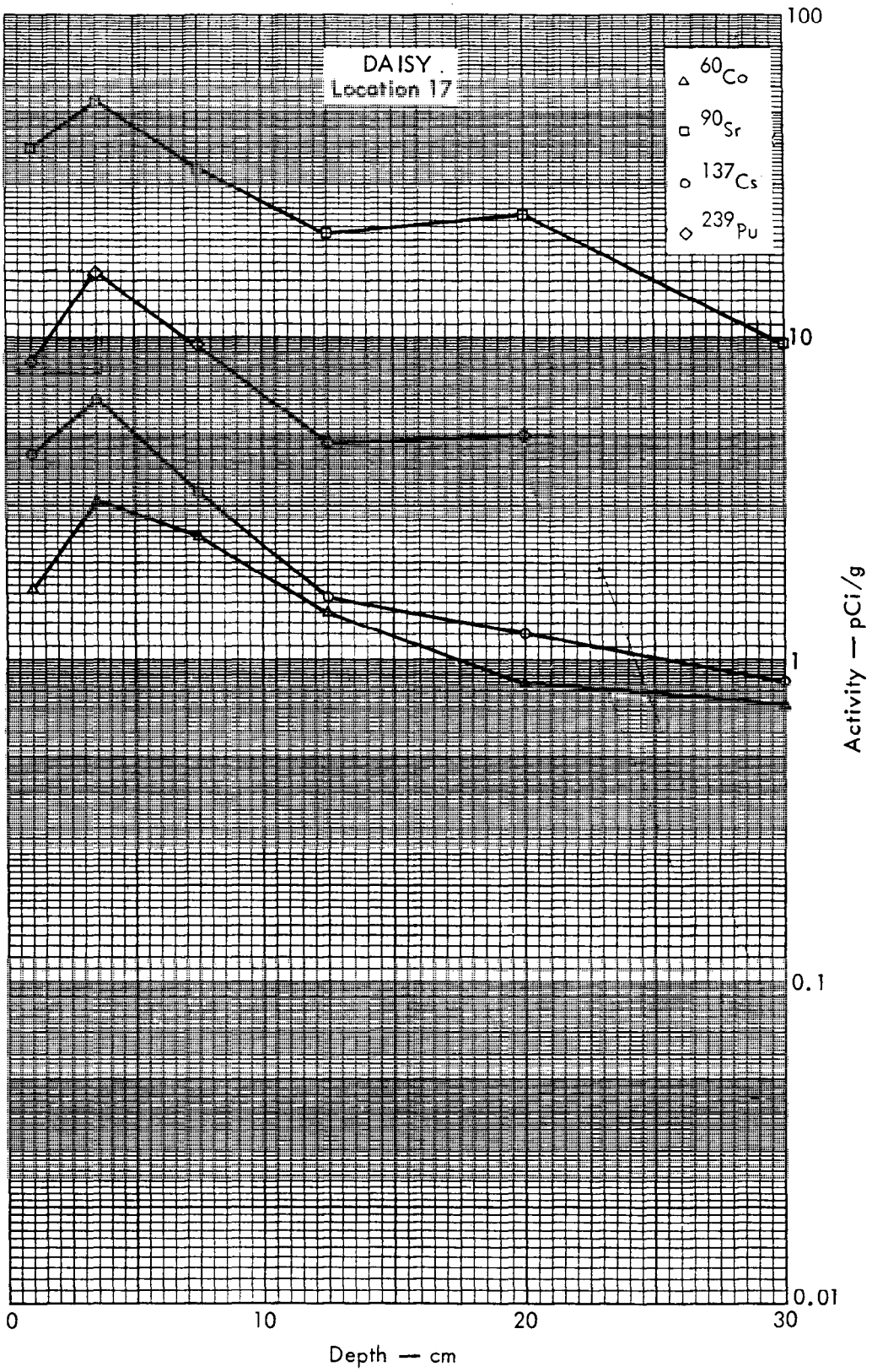

Fig. B.4.2b. Activities of selected radionuclides as a function of soil depth.

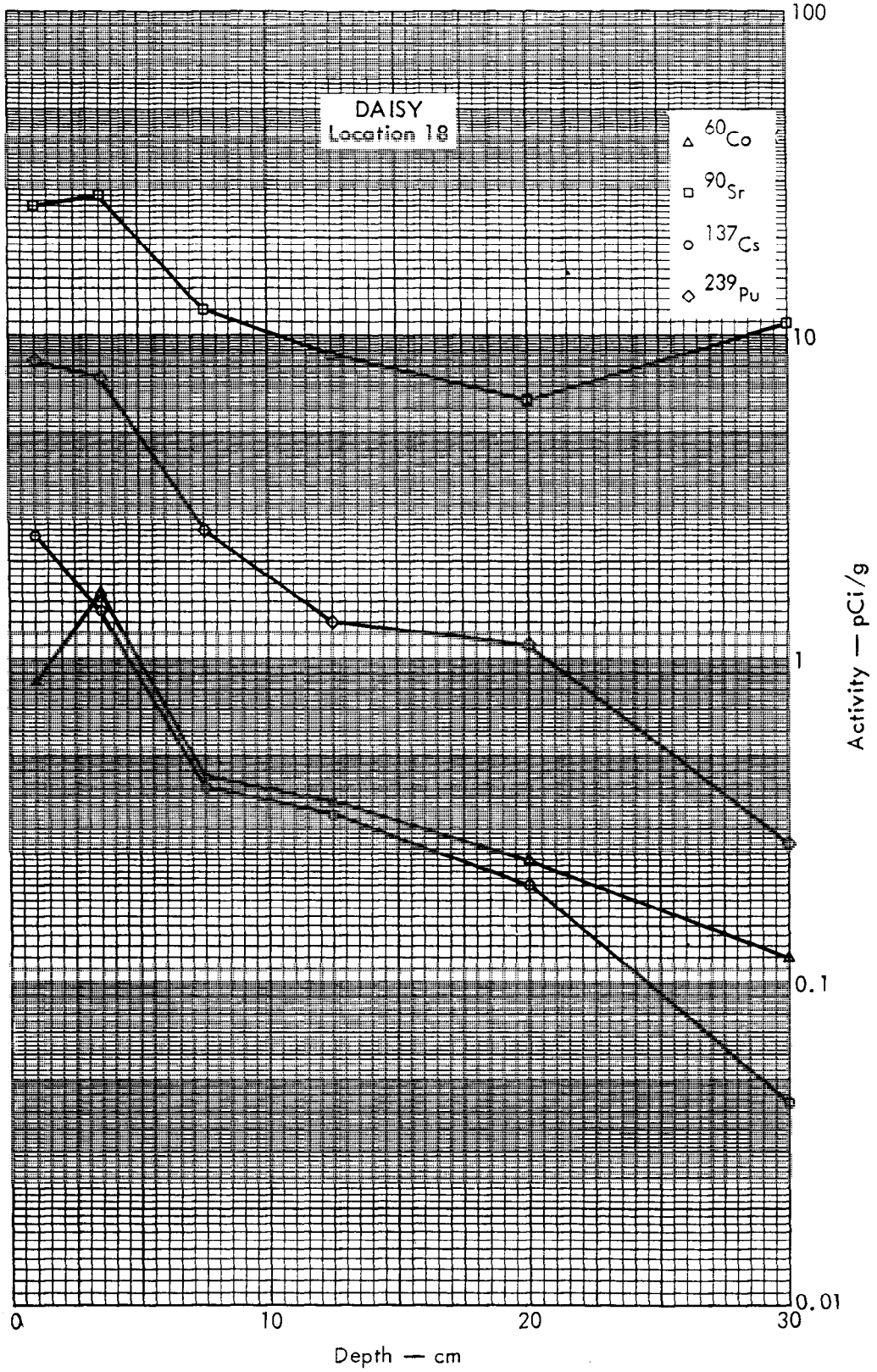

Fig. B. 4. 2c. Activities of selected radionuclides as a function of soil depth.

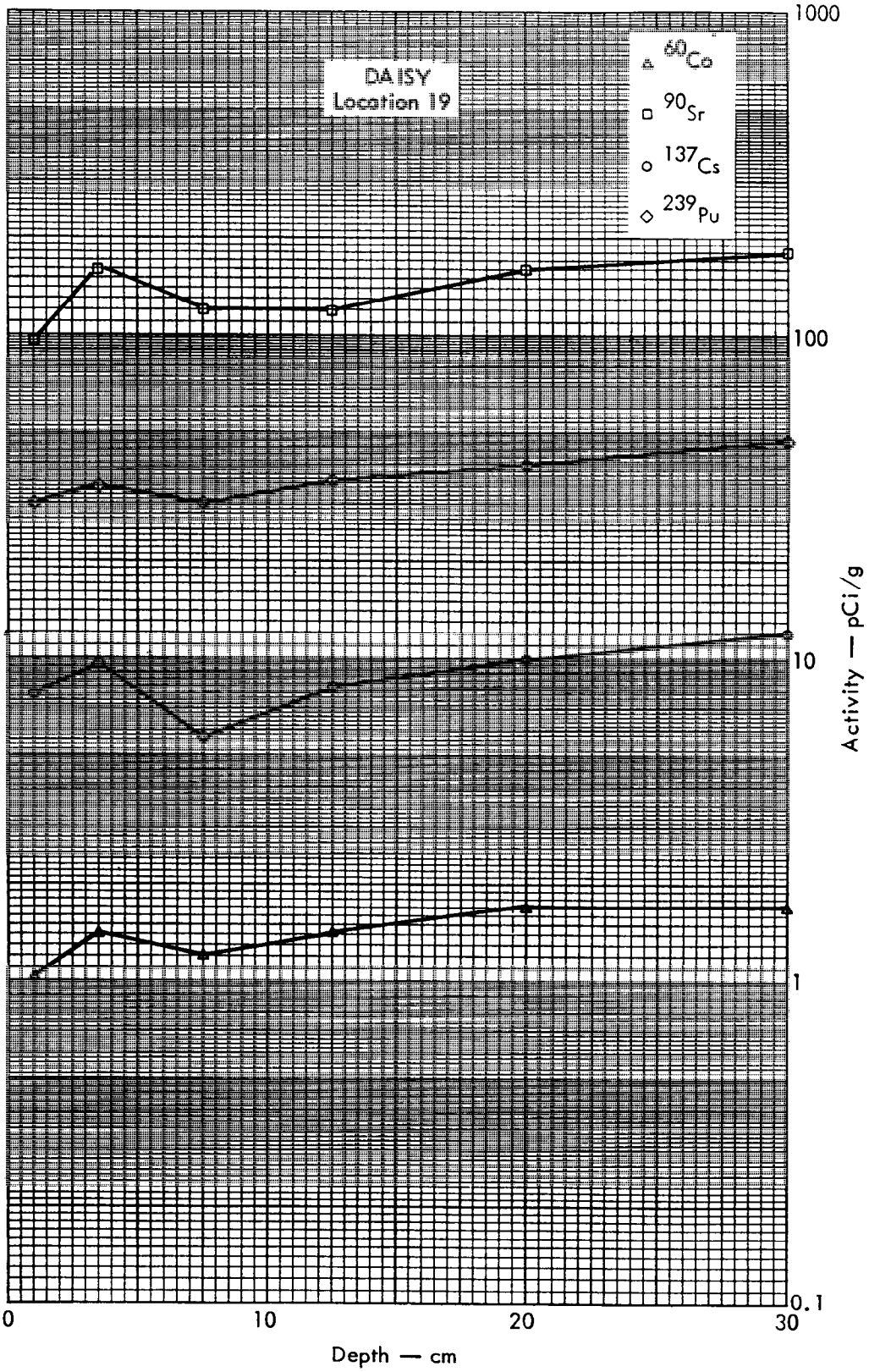

Fig. B. 4. 2d. Activities of selected radionuclides as a function of soil depth.

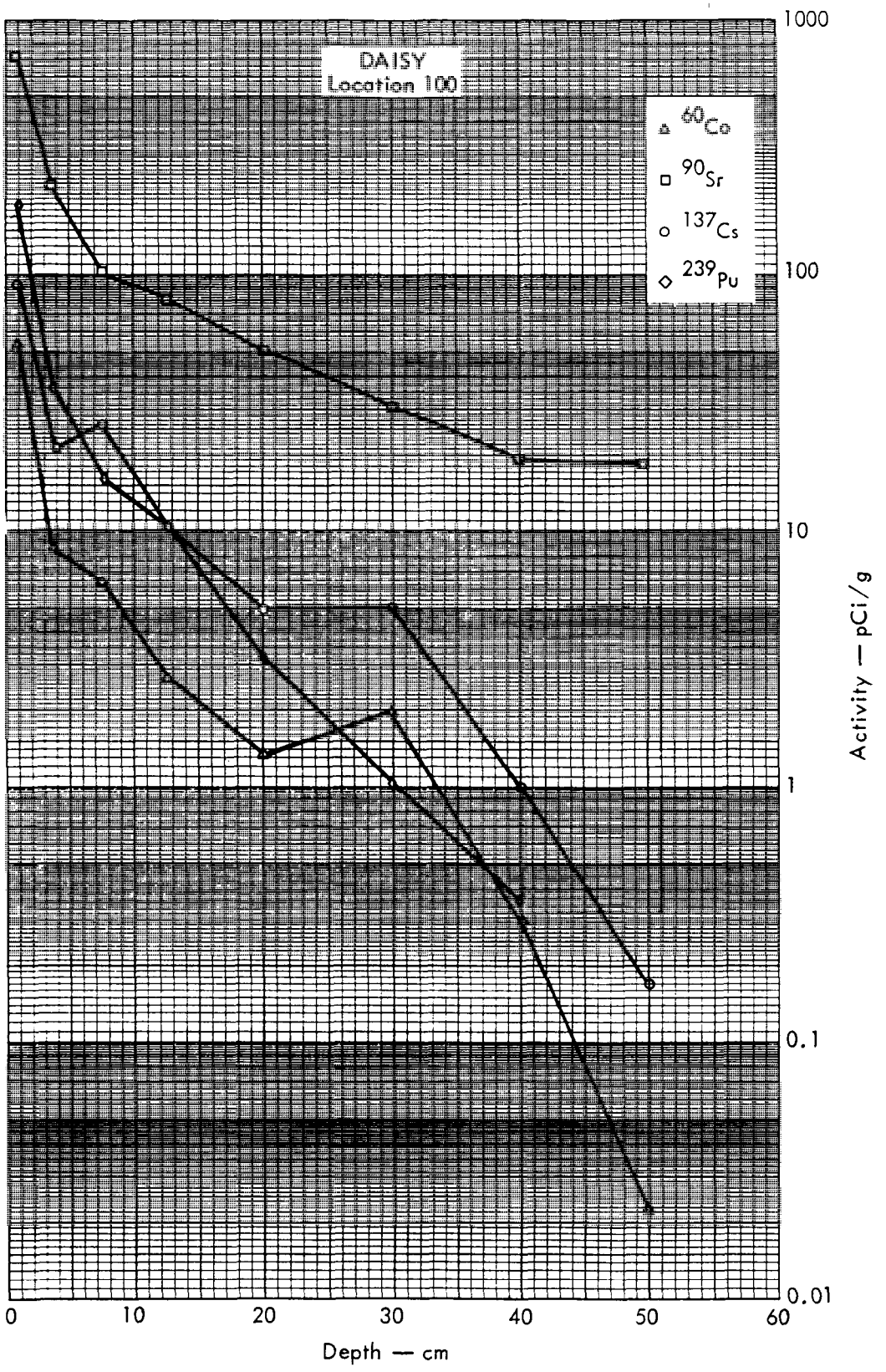

Fig. B.4.2e. Activities of selected radionuclides as a function of soil depth.

Fig. B.5.1.a.

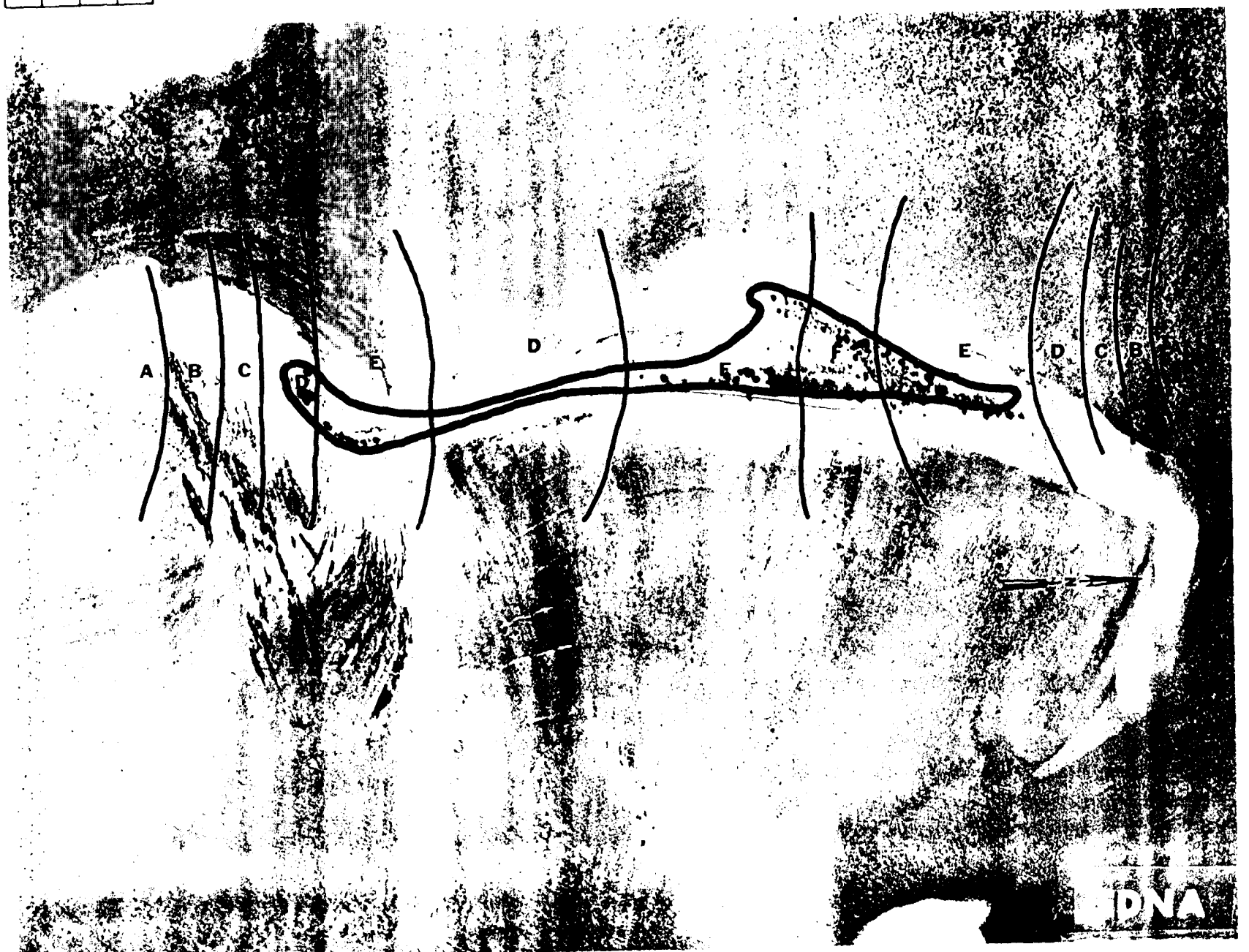

Fig. B.5.1.b. Gross count isoexposure contours. (Refer to alphabetic symbol key in this appendix.)

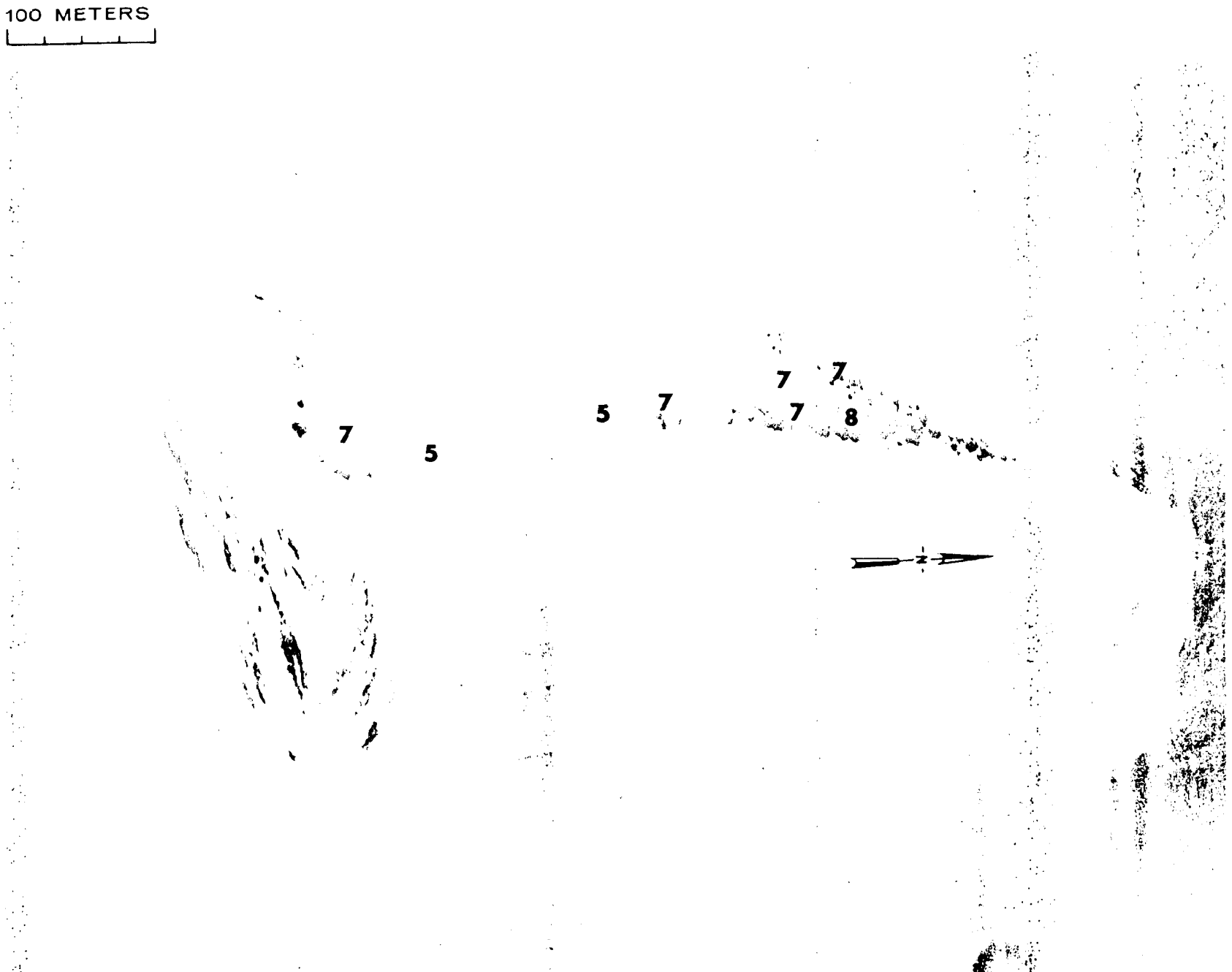

Fig. B.5.1.d. The gamma background exposure rate (μR/hr) at 1 m above the ground, measured with a portable NaI scintillation counter.

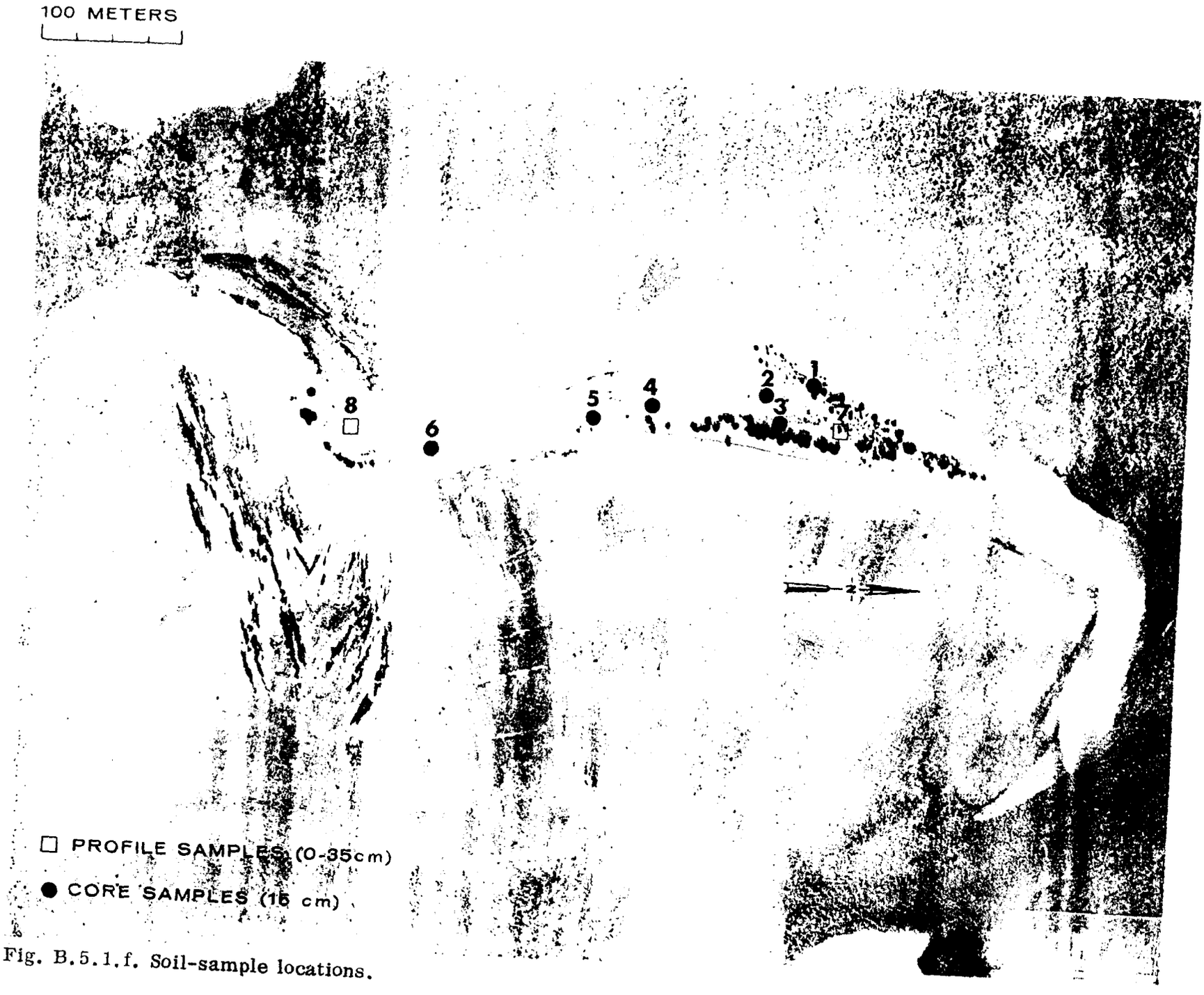

Fig. B.5.1.f. Soil-sample locations.

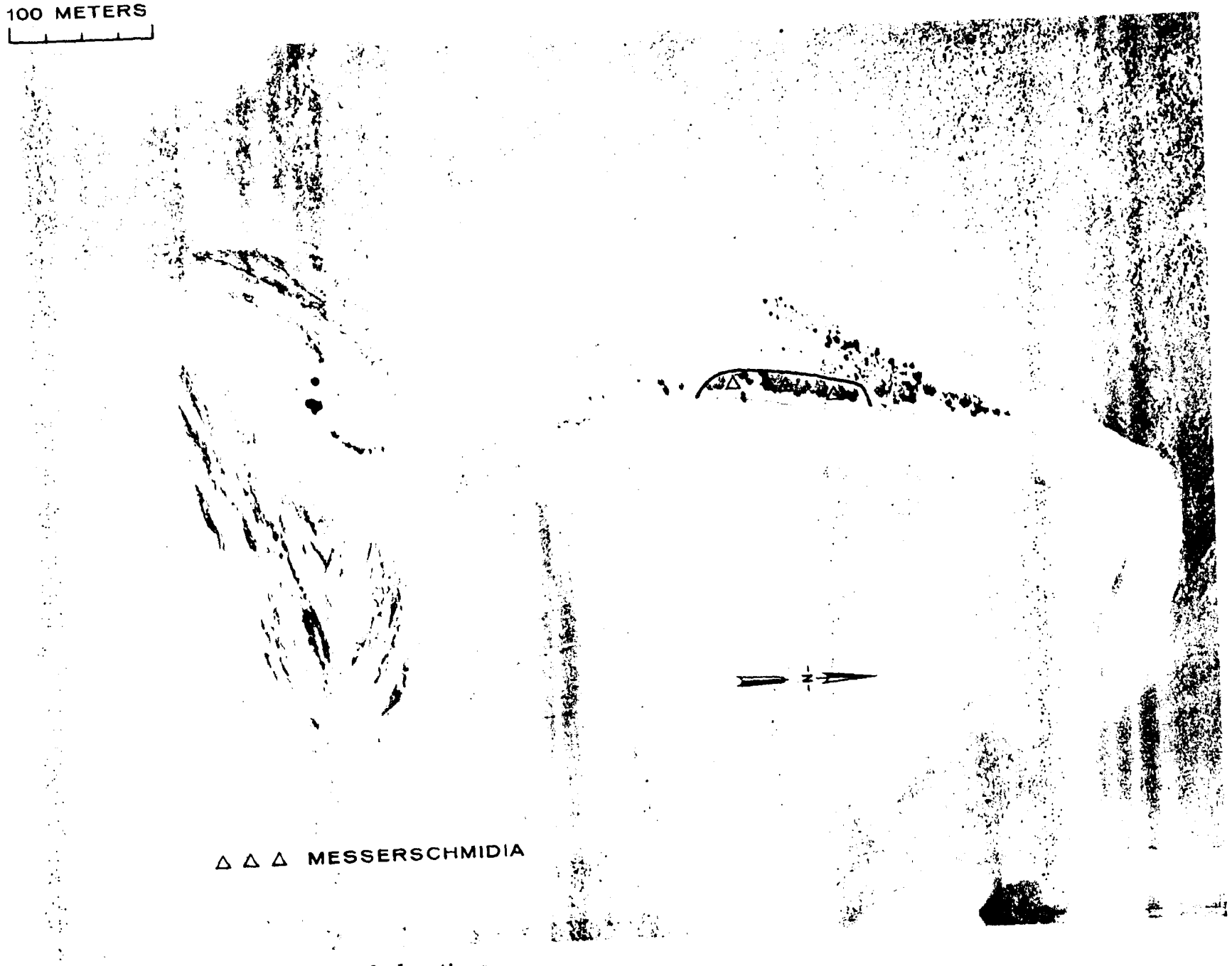

Fig. B.5.1.g. Vegetation sample locations.

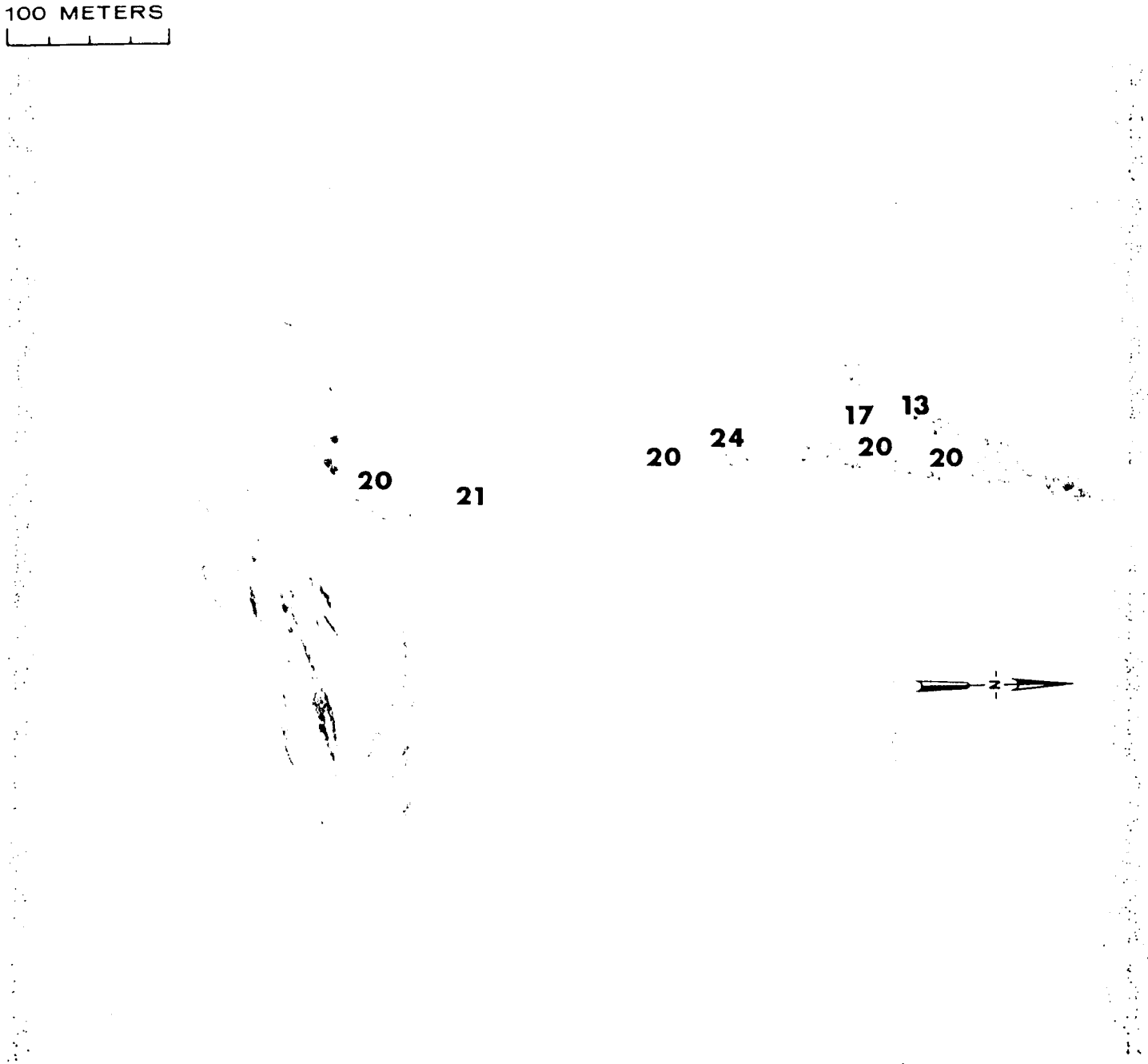

Fig. B.5.1.i. The average ^{239}Pu activities (pCi/g) in soil samples collected to a depth of 15 cm.

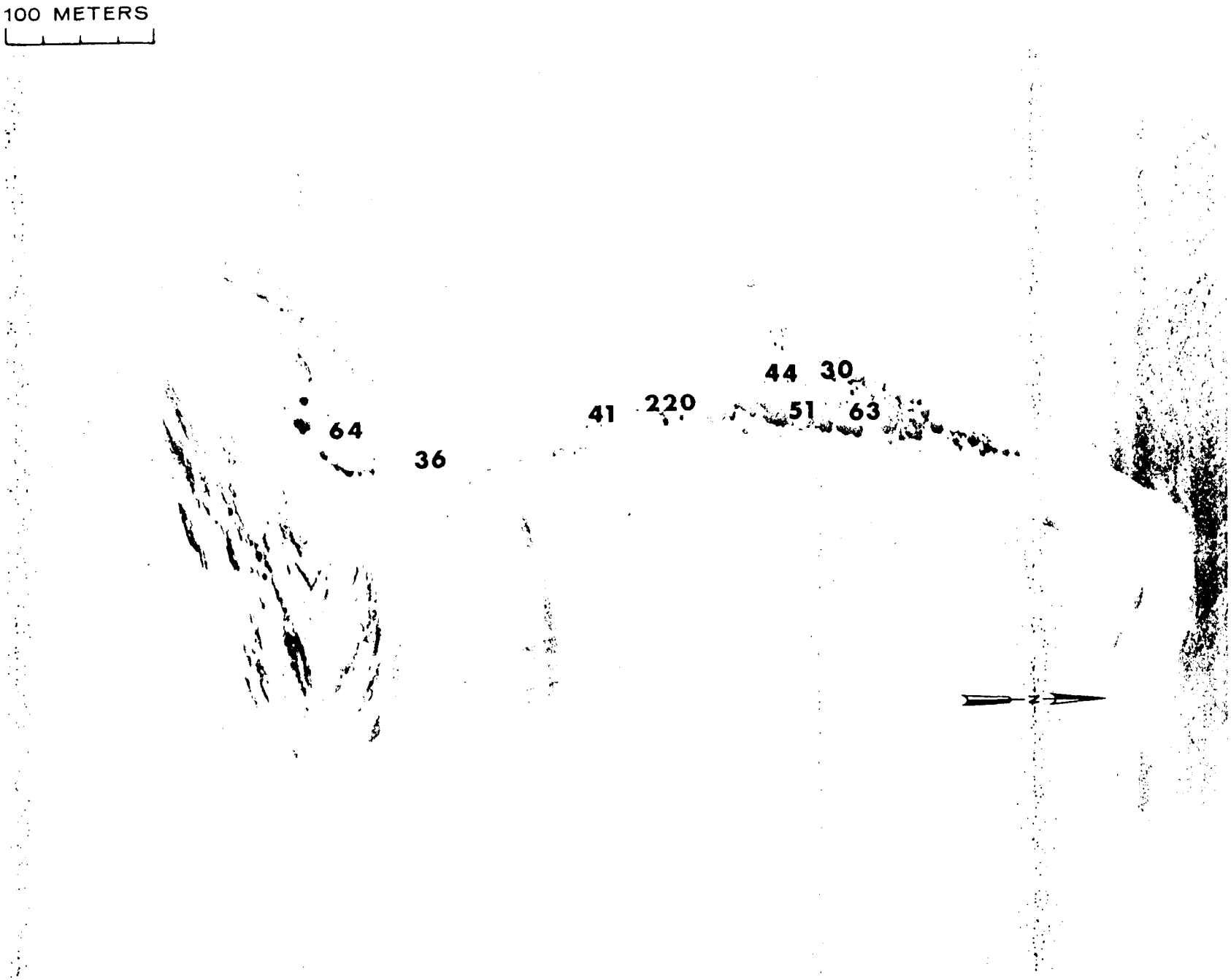

Fig. B.5.1.j. The average ^{90}Sr activities (pCi/g) in soil samples collected to a depth of 15 cm.

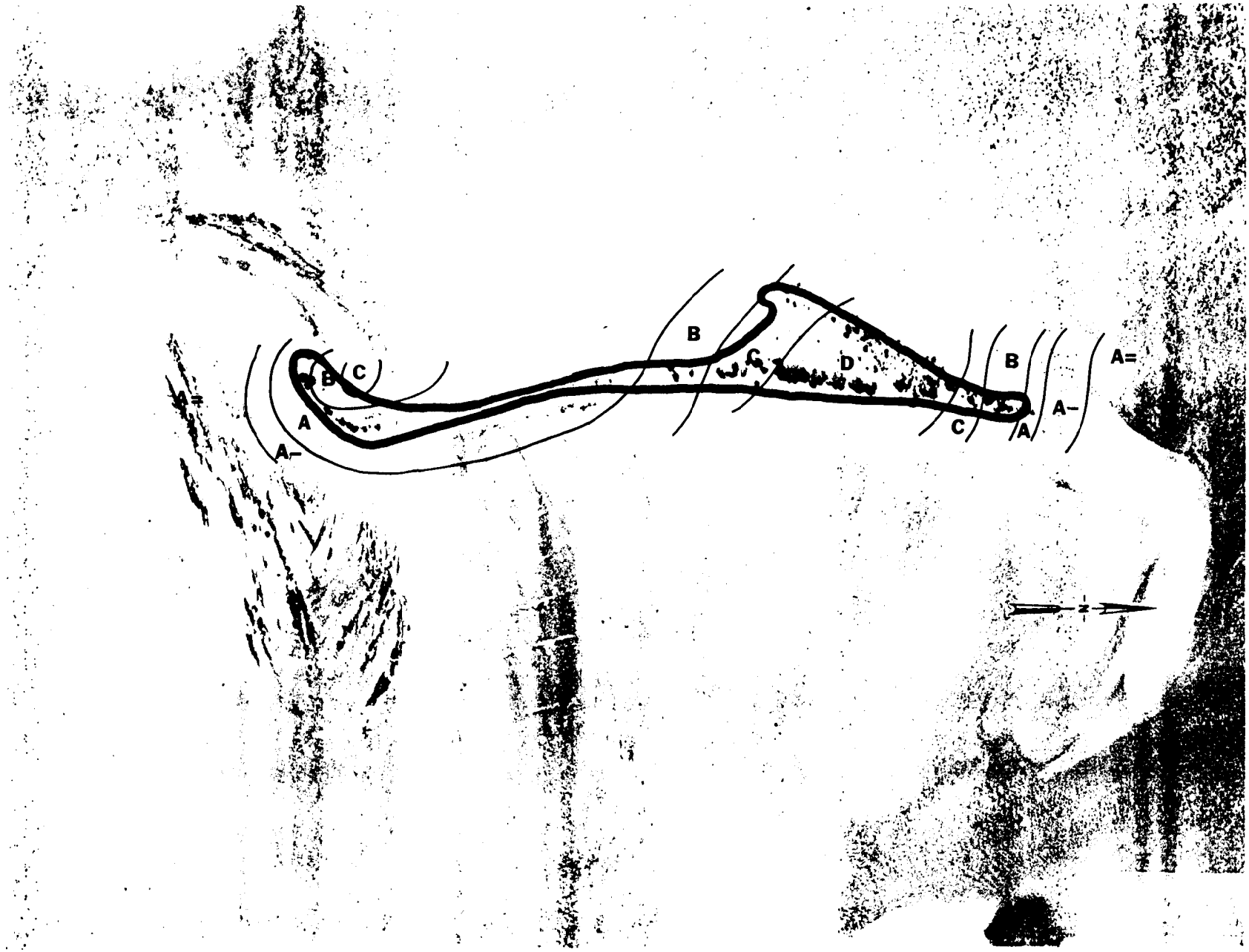

Fig. B.5.1.k. ^{137}Cs isoexposure and isoconcentration contours. (Refer to alphabetic symbol key in this appendix.)

Fig. B.5.1.1. The average ^{137}Cs activities (pCi/g) in soil samples collected to a depth of 15 cm.

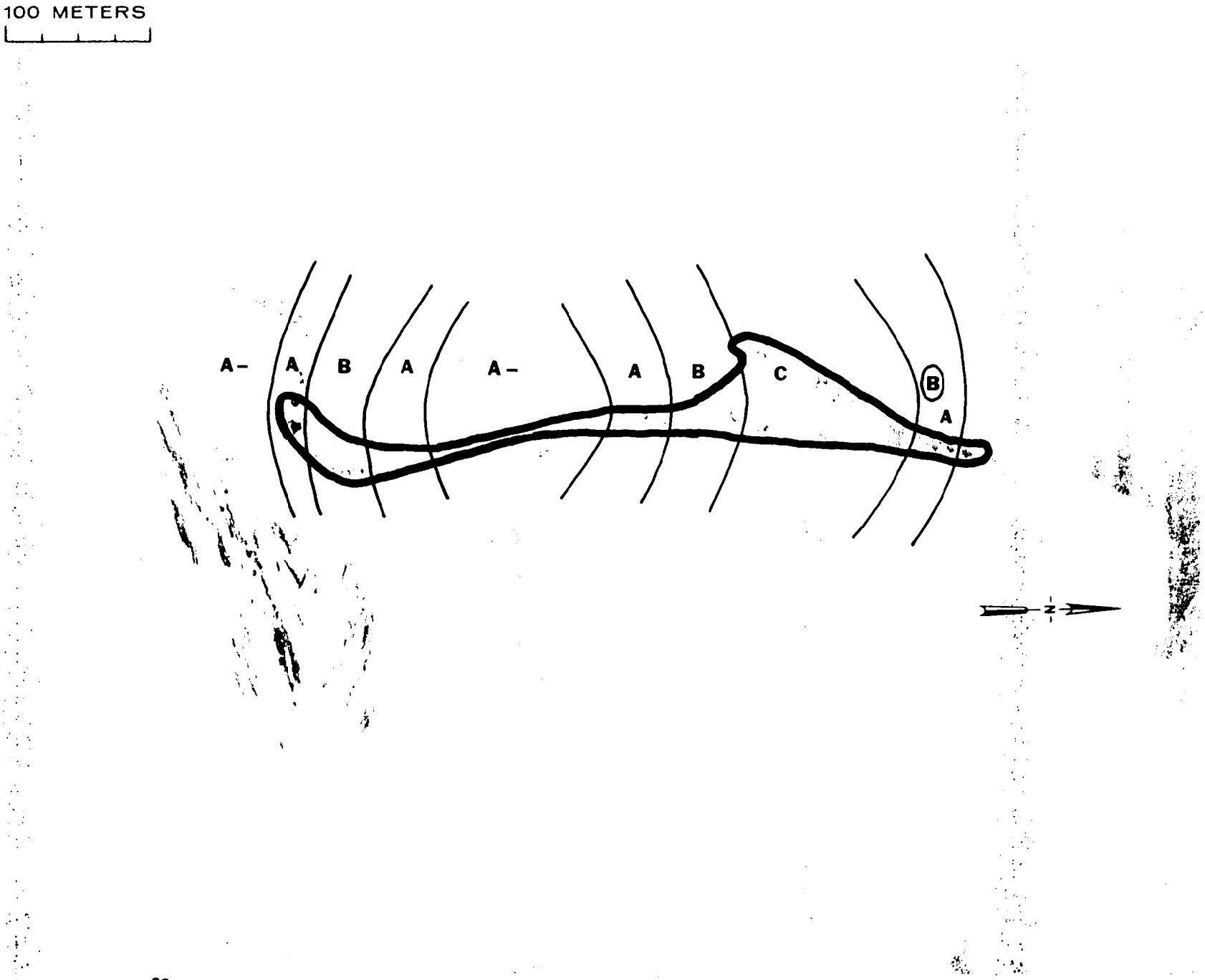

Fig. B.5.1.m. ^{60}Co **isoexposure** and isoconcentration contours. (Refer to alphabetic symbol key in this appendix.)

Fig. B.5.1.n. The average ^{60}Co activities (pCi/g) in soil samples collected to a depth of 15 cm.

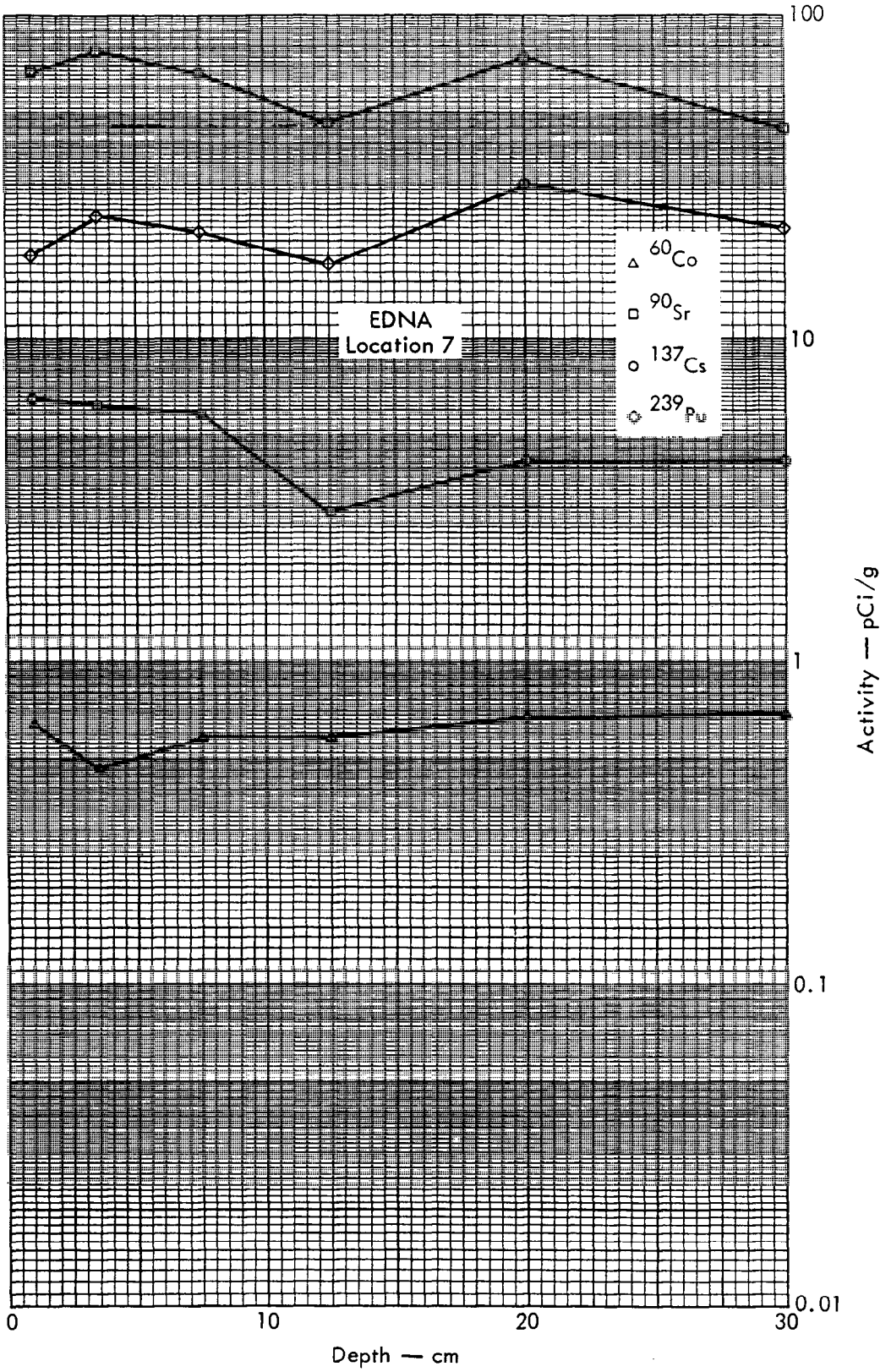

Fig. B.5.2a. Activities of selected radionuclides as a function of soil depth.

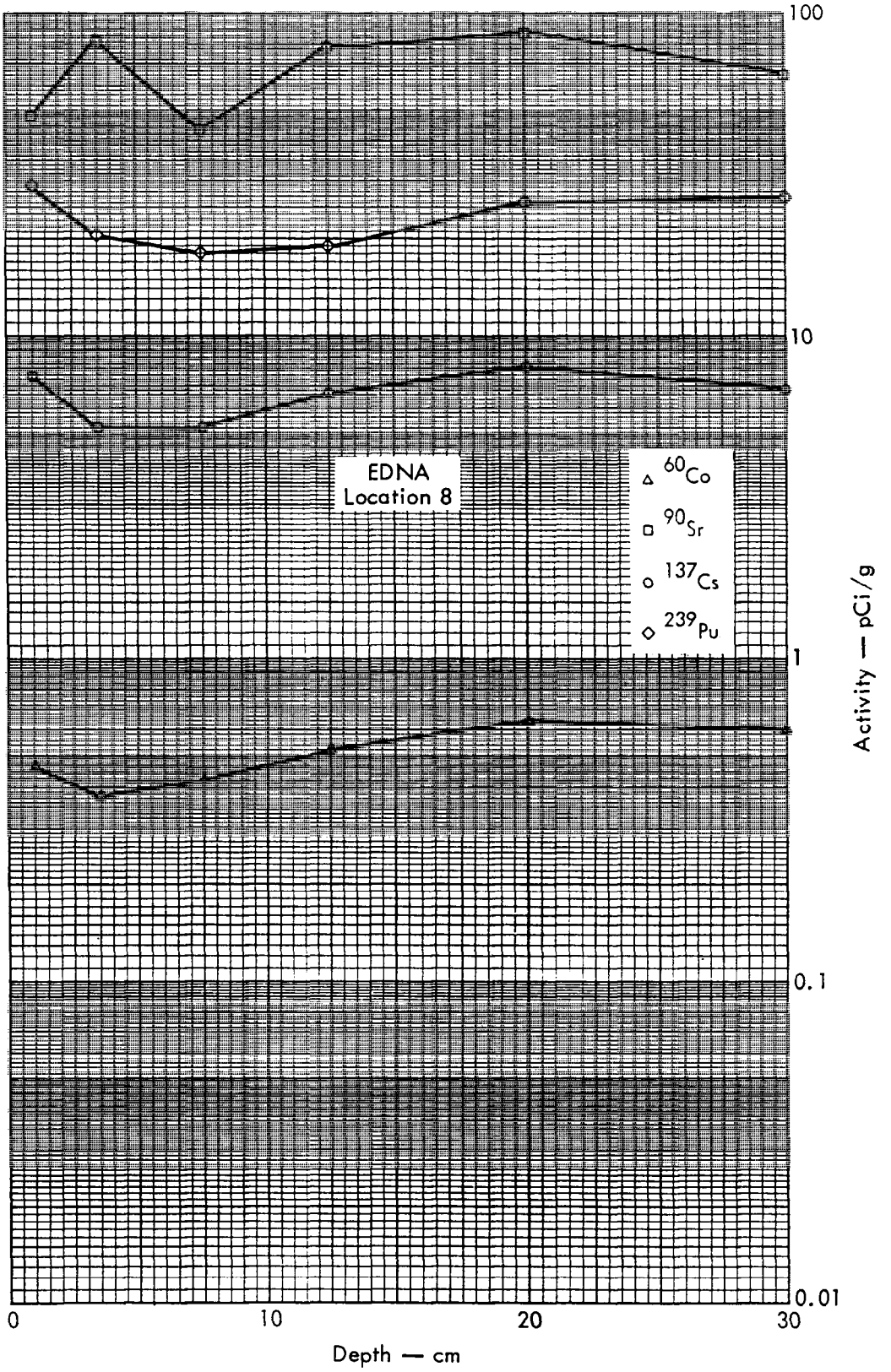

Fig. B.5.2b. Activities of selected radionuclides as a function of soil depth.

Fig. B.6.1.a.

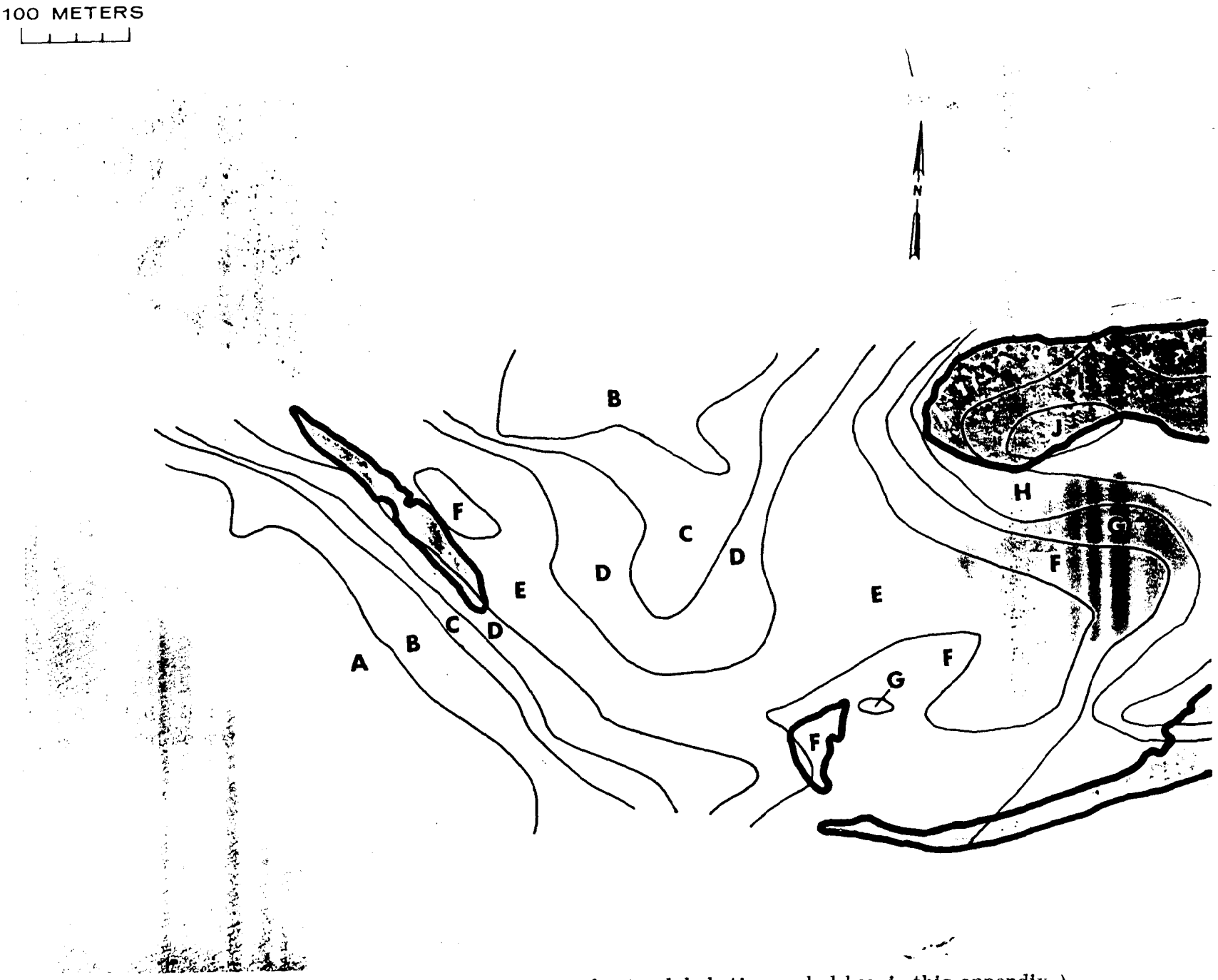

Fig. B.6.1.b. Gross count isoexposure contours. (Refer to alphabetic symbol key in this appendix.)

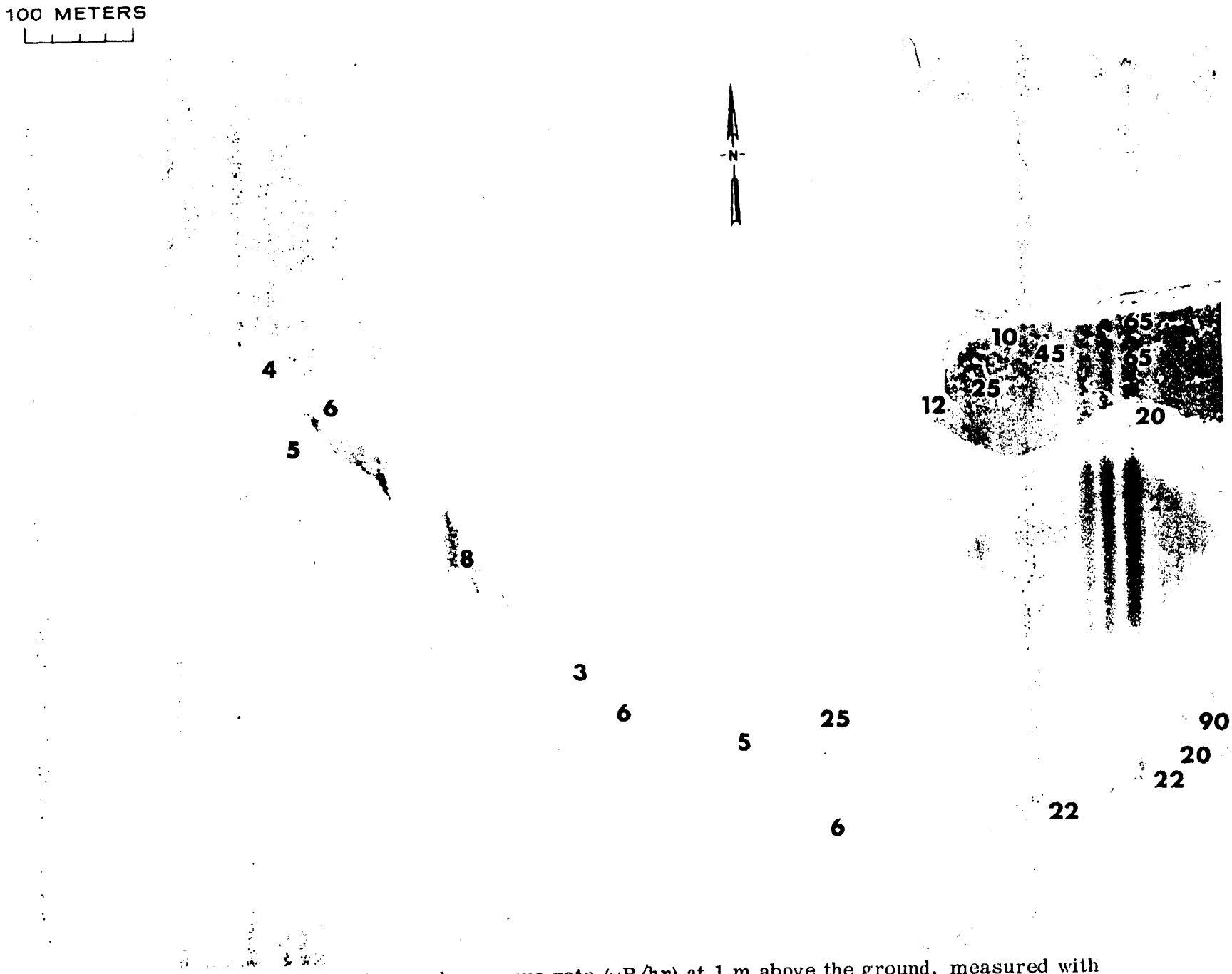

Fig. B.6.1.d. The gamma background exposure rate (μR/hr) at 1 m above the ground, measured with a portable NaI scintillation counter.

Fig. B.6.1.f. Soil-sample locations.

Fig. B.6.1.g. Vegetation sample locations.

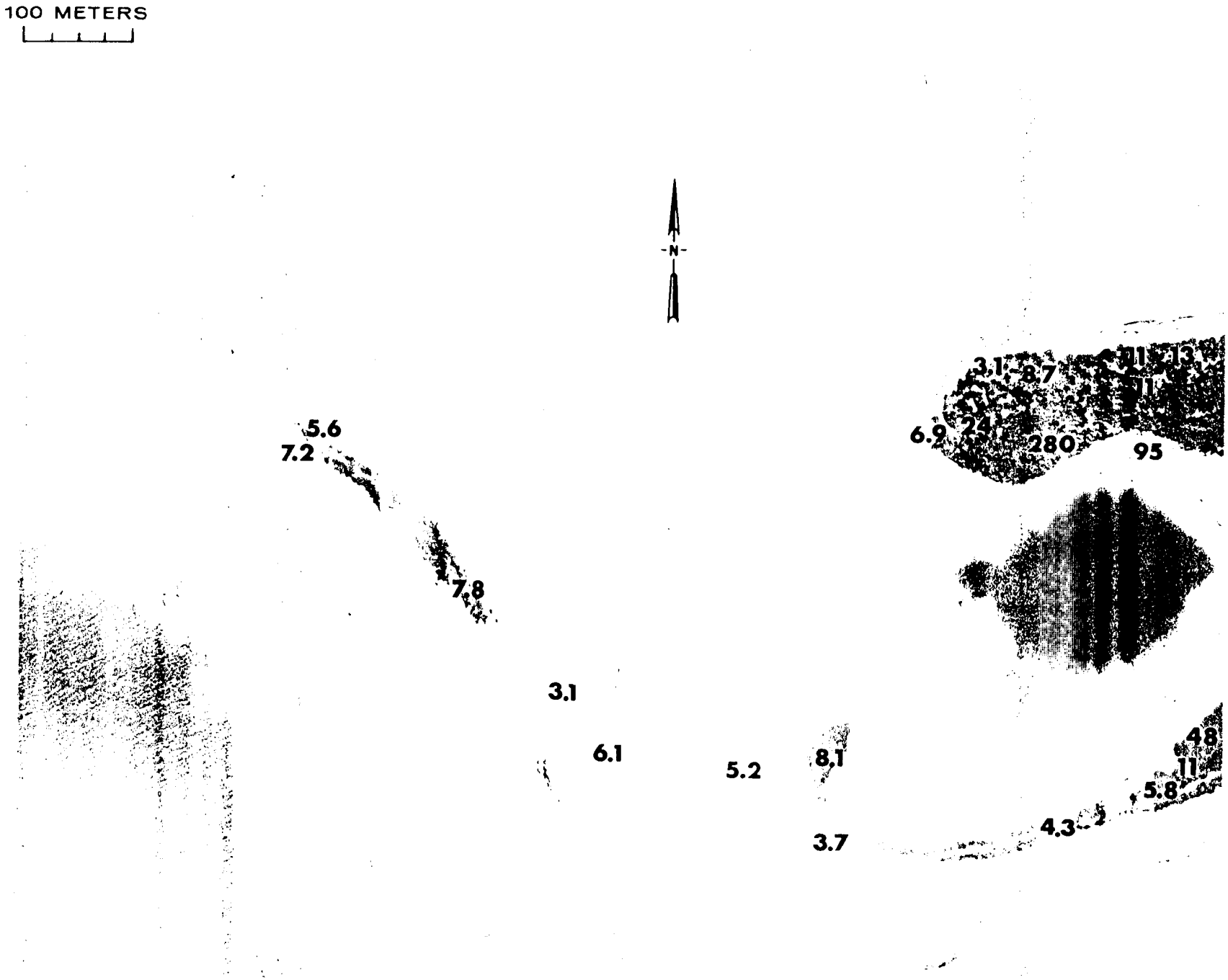

Fig. B.6.1.i. The average ^{239}Pu activities (pCi/gm) in soil samples collected to a depth of 15 cm.

Fig. B.6.1.j. The average ^{90}Sr activities (pCi/gm) in soil samples collected to a depth of 15 cm.

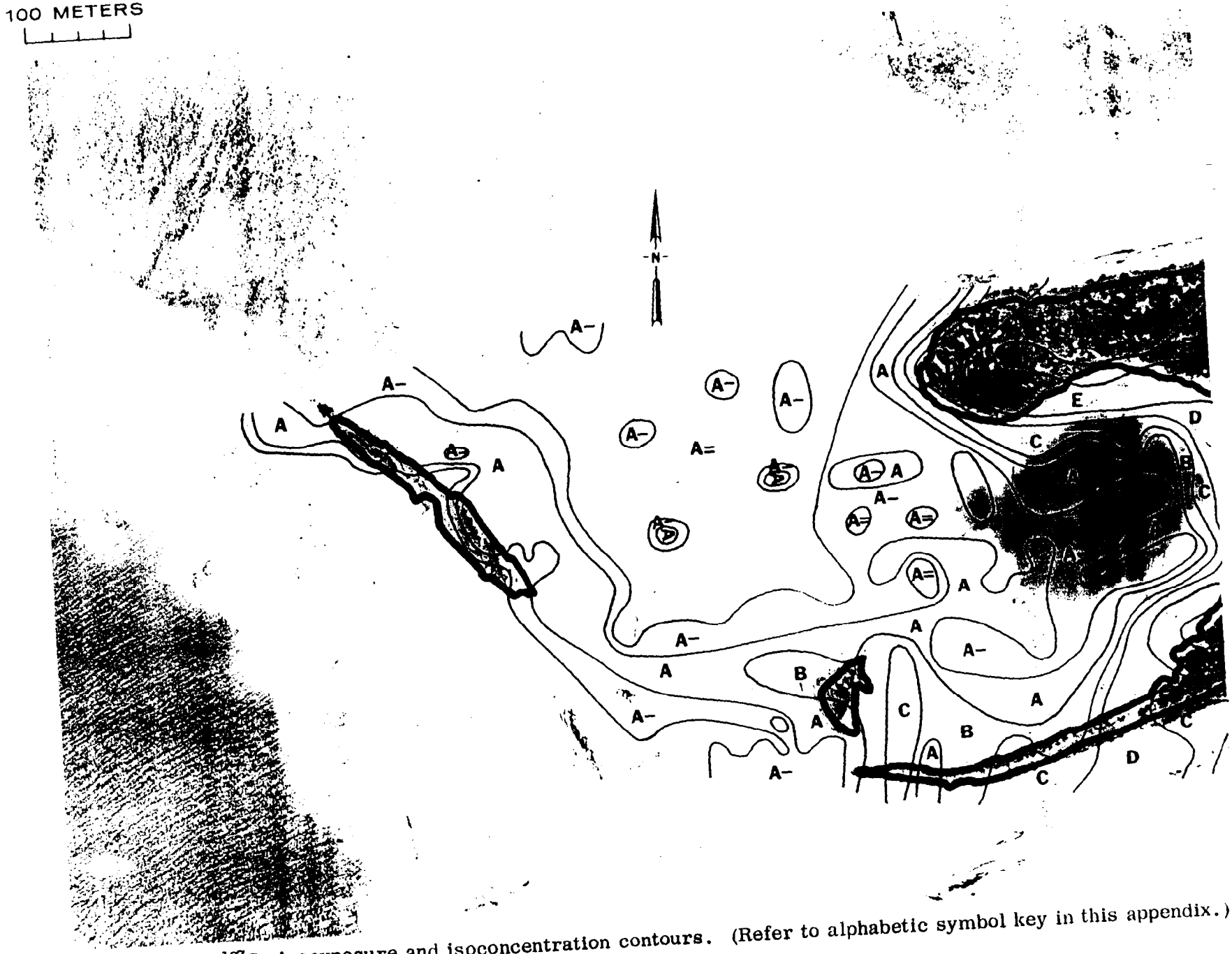

Fig. B.6.1.k. ^{137}Cs isoexposure and isoconcentration contours. (Refer to alphabetic symbol key in this appendix.)

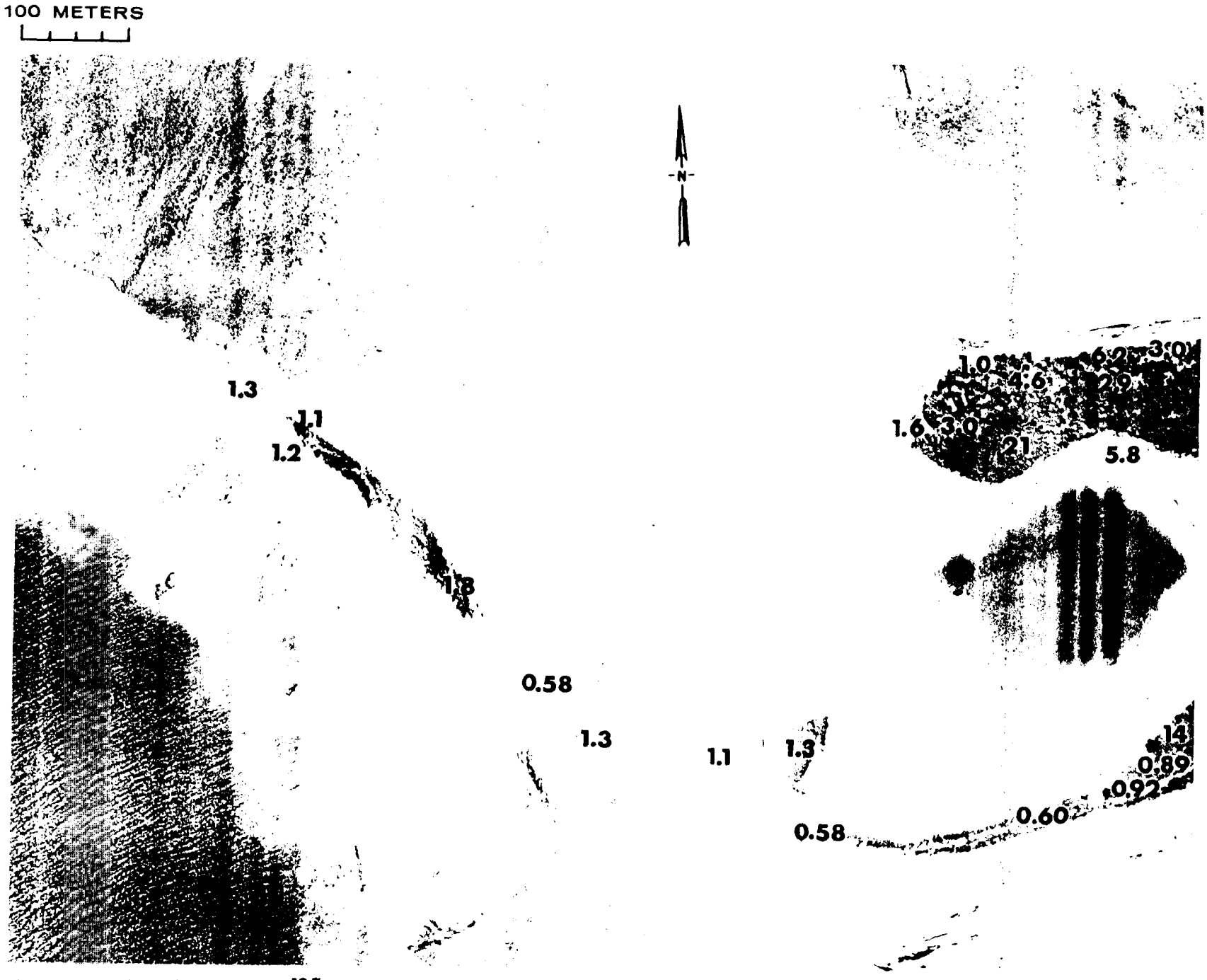

Fig. B.6.1.1. The average ^{137}Cs activities (pCi/gm) in soil samples collected to a depth of 15 cm.

Fig. B.6.1.m. ^{60}Co isoexposure and isoconcentration contours. (Refer to alphabetic symbol key in this appendix.)

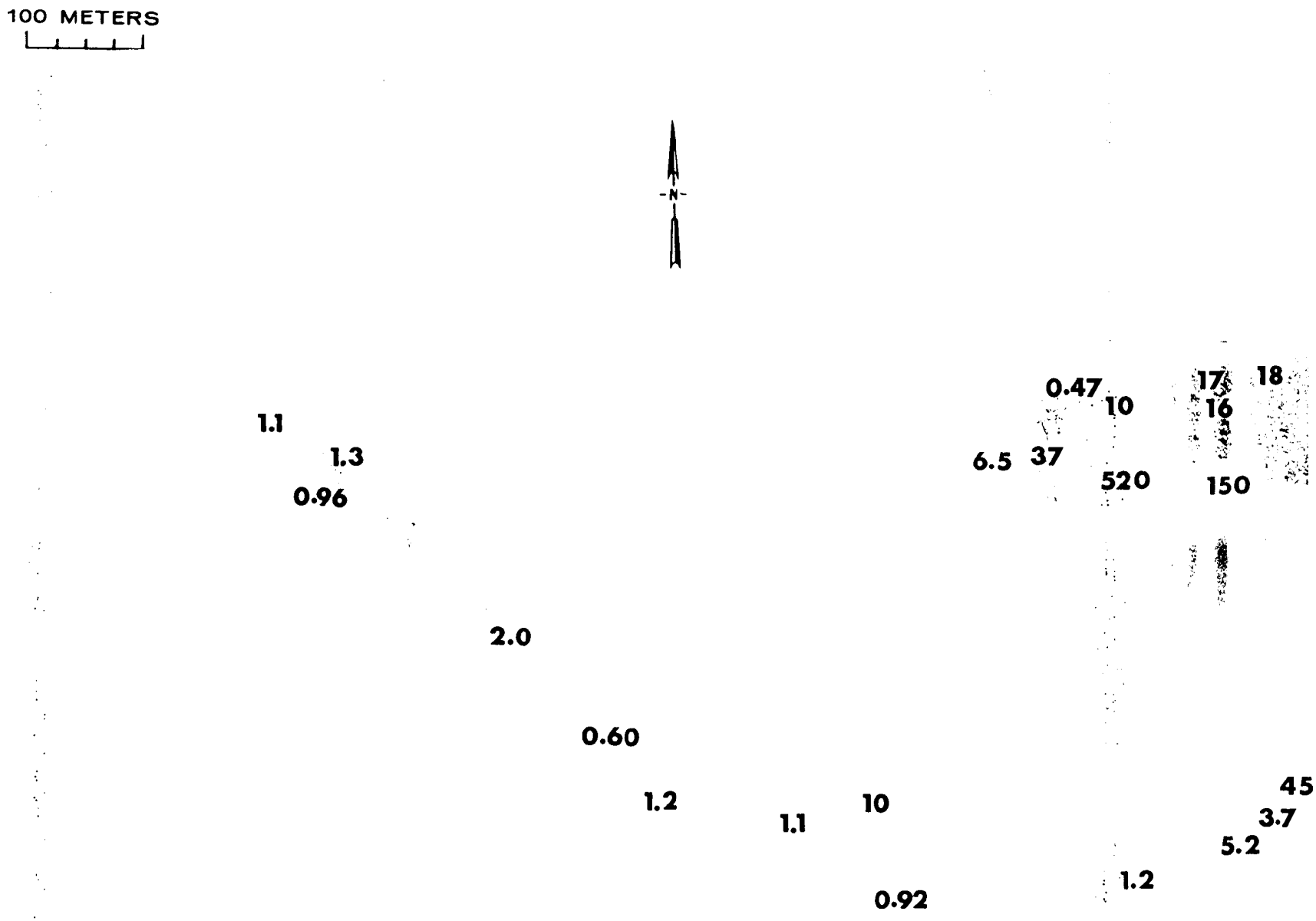

Fig. B.6.1.n. The average ^{60}Co activities (pCi/gm) in soil samples collected to a depth of 15 cm.

Fig. B.6.1.o. Terrestrial animal sample locations.

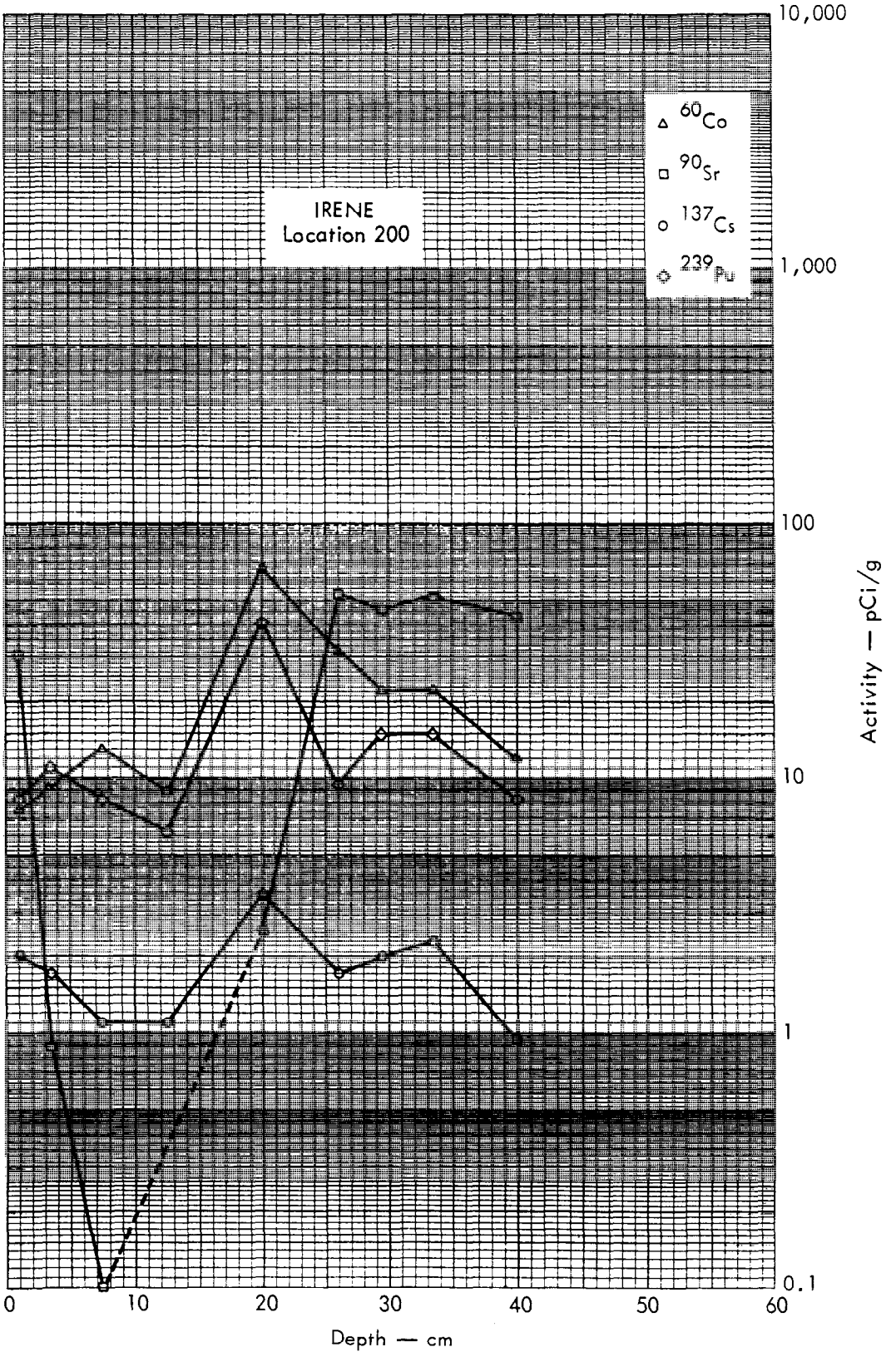

Fig. B. 6.2a. Activities of selected radionuclides as a function of soil depth.

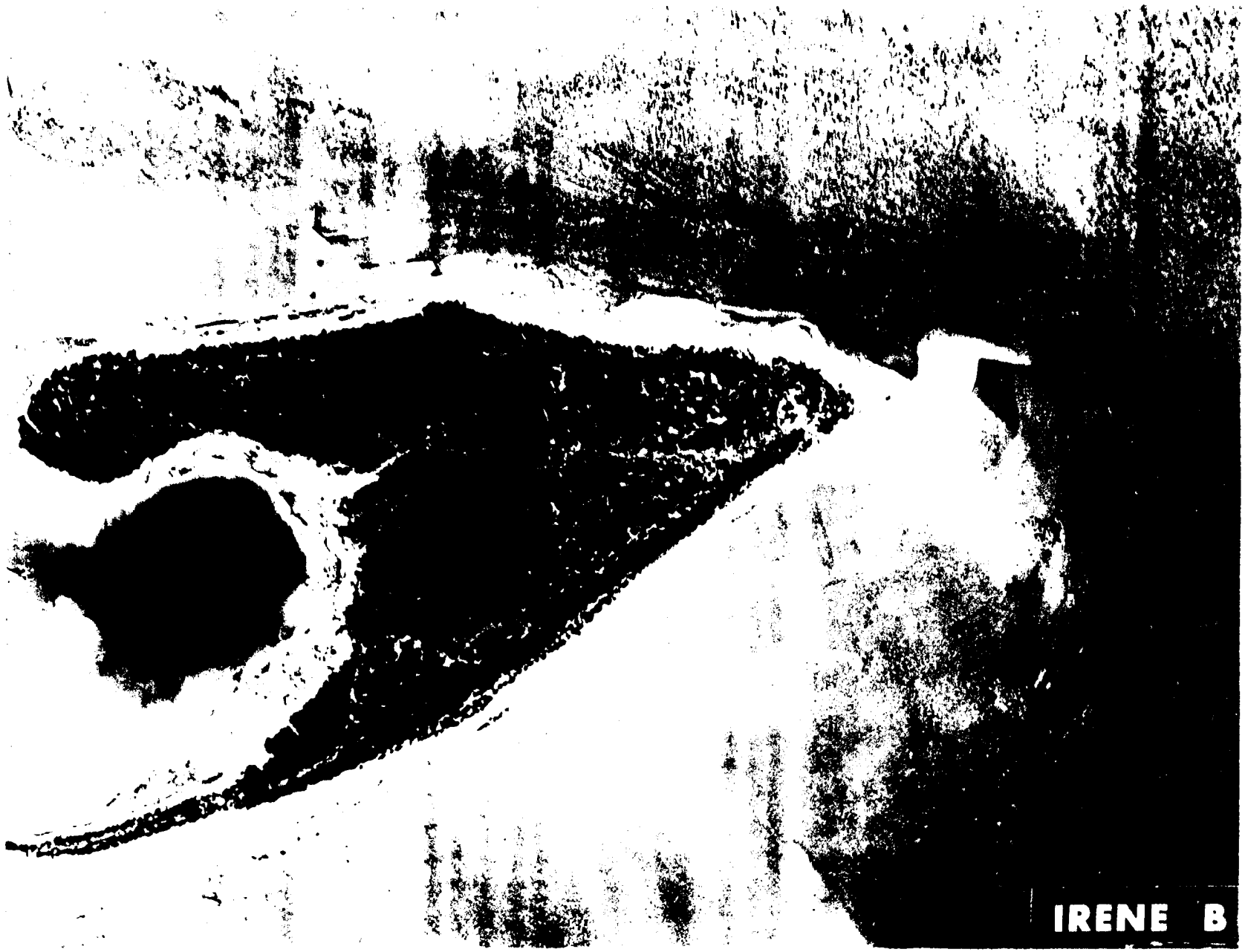

Fig. B.7.1.a.

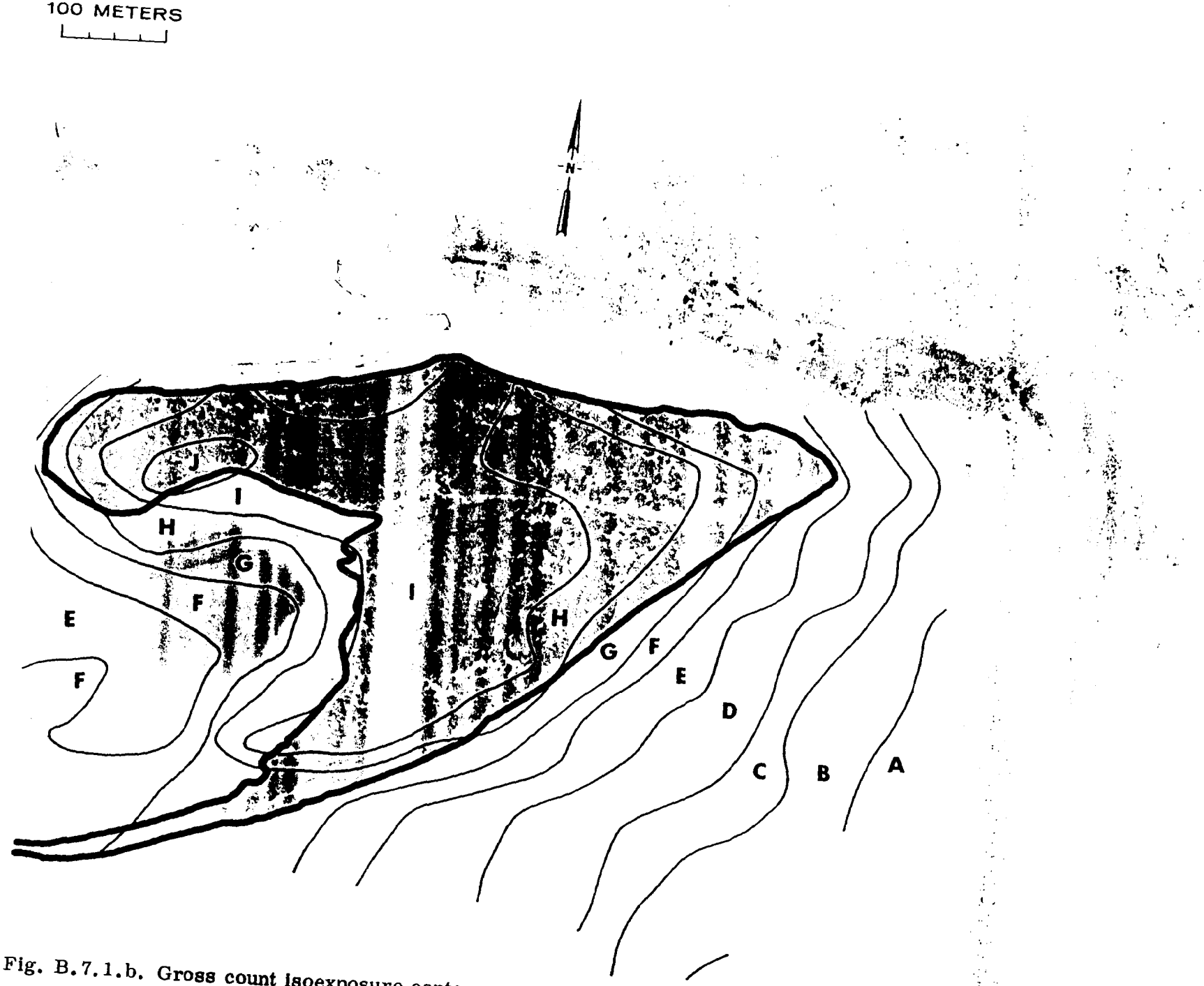

Fig. B.7.1.b. Gross count isoexposure contours. (Refer to alphabetic symbol key in this appendix.)

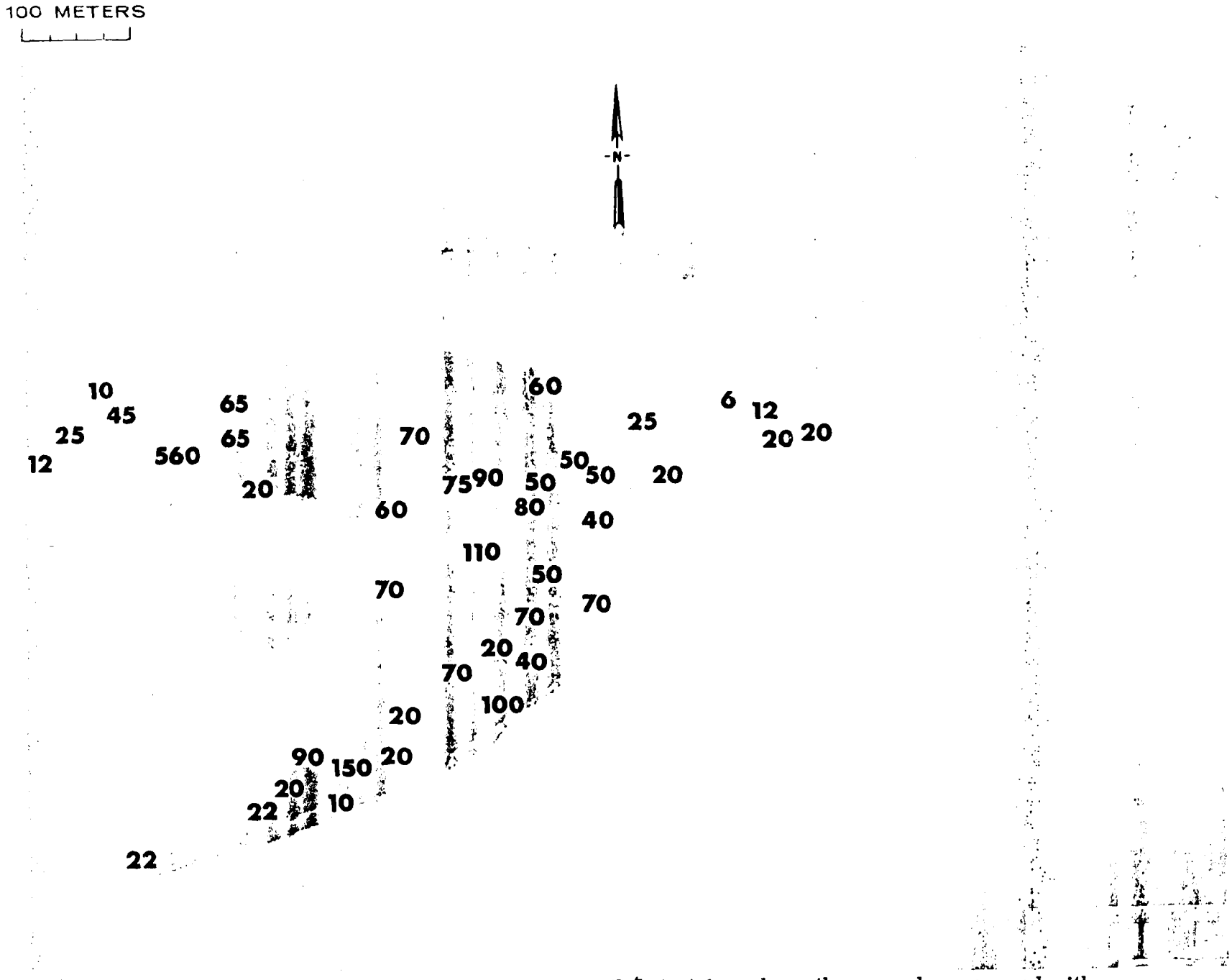

Fig. B.7.1.d. The gamma background exposure rate (μR/hr) at 1 m above the ground, measured with a portable NaI scintillation counter.

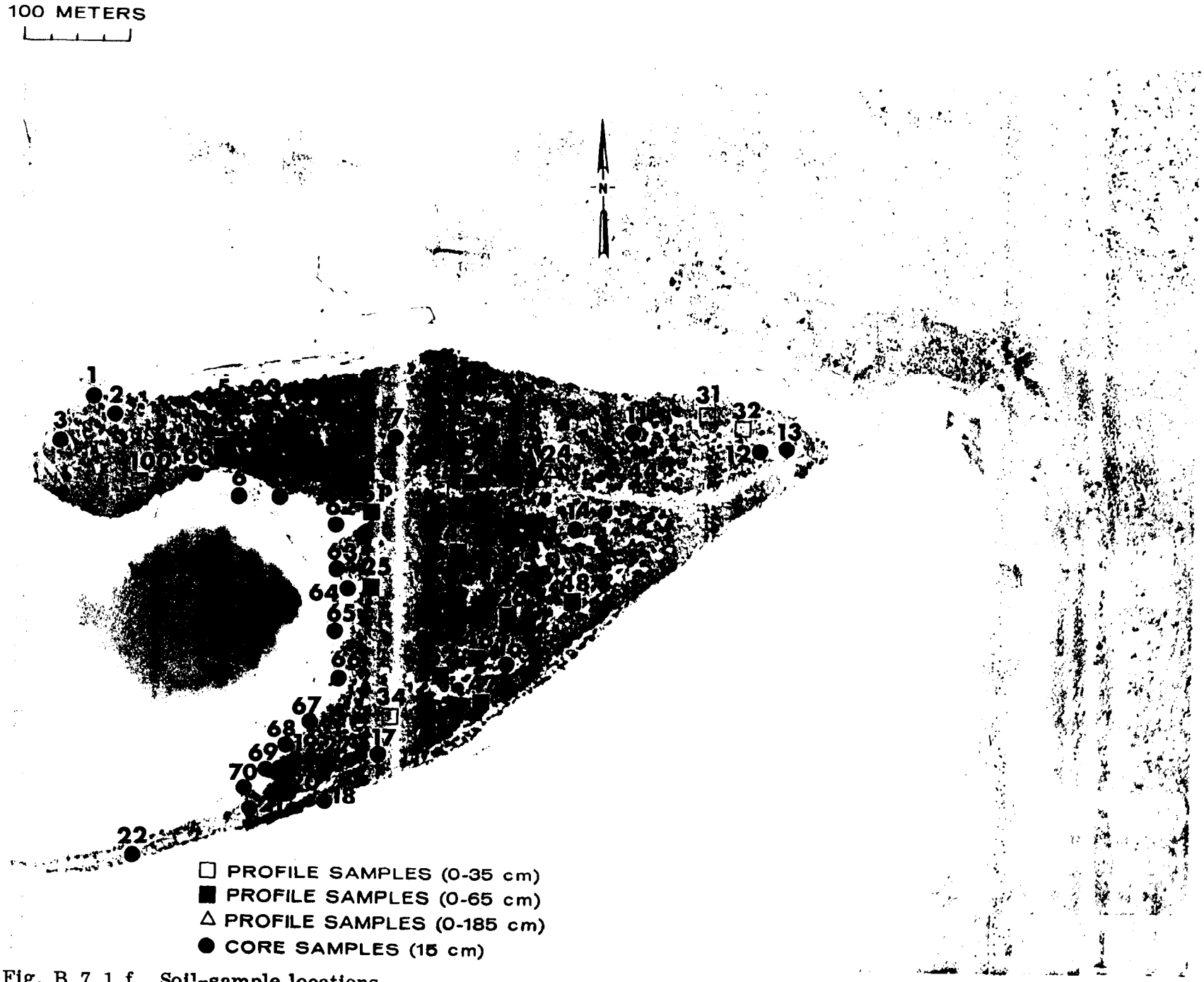

Fig. B.7.1.f. Soil-sample locations.

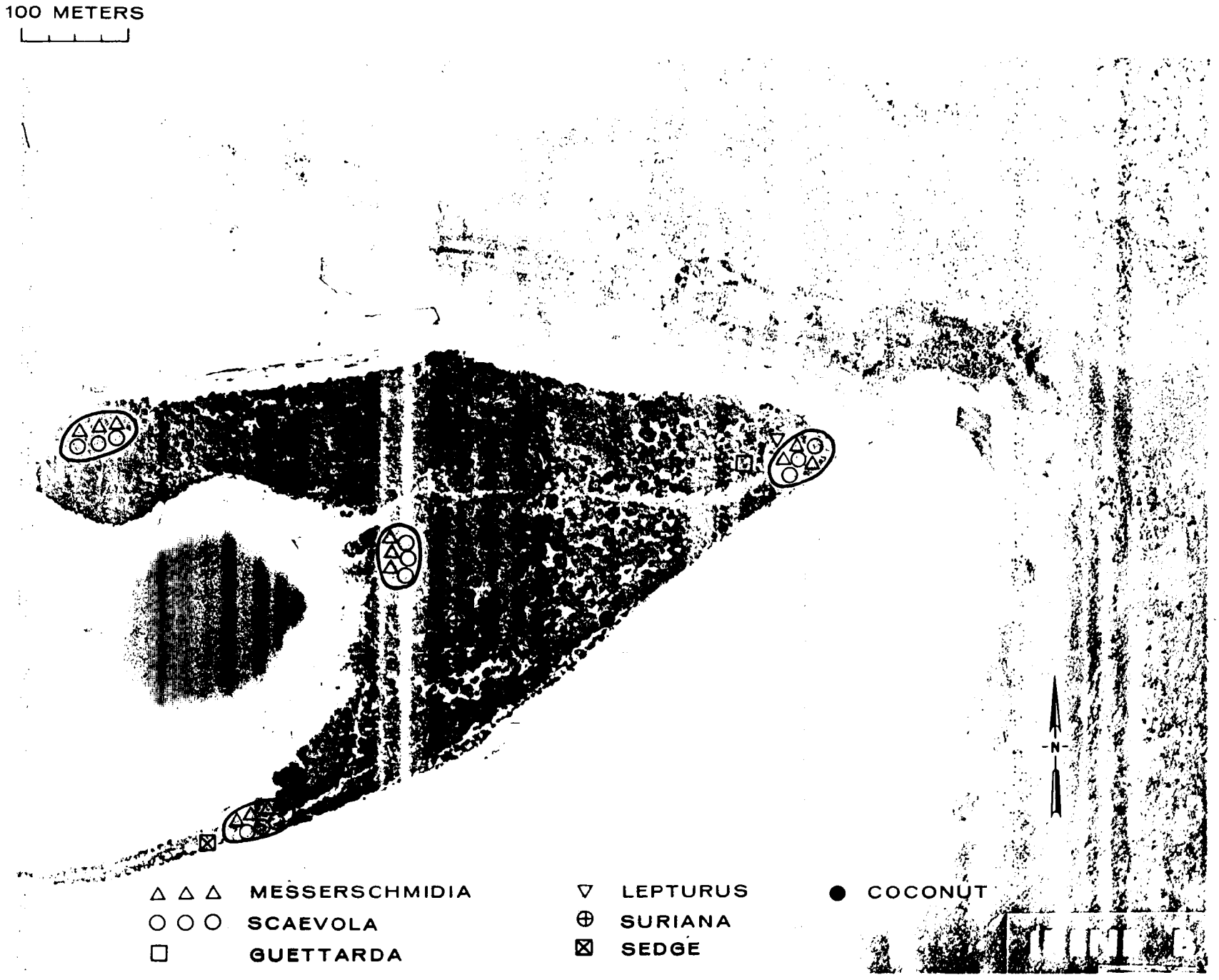

Fig. B.7.1.g. **Vegetation sample locations.**

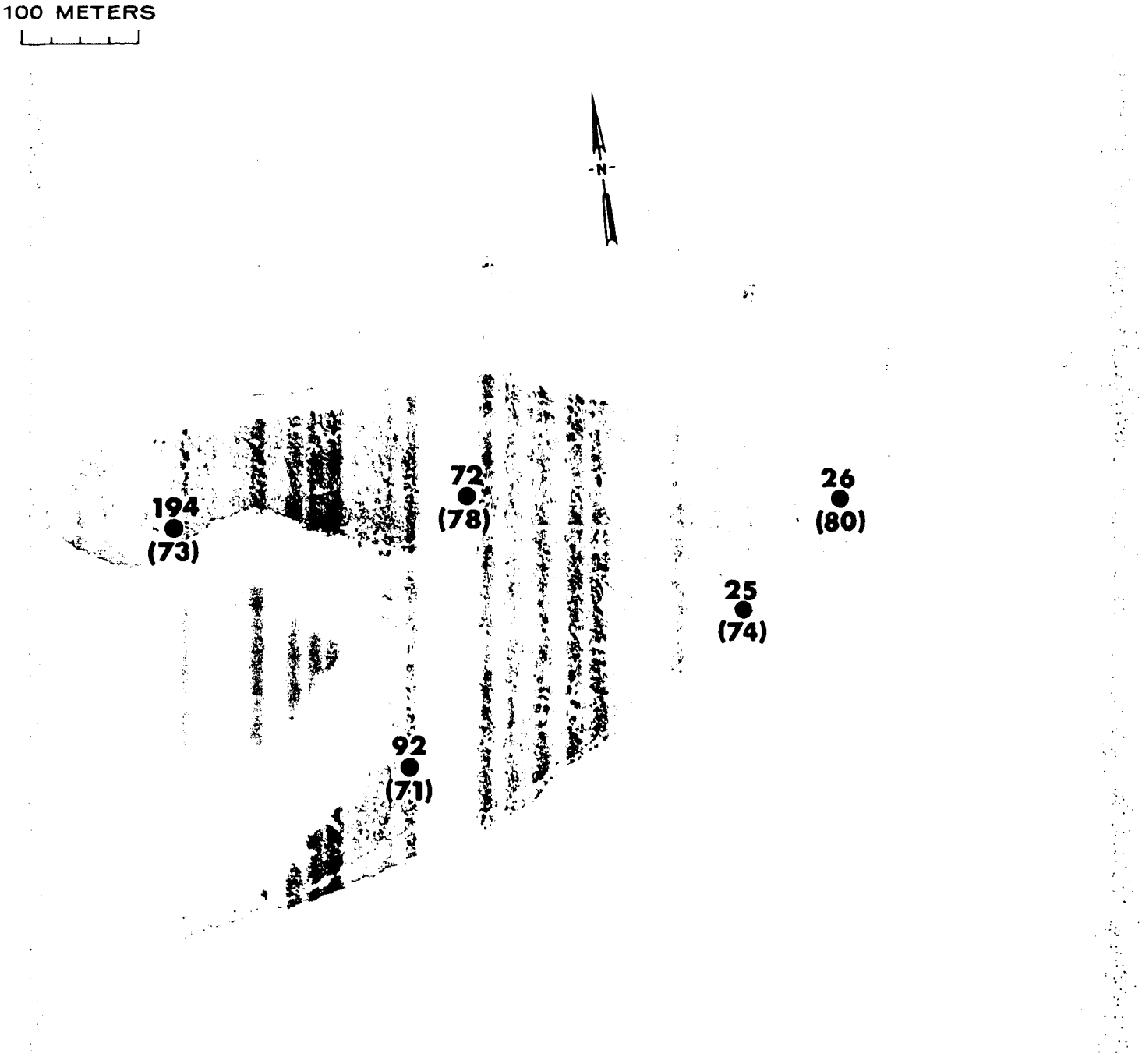

Fig. B.7.1.h. The gamma-ray exposure rates (μR/hr) measured 1 m above the ground by the LiF thermoluminescent dosimeters (TLD). The numbers shown in parentheses denote the location identification numbers.

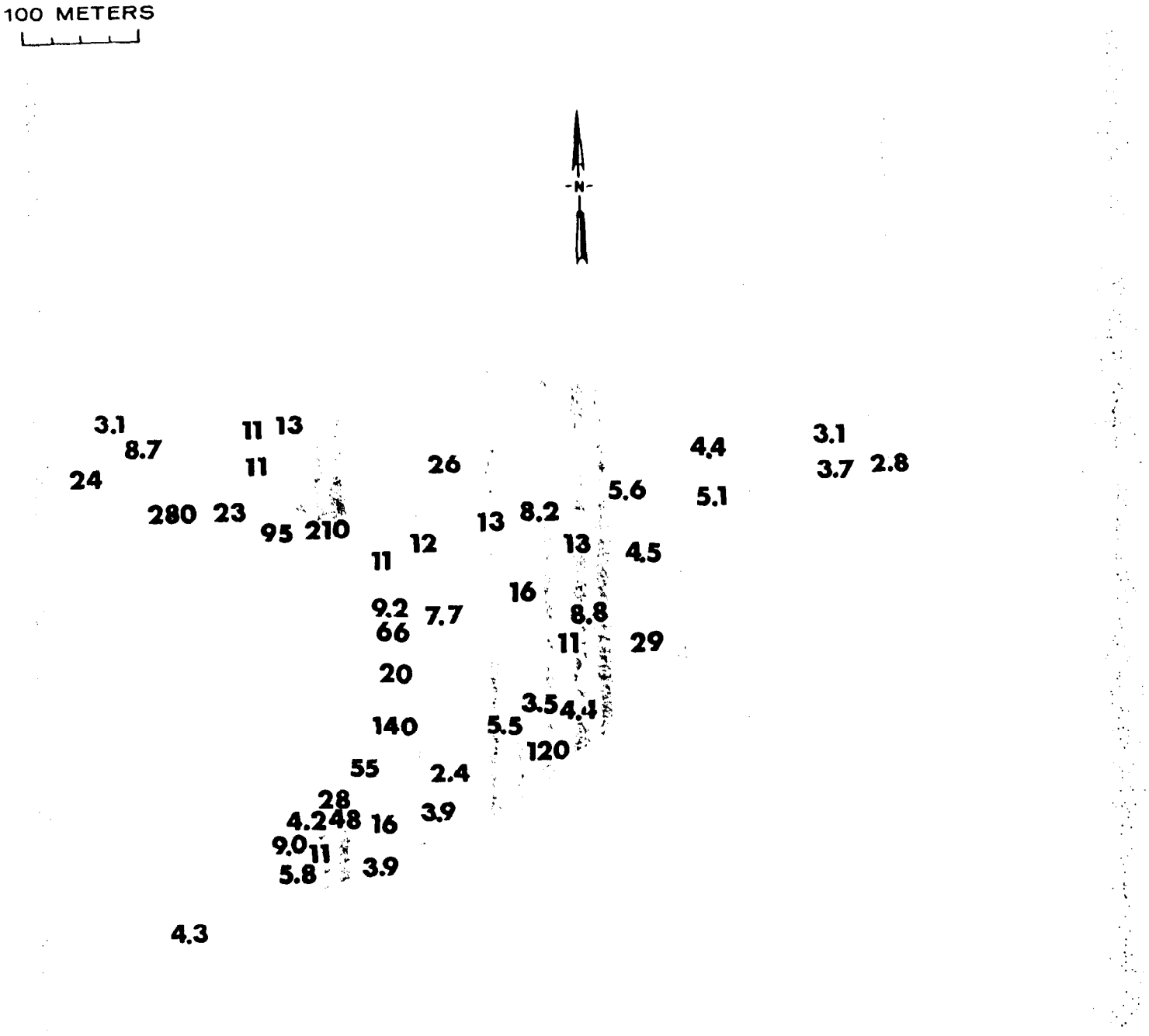

Fig. B.7.1.1. The average ^{239}Pu activities (pCi/gm) in soil samples collected to a depth of 15 cm.

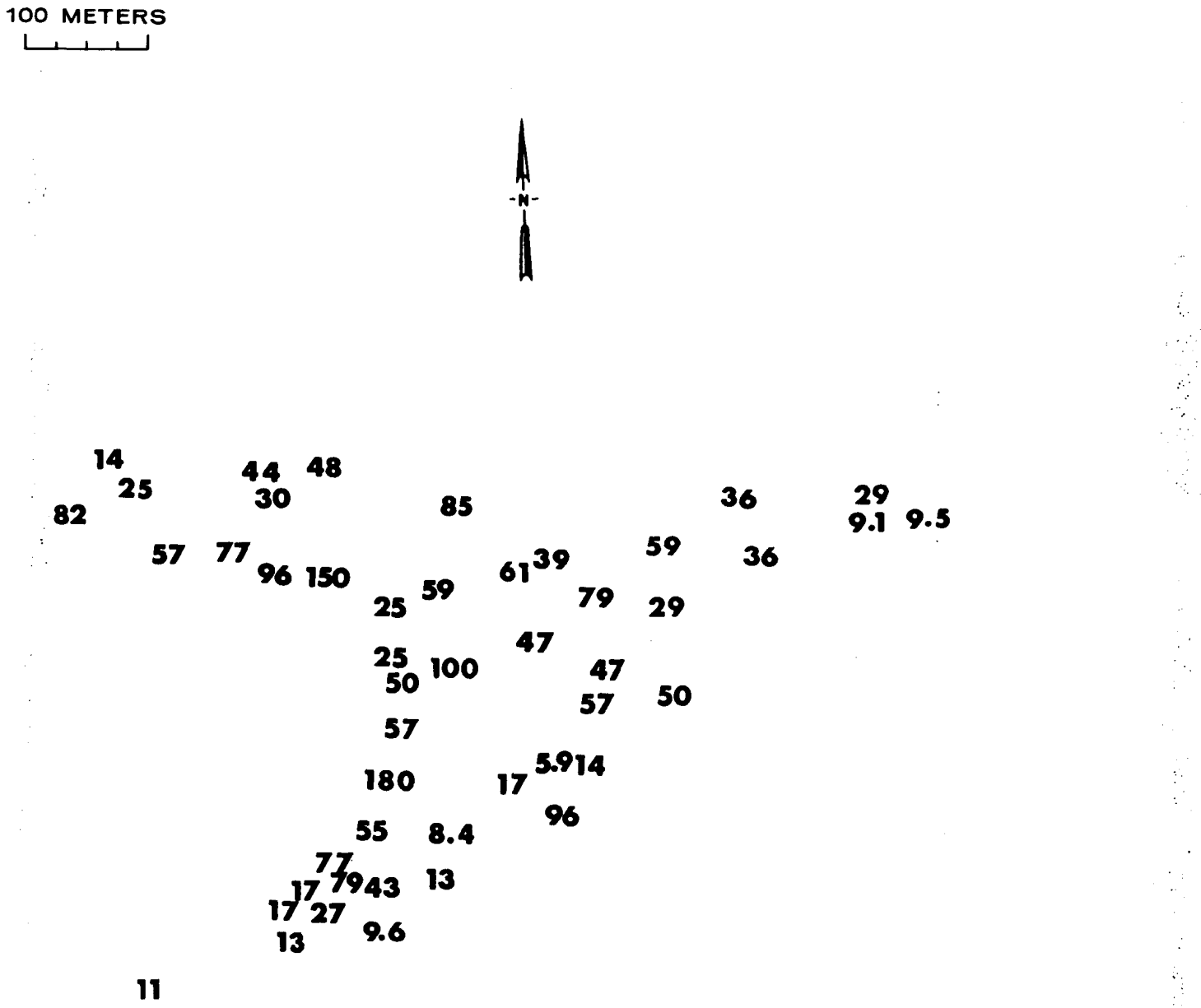

Fig. B.7.1.j. The average ^{90}Sr activities (pCi/gm) in soil samples collected to a depth of 15 cm.

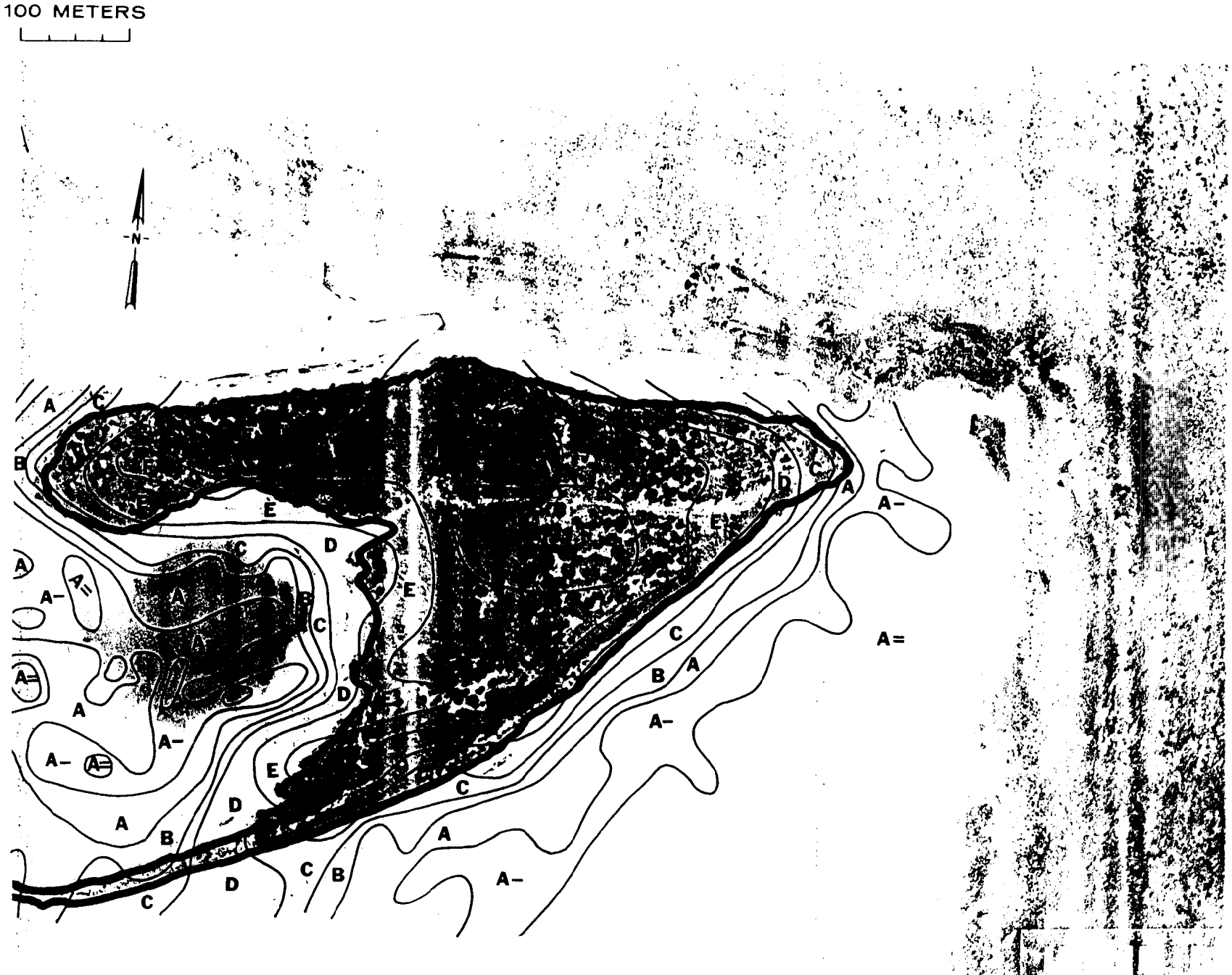

Fig. B.7.1.k. ^{137}Cs isoexposure and isoconcentration contours. (Refer to alphabetic symbol key in this appendix.)

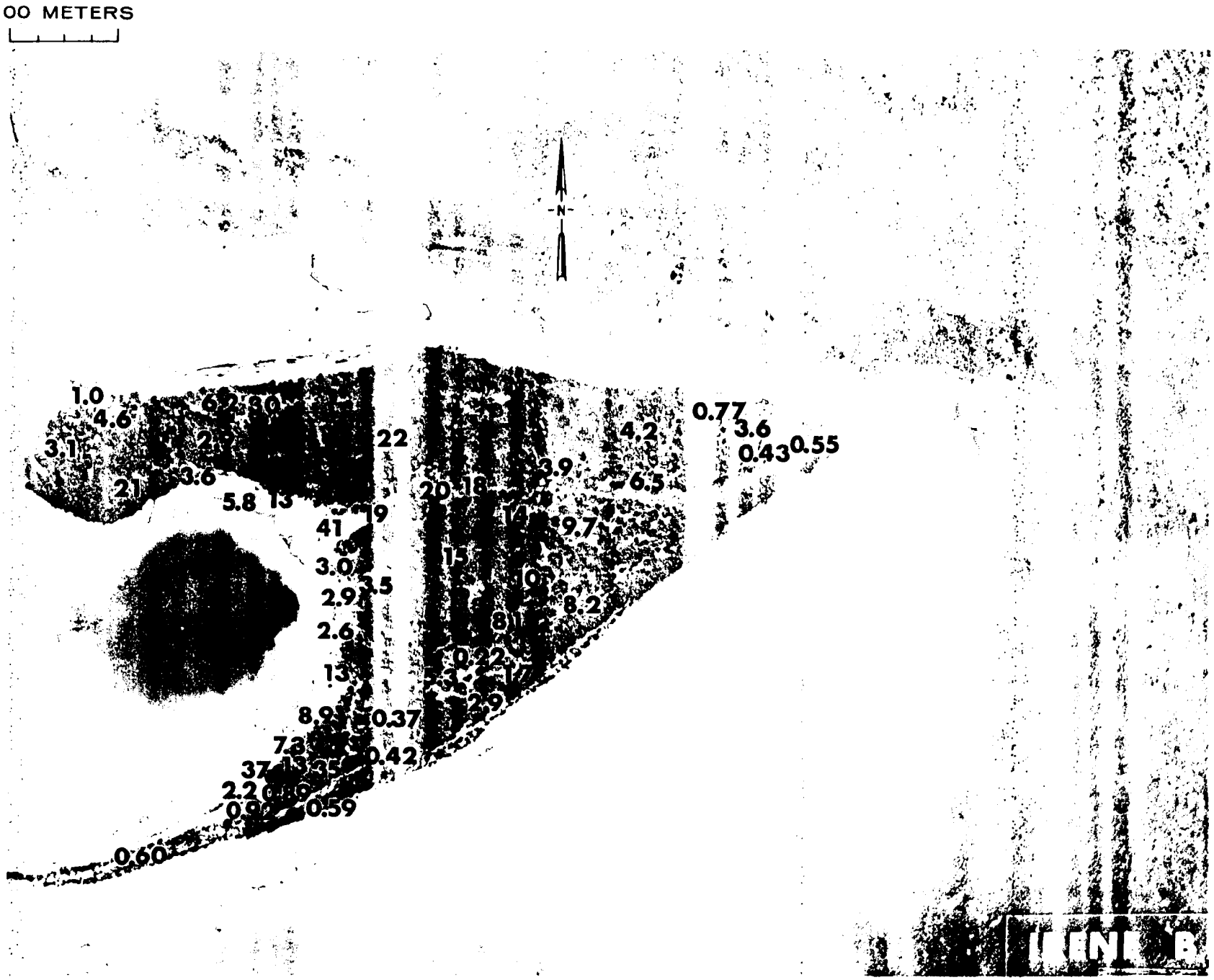

Fig. B.7.1.1. The average ^{137}Cs activities (pCi/gm) in soil samples collected to a depth of 15 cm.

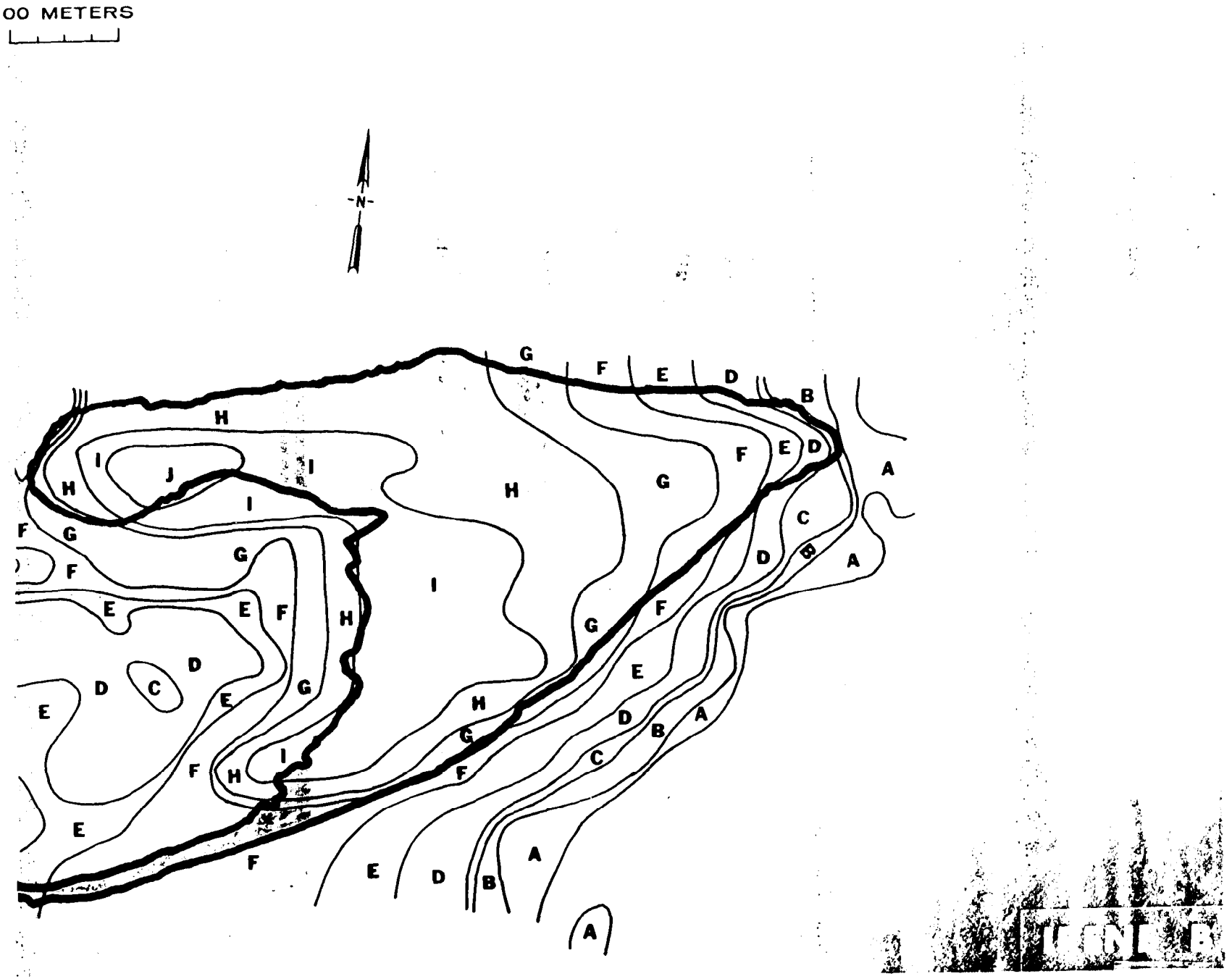

Fig. B.7.1.m. ^{60}Co isoexposure and isoconcentration contours. (Refer to alphabetic symbol key in this appendix.)

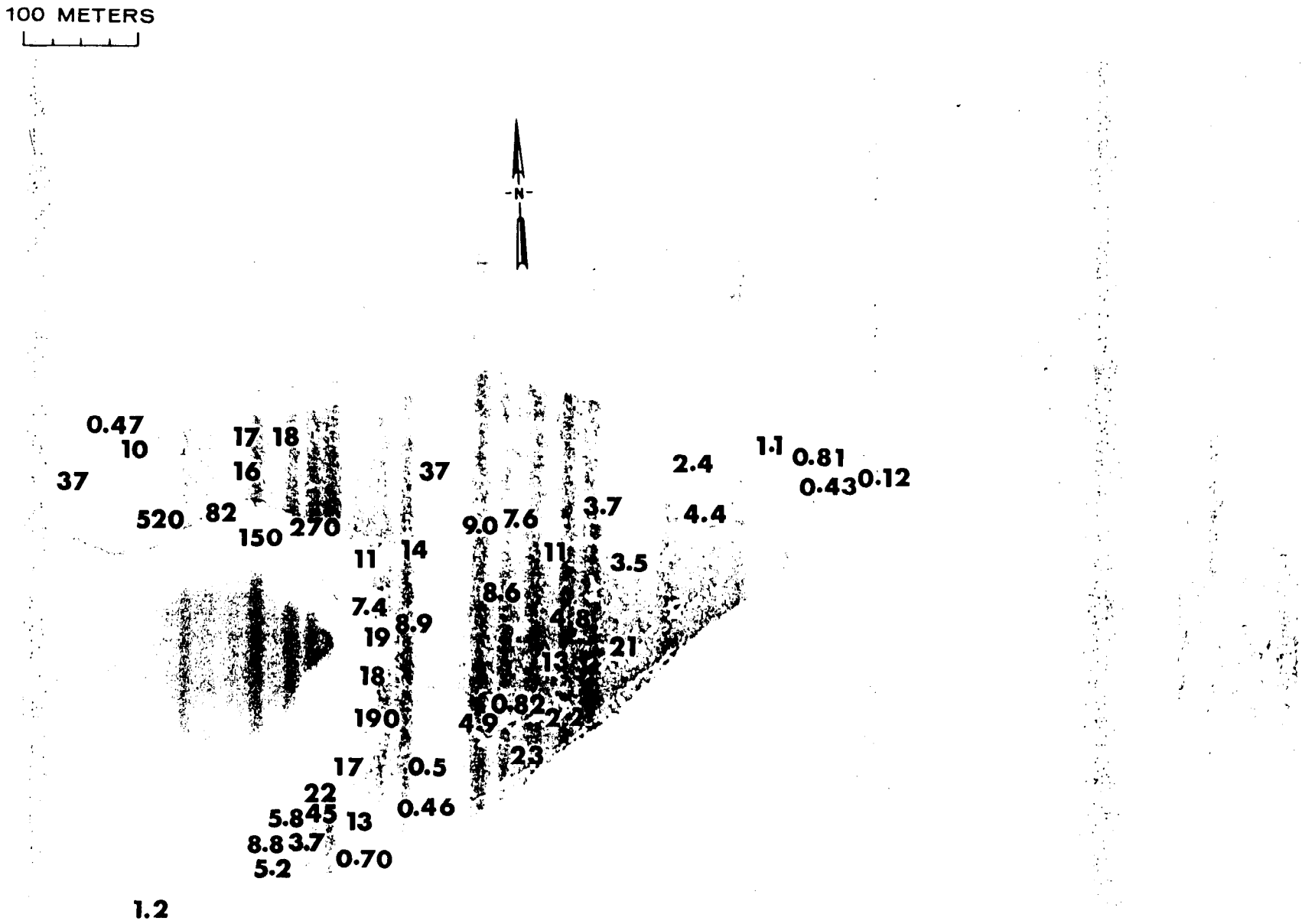

Fig. B.7.1.n. The average ^{60}Co activities (pCi/gm) in soil samples collected to a depth of 15 cm.

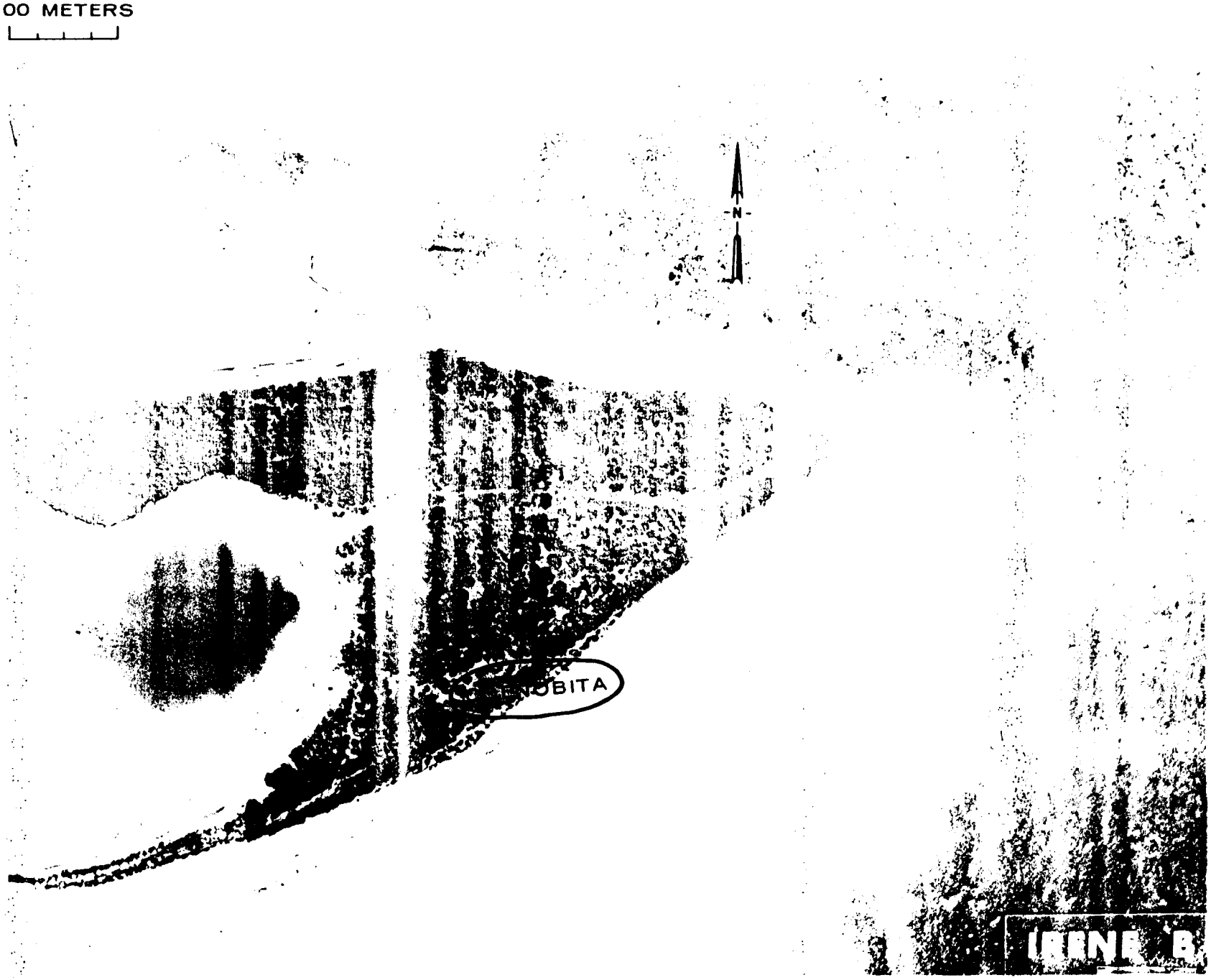

Fig. B.7.1.o. Terrestrial animal sample locations.

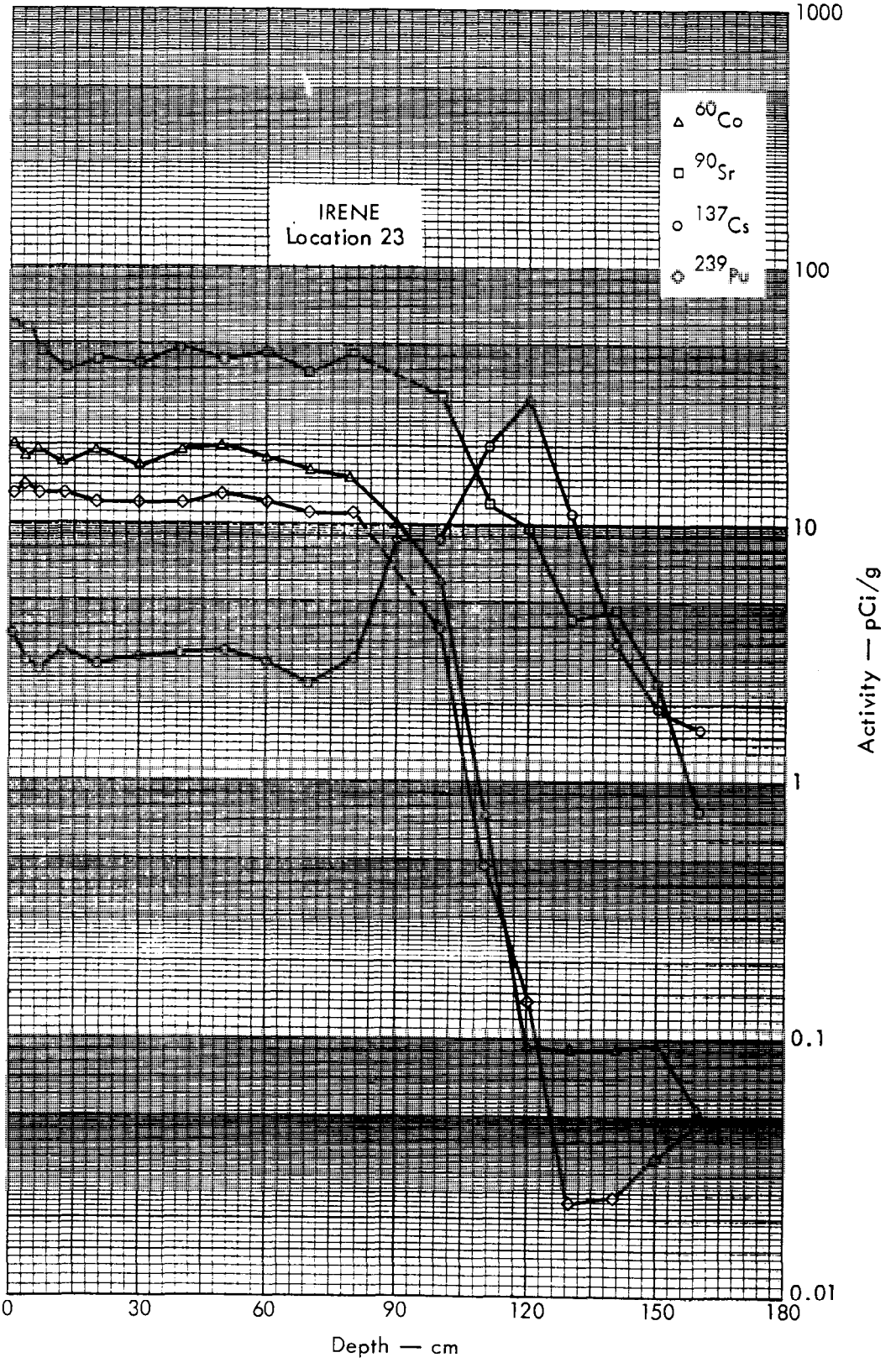

Fig. B.7.2a. Activities of selected radionuclides as a function of soil depth.

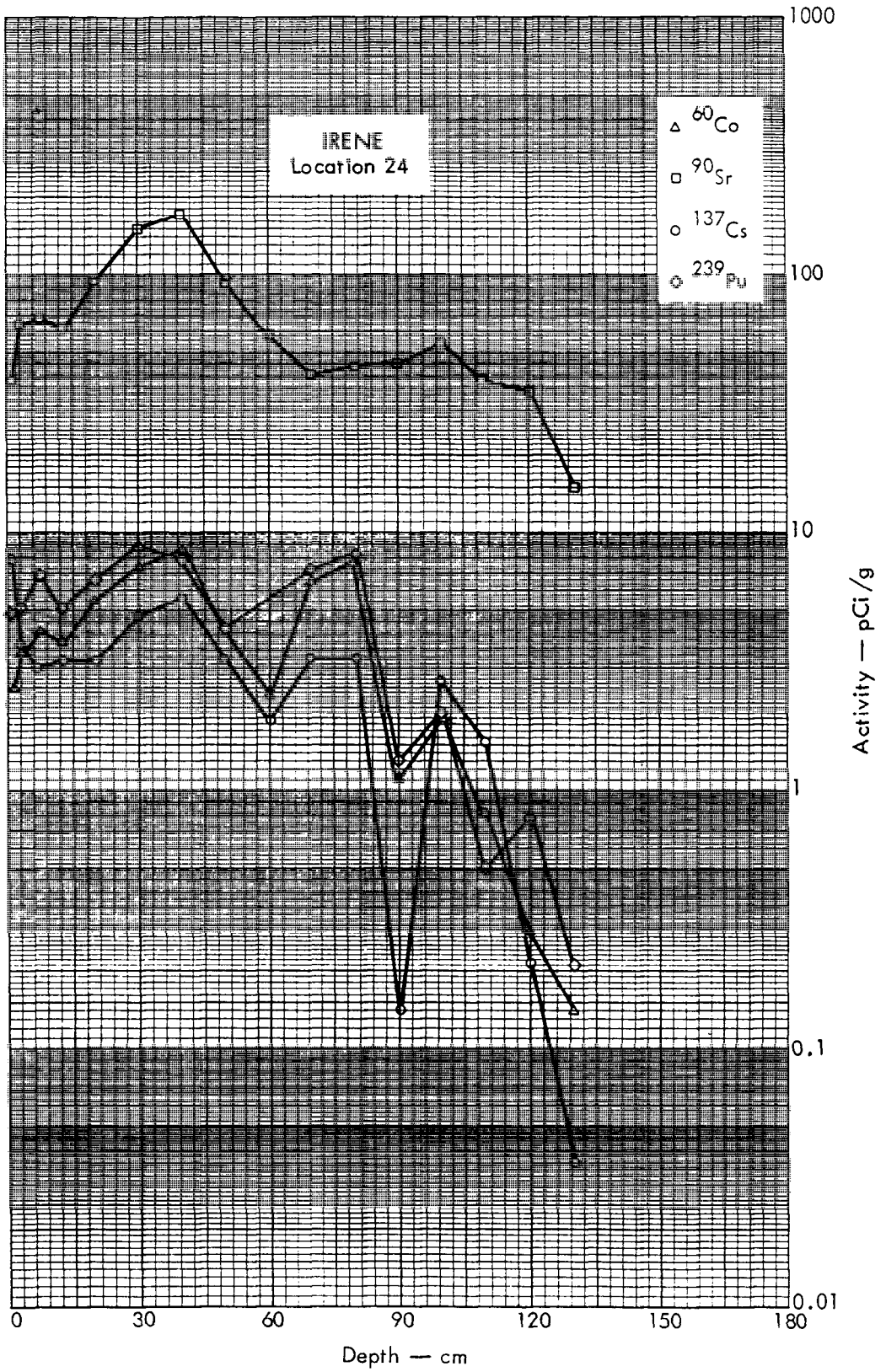

Fig. B.7.2b. Activities of selected radionuclides as a function of soil depth.

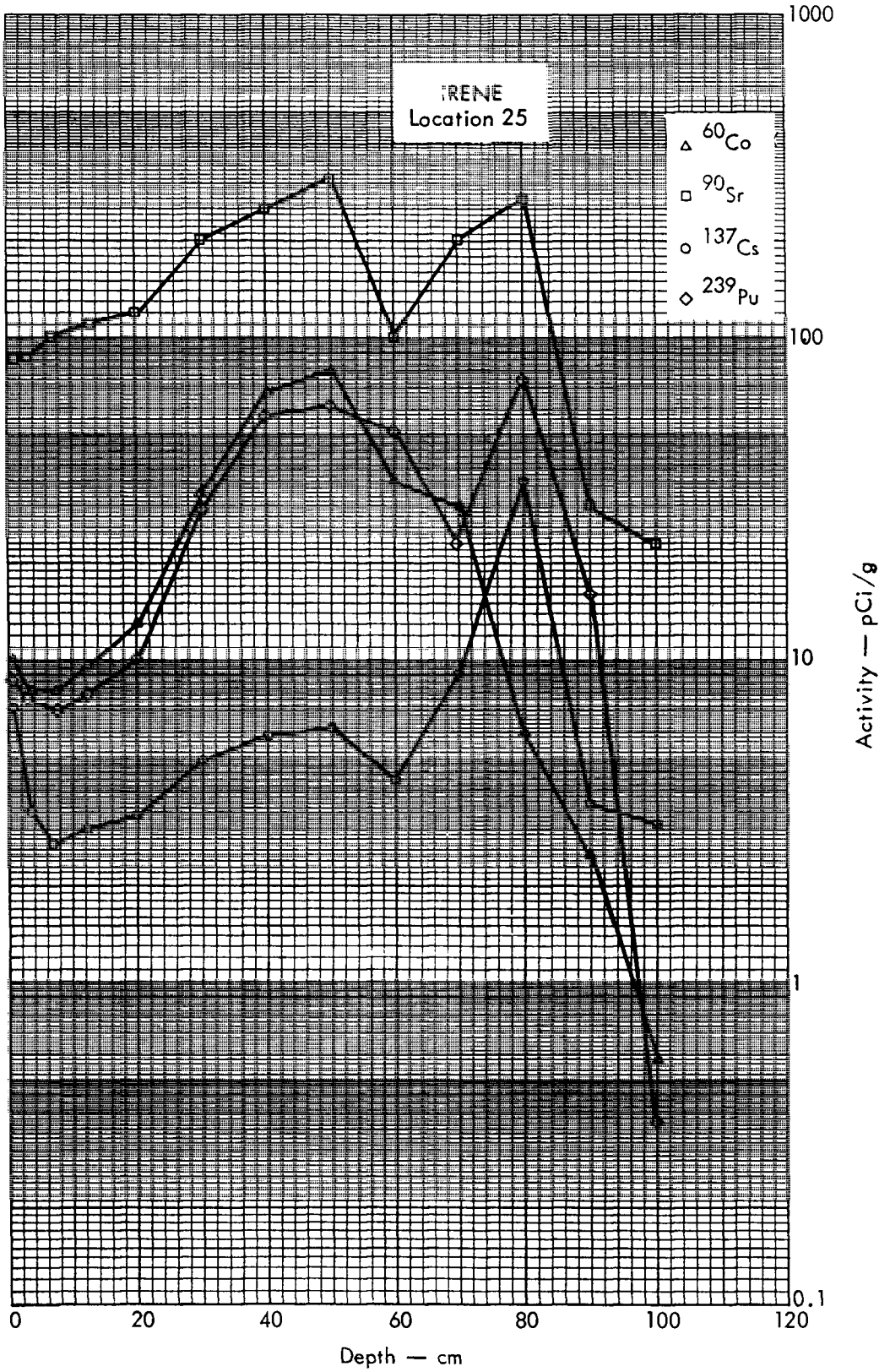

Fig. B.7.2c. Activities of selected radionuclides as a function of soil depth.

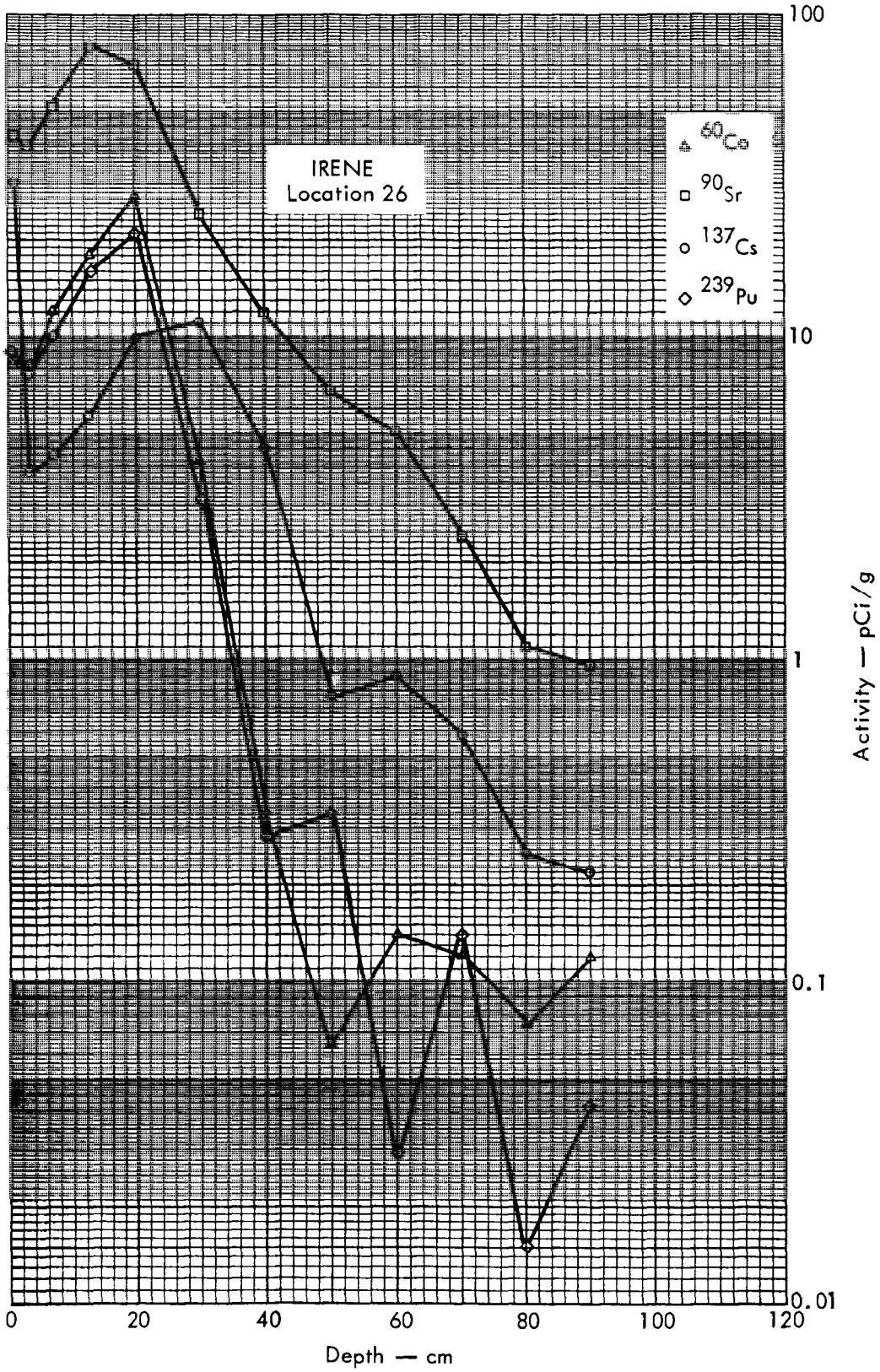

Fig. B.7.2d. Activities of selected radionuclides as a function of soil depth.

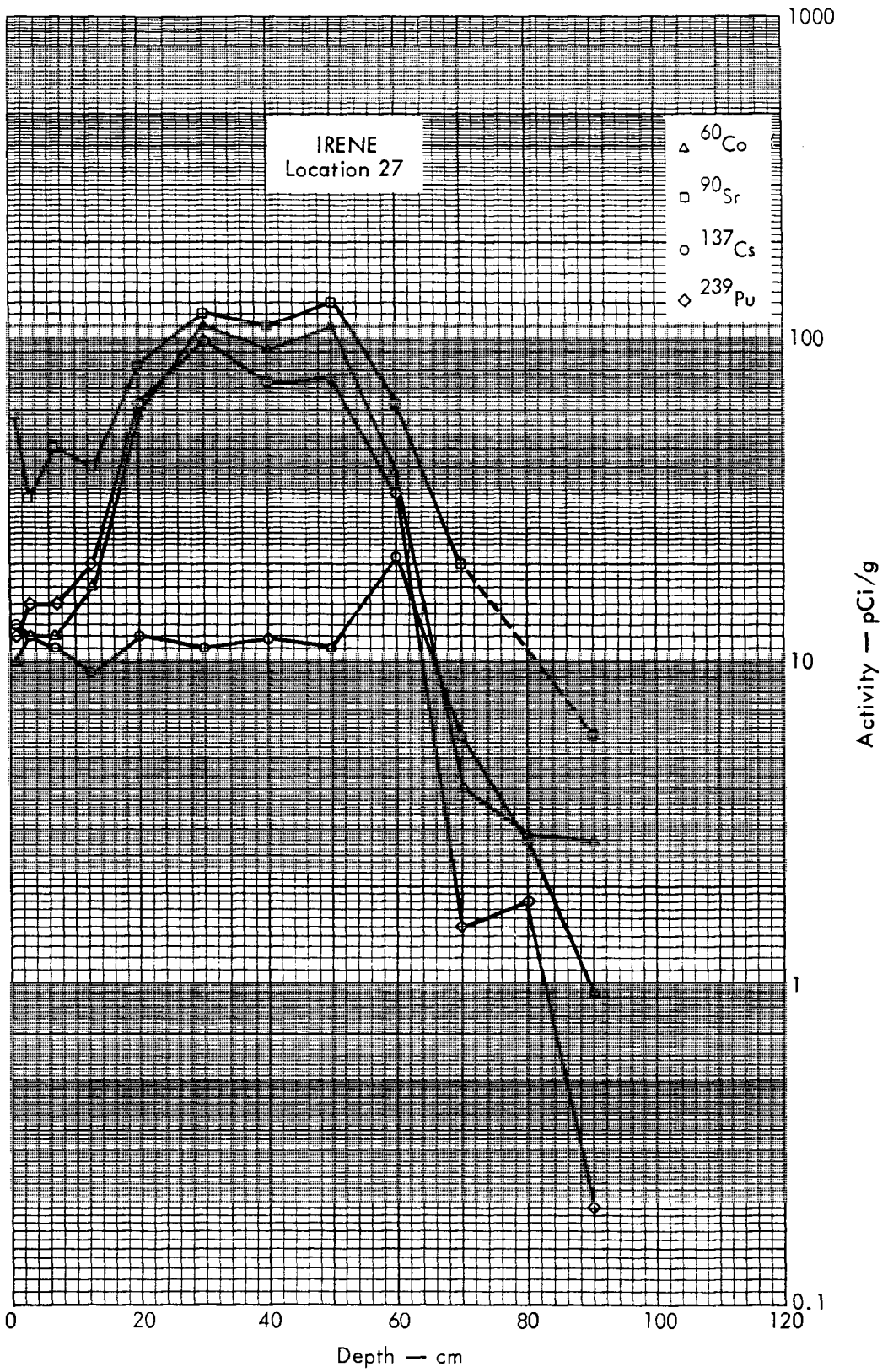

Fig. B.7.2e. Activities of selected radionuclides as a function of soil depth.

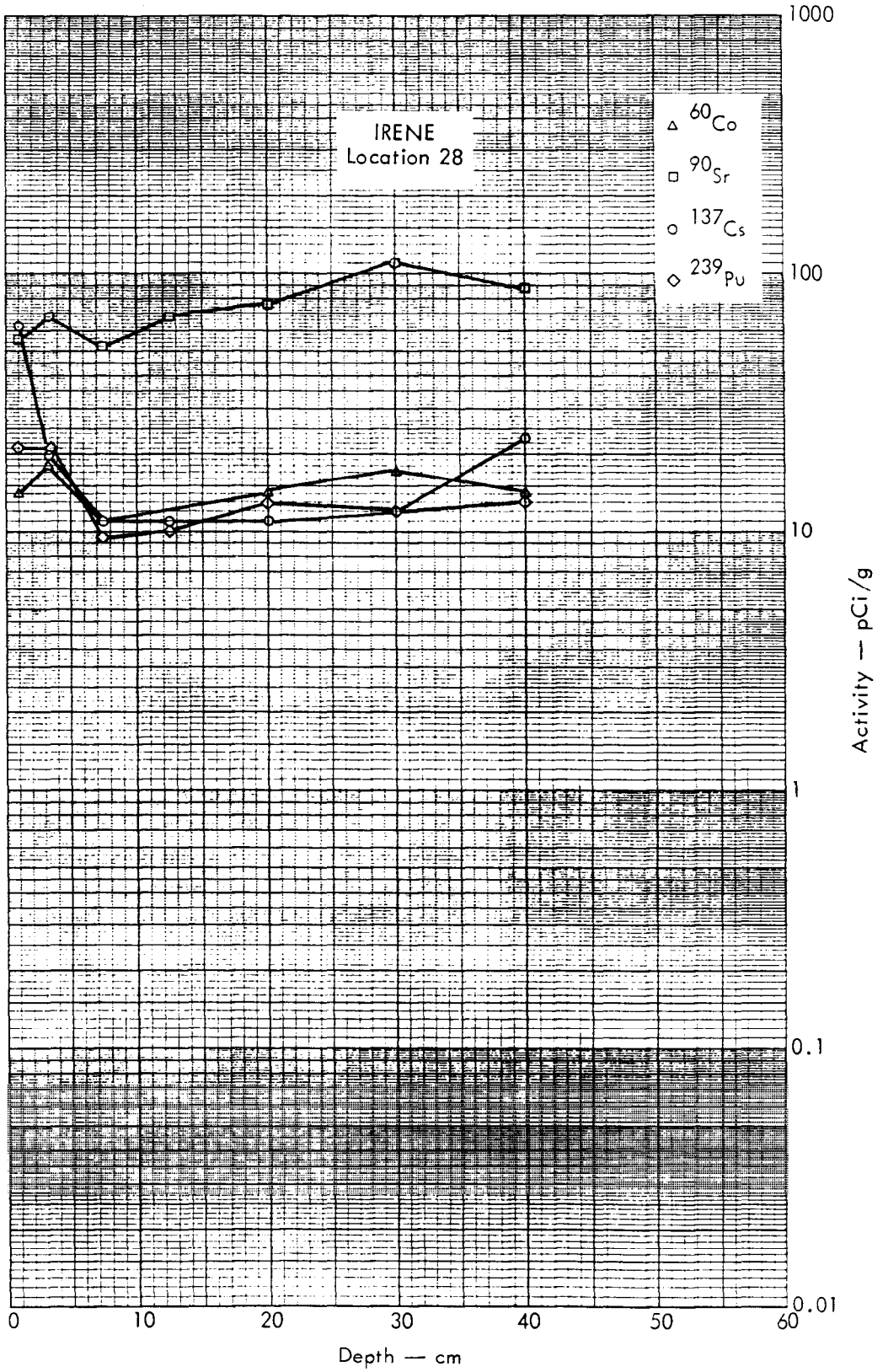

Fig. B.7.2f. Activities of selected radionuclides as a function of soil depth.

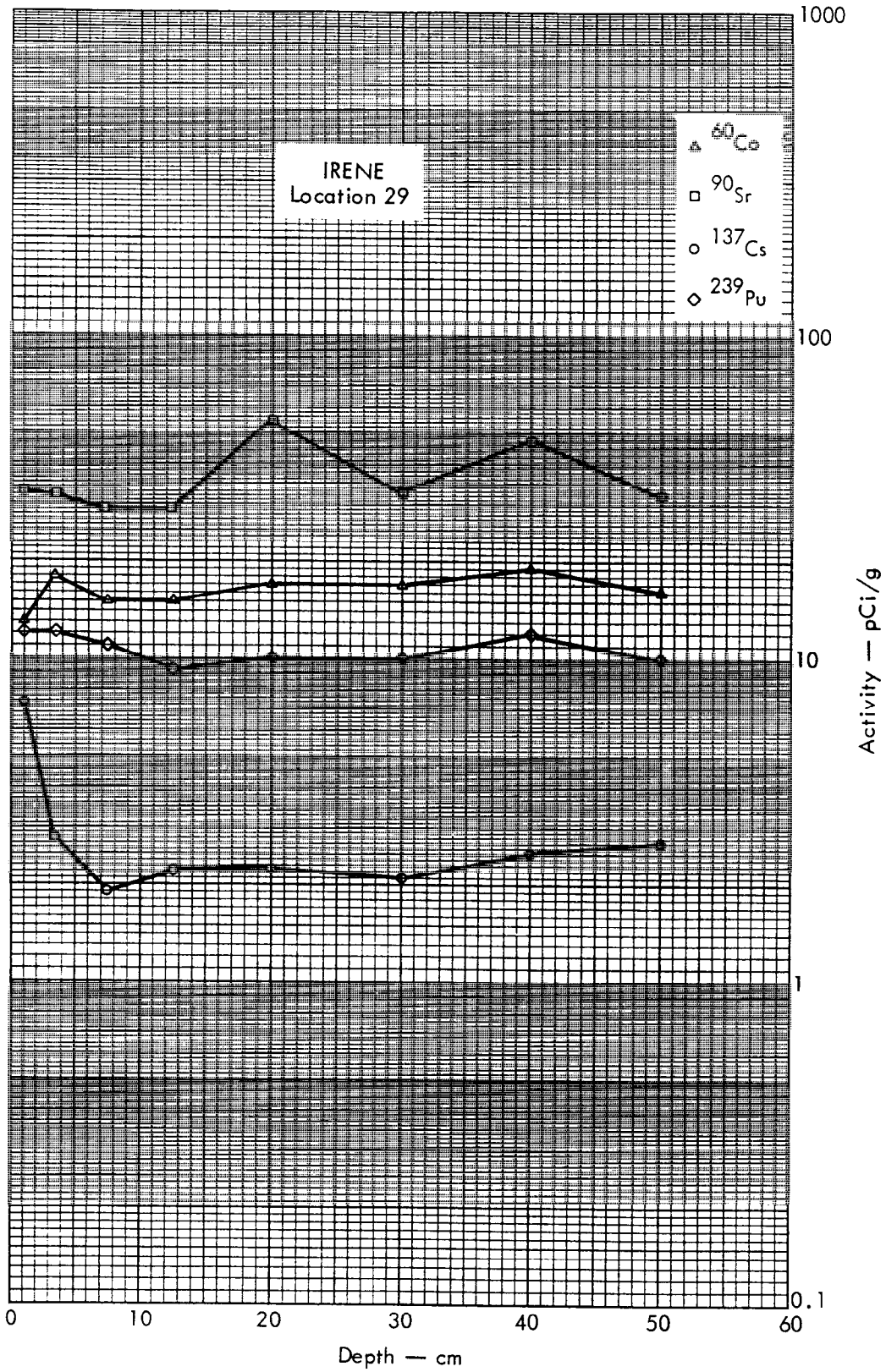

Fig. B.7.2g. Activities of selected radionuclides as a function of soil depth.

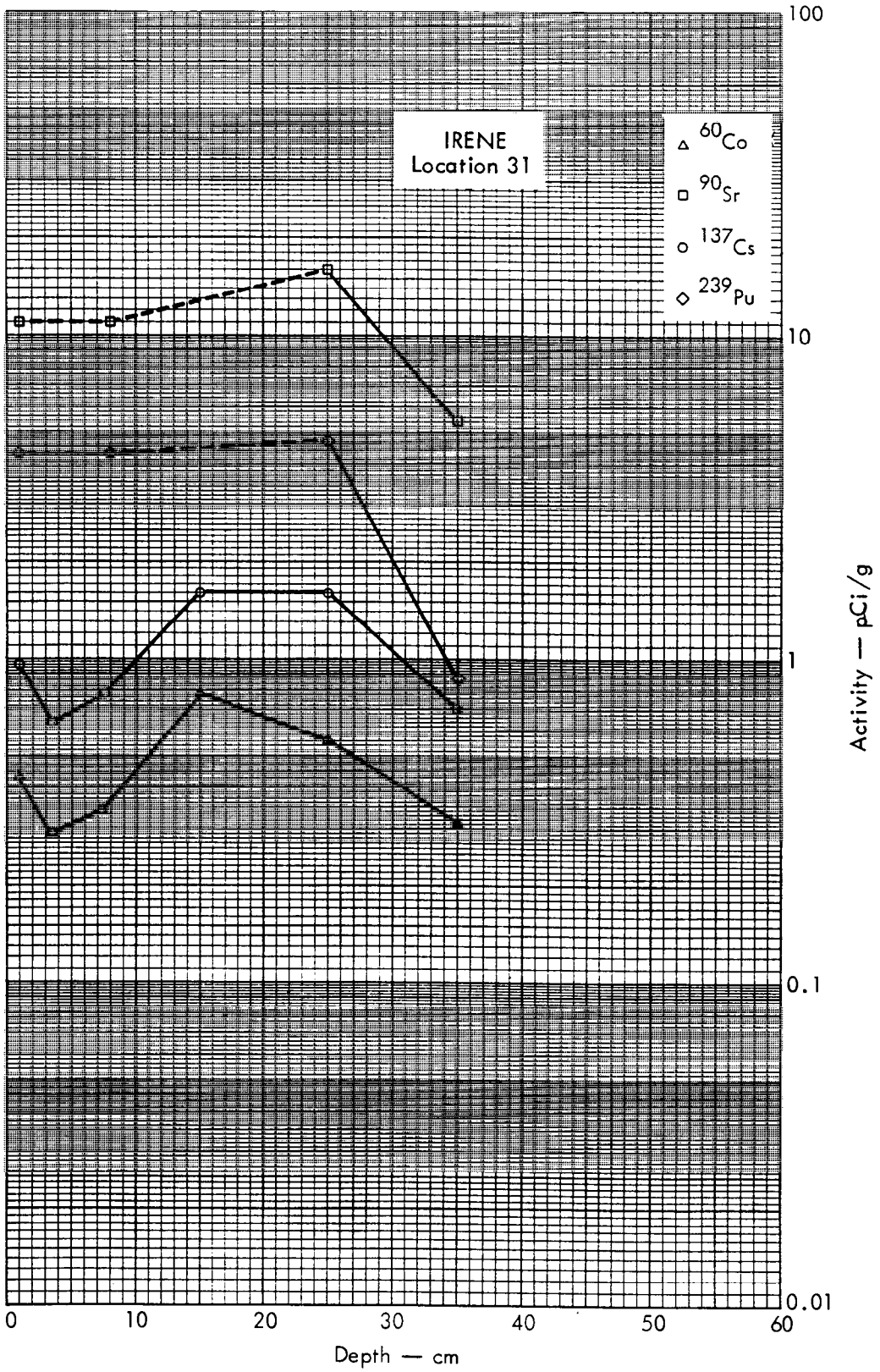

Fig. B.7.2h. Activities of selected radionuclides as a function of soil depth.

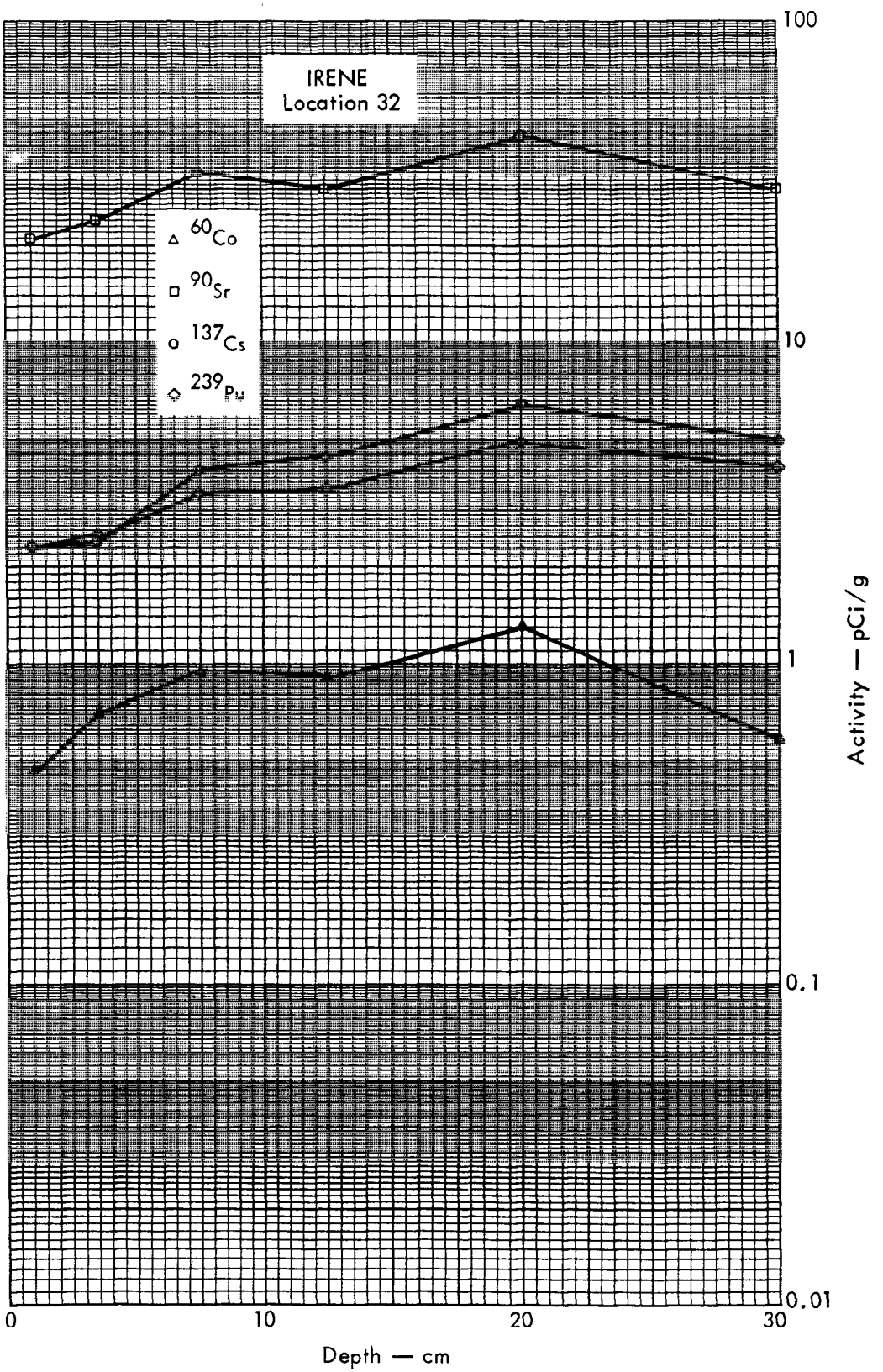

Fig. B.7.2i. Activities of selected radionuclides as a function of soil depth.

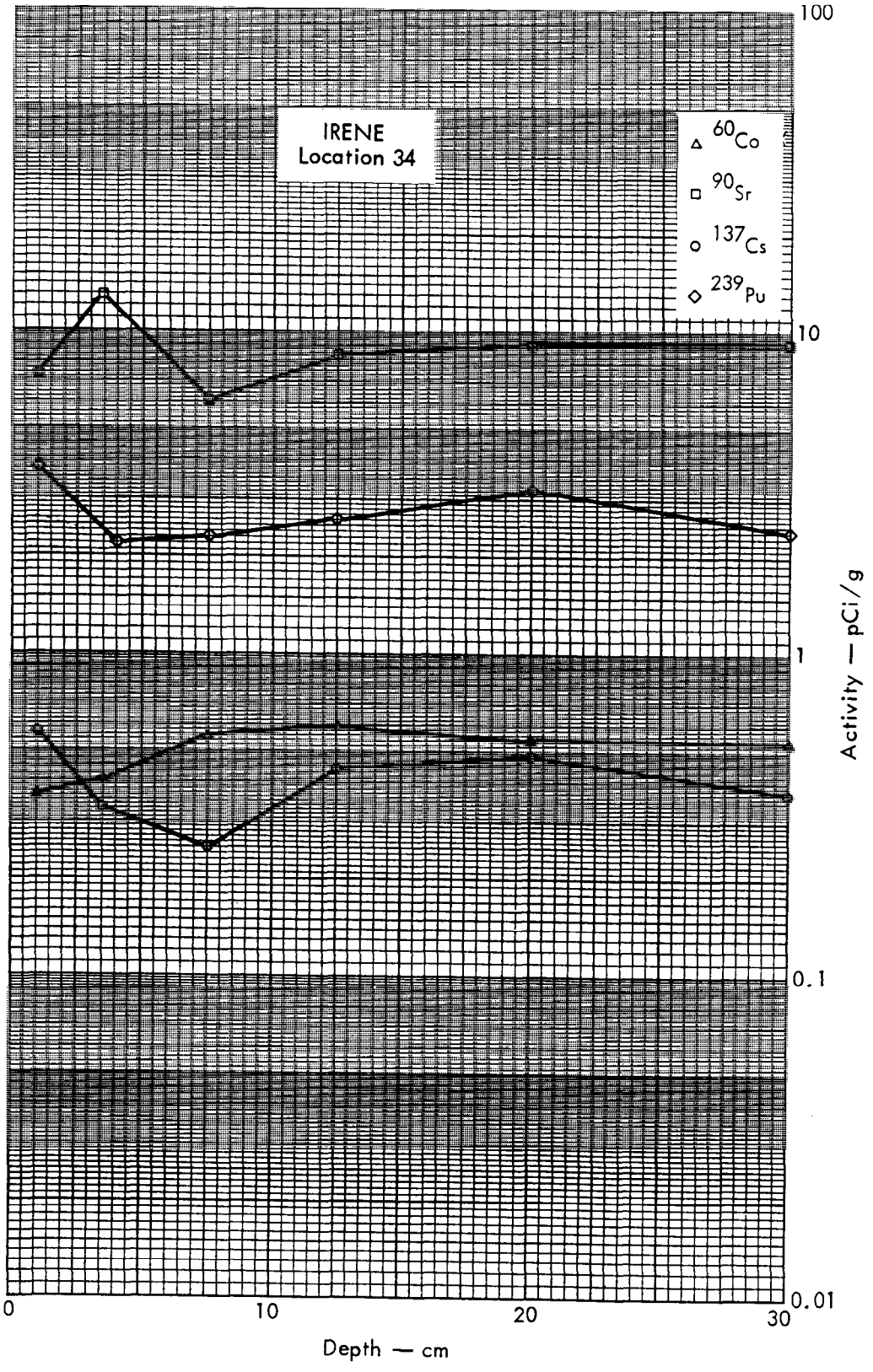

Fig. B.7.2j. Activities of selected radionuclides as a function of soil depth.

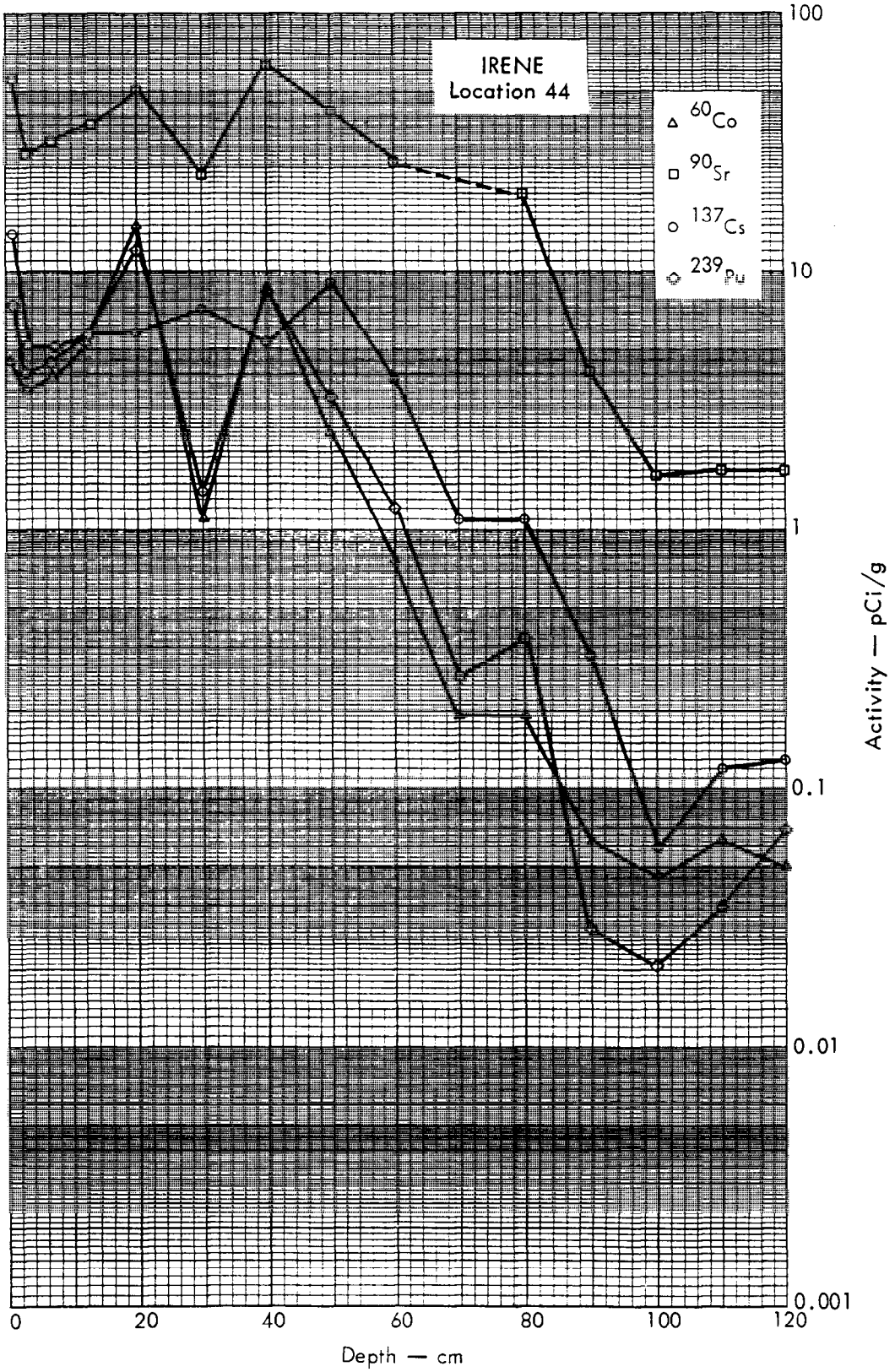

Fig. B.7.2k. Activities of selected radionuclides as a function of soil depth.

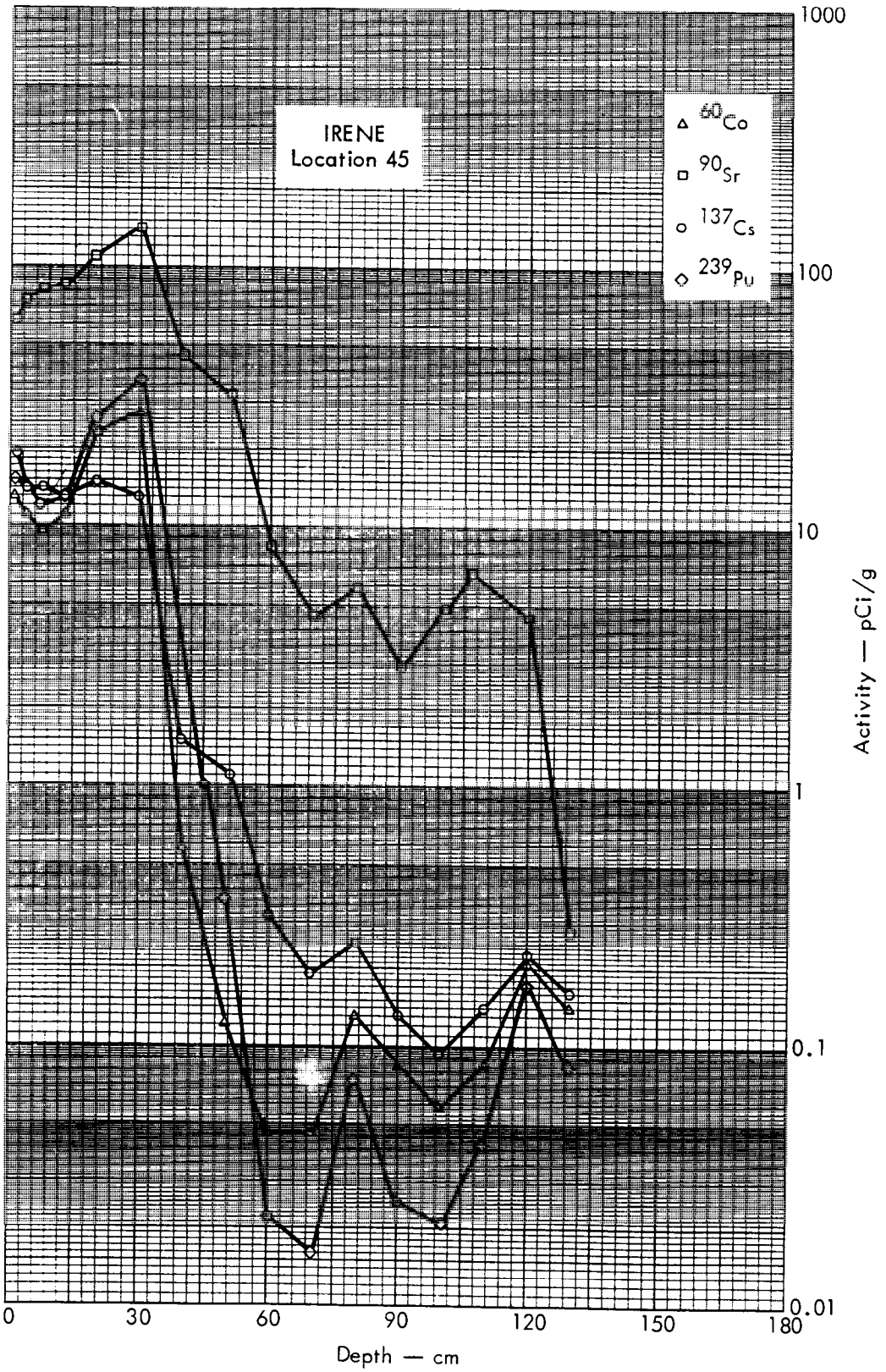

Fig. B.7.21. Activities of selected radionuclides as a function of soil depth.

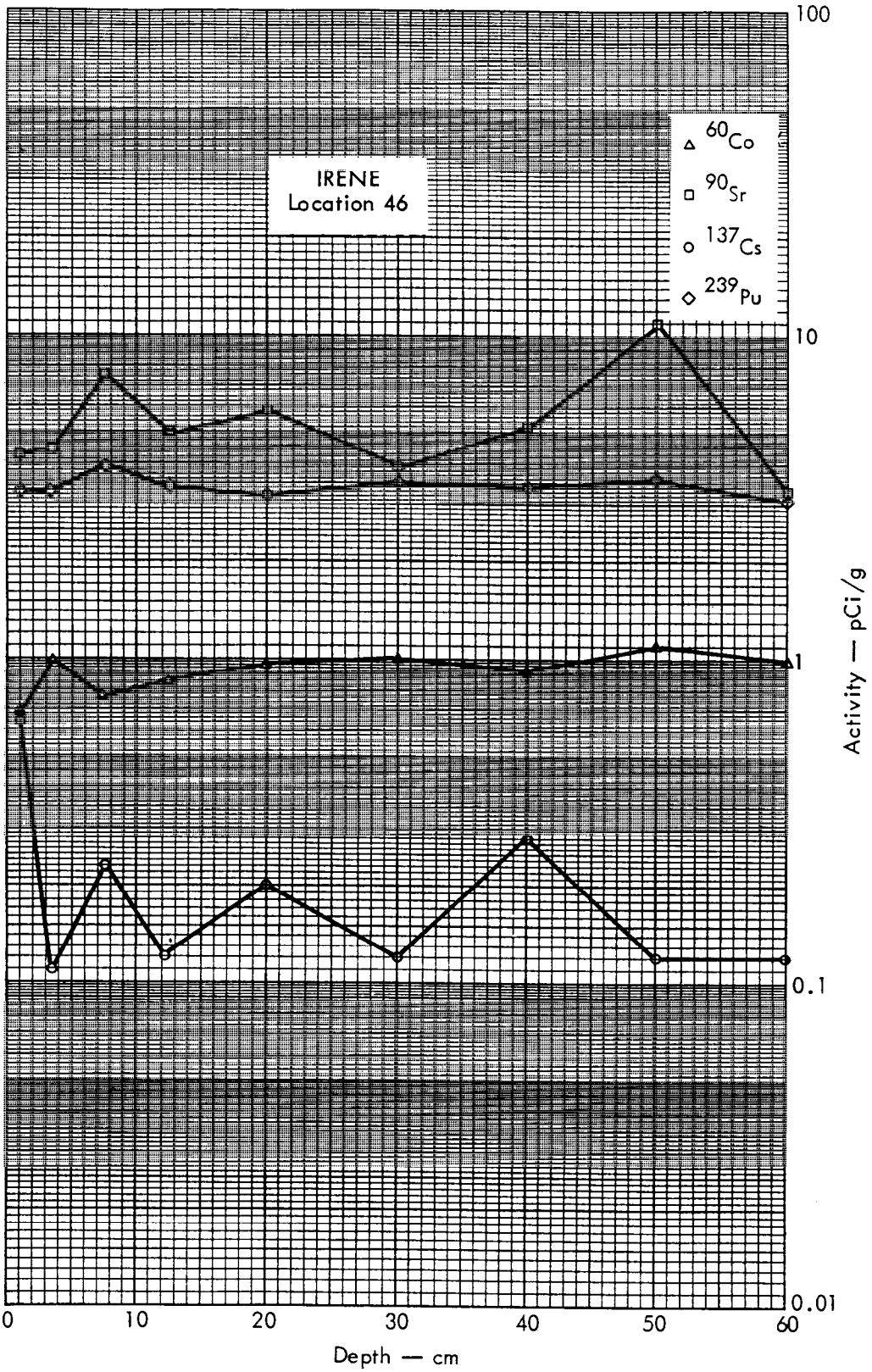

Fig. B.7.2m. Activities of selected radionuclides as a function of soil depth.

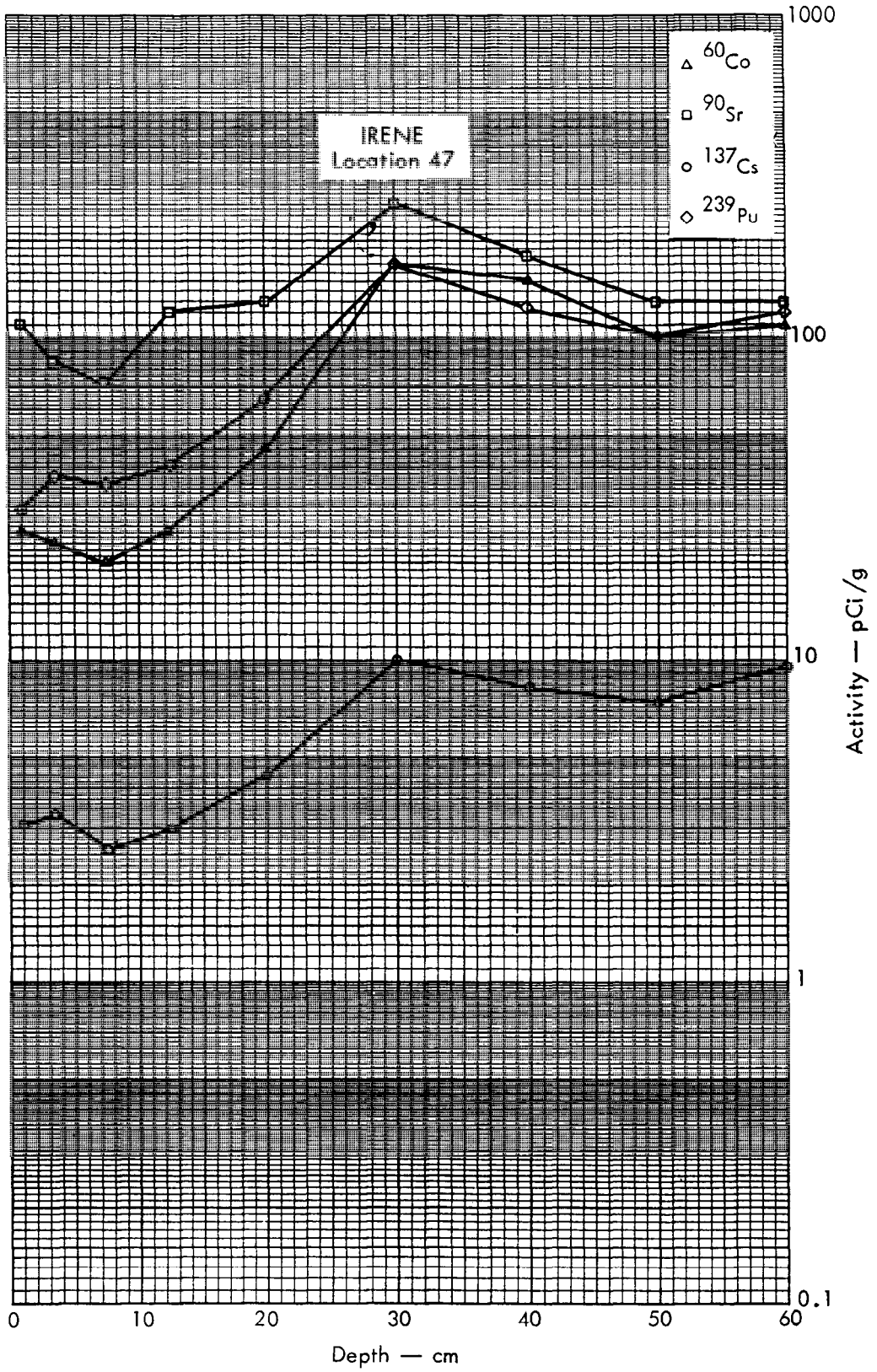

Fig. B.7.2n. Activities of selected radionuclides as a function of soil depth.

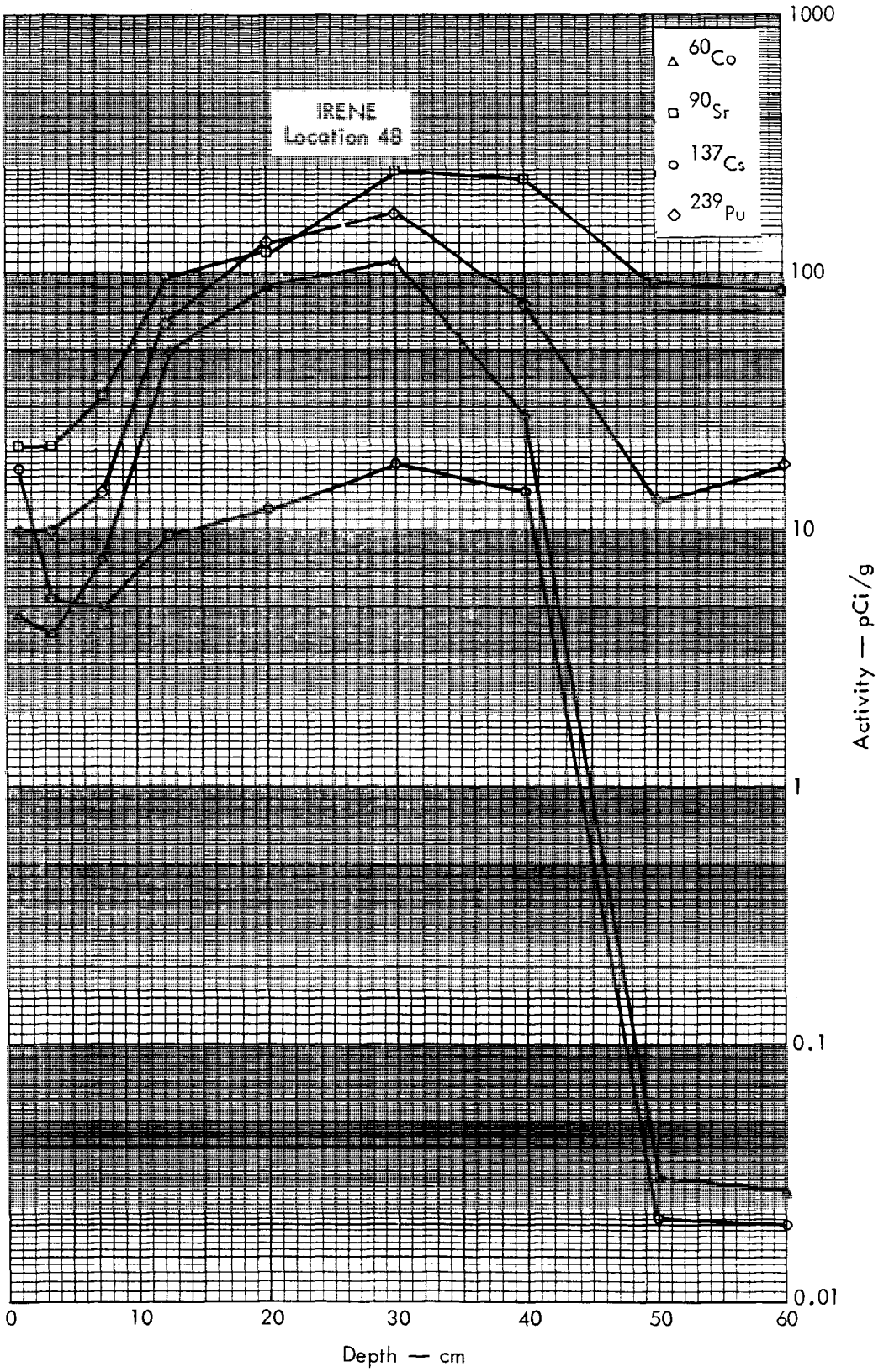

Fig. B.7.2o. Activities of selected radionuclides as a function of soil depth.

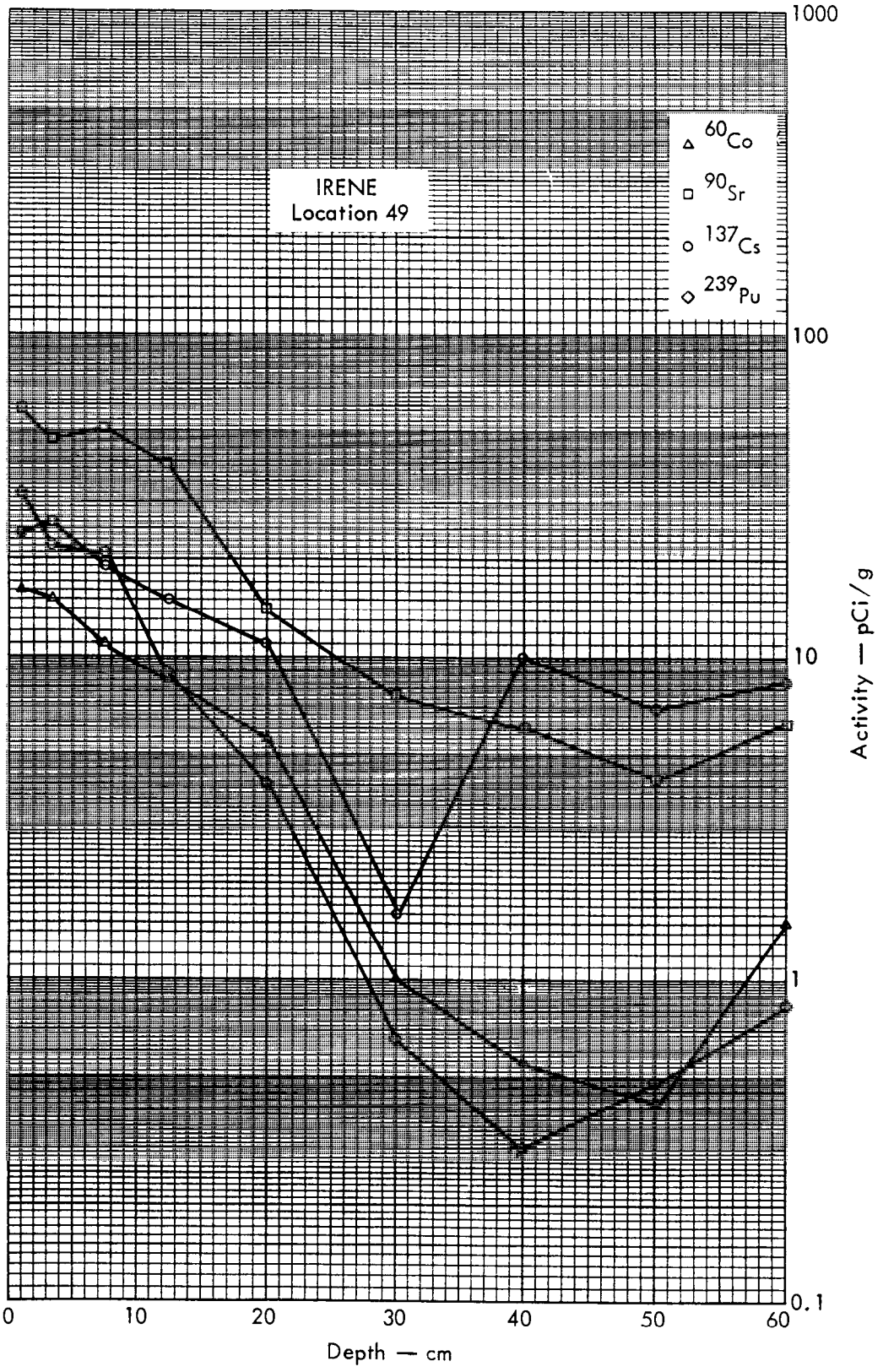

Fig. B.7.2p. Activities of selected radionuclides as a function of soil depth.

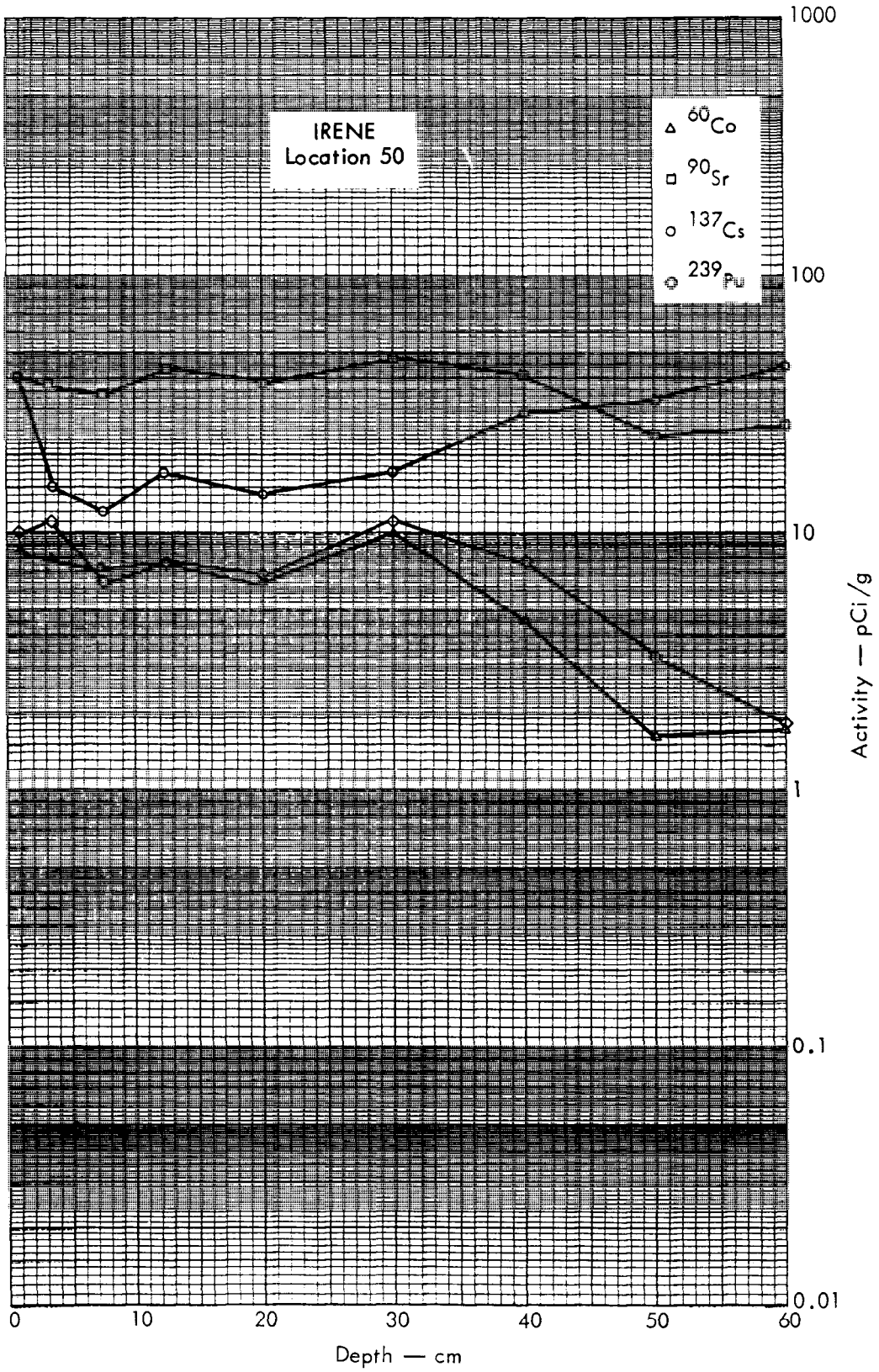

Fig. B.7.2q. Activities of selected radionuclides as a function of soil depth.

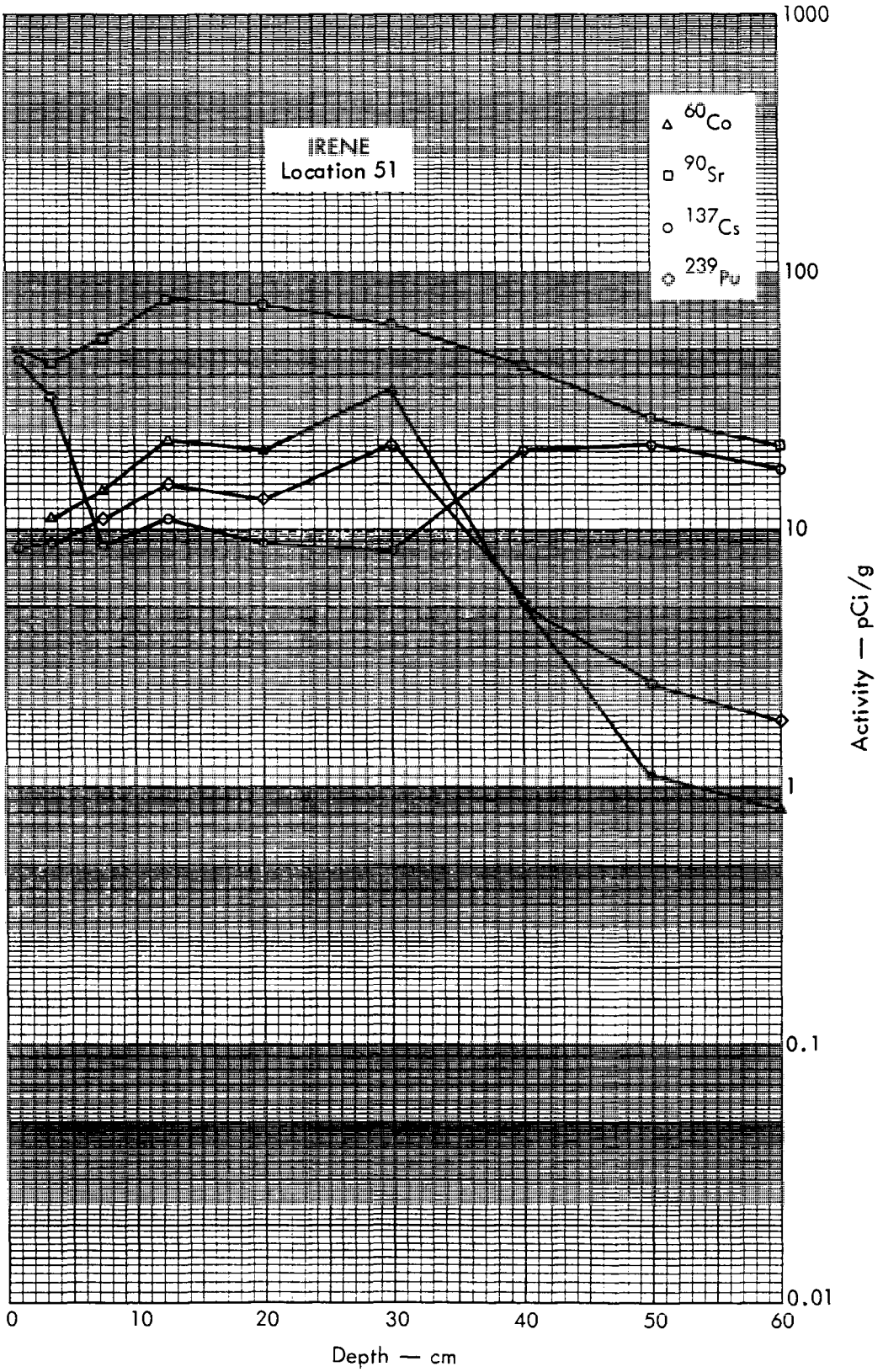

Fig. B.7.2r. Activities of selected radionuclides as a function of soil depth.

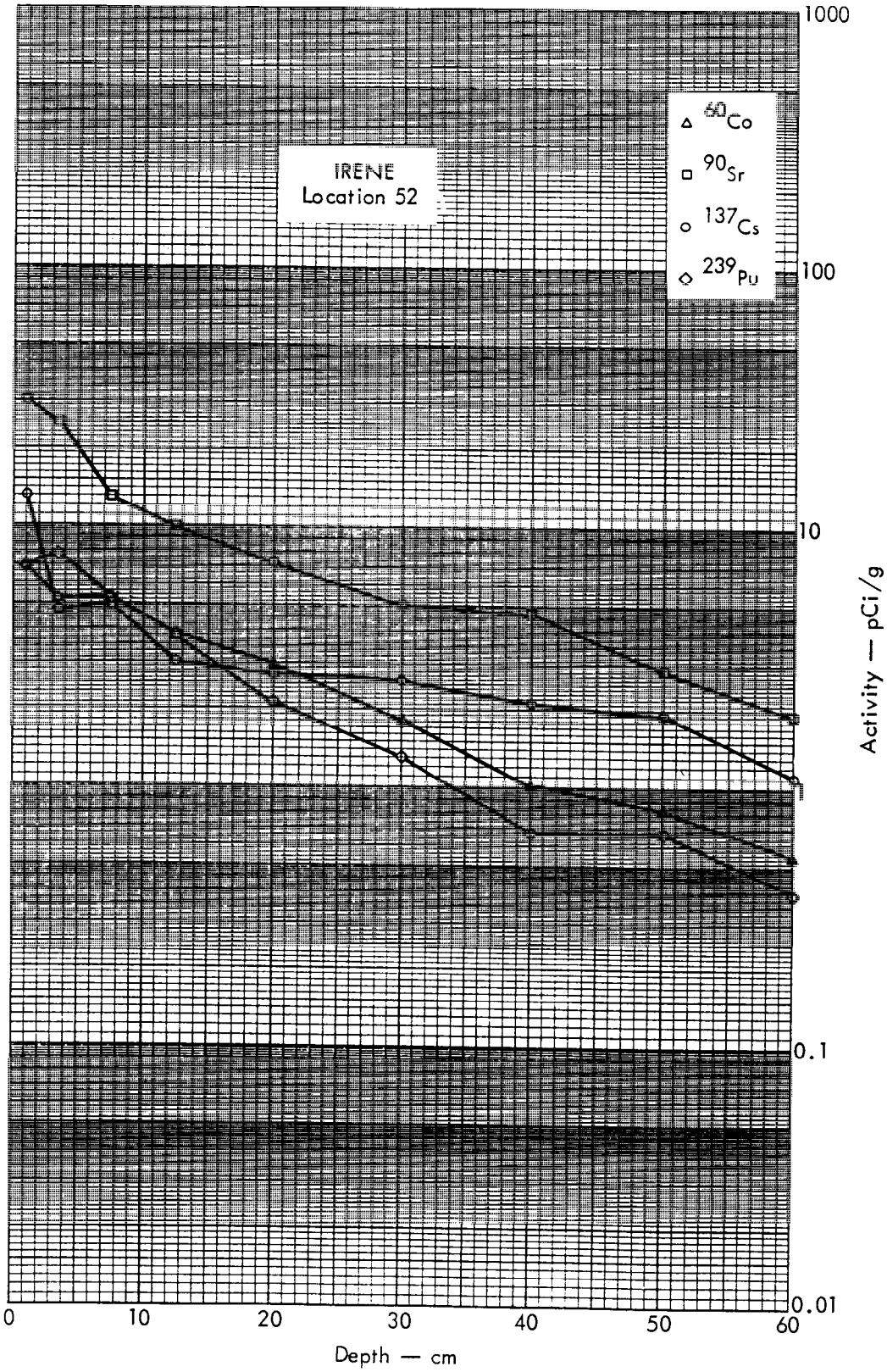

Fig. B.7.2s. Activities of selected radionuclides as a function of soil depth.